STRUCTURAL AND FUNCTIONAL STUDIES OF MUNC18 AND SNARE PROTEINS

APPROVED BY SUPERVISORY COMMITTEE

_____

Jose Rizo-Rey, Ph.D.

_____

Helen Yin, Ph.D.

_____

Xuewu Zhang, Ph.D.

_____

Diana R. Tomchick, Ph.D.

Dedication

To my family who gave me endless love and inspiration

STRUCTURAL AND FUNCTIONAL STUDIES OF MUNC18 AND SNARE PROTEINS

by

Yi Xu

DISSERTATION

Presented to the Faculty of the Graduate School of Biomedical Sciences
The University of Texas Southwestern Medical Center at Dallas
In Partial Fulfillment of the Requirements
For the Degree of

DOCTOR OF PHILOSOPHY

The University of Texas Southwestern Medical Center at Dallas
Dallas, TX
February, 2011

Acknowledgements

I believe this is the most important part of my thesis where I can express my gratitude to all the people that made this work possible. First and foremost, I owe my deepest gratitude to my supervisor, Dr. Jose Rizo-Rey, for offering me an opportunity to work in his laboratory. His persistent enthusiasm for both science and life made him a great scientist, an admirable mentor and a good friend for me. I appreciate working with him for these years and I could not make my achievement without his patience, encouragements, continual guidance, and inspiring discussion on all aspects concerning this thesis. I have learned a lot from him about how to be a good scientist and I will benefit from them for the rest of my life.

I would also like to give my thanks to lab members who have been working with Munc18. I am especially grateful to Dr. Irina Dulubova for giving me the initial recruit training, which later developed into my core skills underlining this thesis. This thesis would not have been possible unless Dr. Dulubova found that the interaction of Munc18-1 and SNARE complex involved Habc domain and SNARE motif and went on to design mutations to disrupt the binding. Lijing Su, a graduate student in the Munc18 group, has a pair of golden hands. In the laboratory, she is such a perfectionist that every single one of her experiments was carried out immaculately, down to the slightest details. But aside from work, she is an easygoing friend and the crowd pleaser, which contribute a lot to our nice environment. She has put a lot of effort in solving the structure of SM/SNAREs and she has found squid Munc18-1 behaves better than rat Munc18-1. I would also like to thank Alpay B. Seven, another graduate student, for his expertise in Cryo-EM, which

lead to the key observation about liposome fusion caused by Munc18-1. All together, these works paved the way for biophysical studies of Munc18-1.

I am heartily thankful to my wonderful dissertation committee formed by Dr. Helen Yin, Dr. Xuewu Zhang and Dr. Diana R. Tomchick, for the constructive suggestions and warm encouragements they gave me in the committee meetings along the way. I am also appreciative of all the current and former members of the laboratory, including Dr. Cong Ma for his sparkling ideas and technical support, and Yibin Xu for her intellectual discussion. It is also my pleasure to thank Kyle Brewer, Dr. Junjie Xu, Dr. Wei Li, Dr. Erin Horns, and Yi Zhang, Yilun Sun for their support and friendship. It has been really a great pleasure to work together with them.

Finally, I would like to thank my family, especially my parents, Dongmei and Changyan, my husband, Shuoyong, and my daughter, Fanqi, for their love, encouragement and support throughout my graduate studies.

STRUCTURAL AND FUNCTIONAL STUDIES OF MUNC18 AND SNARE PROTEINS

Yi Xu, Ph.D.

The University of Texas Southwestern Medical Center at Dallas, 2010

Supervising Professor: JOSE RIZO-REY, Ph.D.

Release of neurotransmitters is a tightly regulated process and a key event in interneuron communication. Release involves a series of steps, including vesicles docking to the active zone of the plasma membrane, priming to a readily releasable state, and Ca^{2+}-triggered membrane fusion. These steps are tightly controlled by an intricate protein machinery.

Essential components of this machinery are proteins from the Sec1/Munc18 (SM) and SNARE (soluble *N-ethyl*maleimide sensitive factor attachment protein receptors) families. SNAREs function by forming a four-helix bundle called SNARE complex; assembly of the SNARE complex brings two membranes together and is key for membrane fusion. The function of SM proteins is less clear. The neuronal SM proteins

Munc18-1 was identified and linked to synaptic vesicle fusion due to its tight binding to syntaxin-1. The strict requirement of Munc18-1 for release is illustrated by the observation that, in mice, deletion of Munc18-1 abolished neurotransmitter release completely.

Munc18-1 binds to the closed conformation of syntaxin-1 as well as to assembled SNARE complexes containing open syntaxin-1. Analysis of point mutations on Munc18-1 showed that binding of Munc18-1 to the Habc domain of open syntaxin-1 is critical for synaptic vesicle priming but not for the release step. The fact that Munc18-1 and complexin-1 could bind simultaneously to the SNARE complex suggested Munc18-1 remained bound to a macrocomplex that is poised for Ca2+ triggering of fusion.

Analysis using diverse biophysical approaches revealed that Munc18-1 indeed binds to the C-terminus of the synaptobrevin SNARE motif and to the SNARE four-helix bundle. Both interactions have similar affinities and the N-terminal region of syntaxin-1 competes with the SNARE four-helix bundle and synaptobrevin for Munc18-1 binding, suggesting that the interaction between Munc18-1 and the SNARE four-helix bundle involves the same cavity of Munc18-1 that binds to syntaxin-1.

To directly test Munc18-1's role in fusion, I reconstituted v- and t-SNAREs into separate liposomes. Fusion between these proteoliposomes in the presence of Munc18-1 was monitored with a lipid mixing assay. Intriguingly, I found that enhanced lipid mixing caused by rat Munc18-1 alone was observed. Biochemistry studies showed that denaturation of rat Munc18-1 or squid Munc18-1 causes membrane lipid mixing in the absence of SNAREs proteins.

TABLE OF CONTENTS

PRIOR PUBLICATION

Xu Y, Su L, Rizo J (2010) Binding of Munc18-1 to synaptobrevin and to the SNARE four-helix bundle. Biochemistry 49:1568–1576

Deák F, Xu Y, Chang WP, Dulubova I, Khvotchev M, Liu X, Südhof TC, Rizo J. (2009) Munc18-1 binding to the neuronal SNARE complex controls synaptic vesicle priming. J Cell Biol. 184(5):751-64 (Co-first author)

Xu L, Xu Y, Dong A, Sun Y, Pi L, Huang H (2003) Novel as1 and as2 defects in leaf adaxial–abaxial polarity reveal the requirement for ASYMMETRIC LEAVES1 and 2 and ERECTA functions in specifying leaf adaxial identity. Development 130:4097–4107

Xu Y, Sun Y, Liang W, Huang H (2002) The Arabidopsis AS2 gene encoding a predicted leucine-zipper protein is required for the leaf polarity formation. Acta Bot Sin 44:1194–1202

Chen C, Xu Y, Zeng M, Huang H (2001) Genetic control by Arabidopsis genes LEUNIG and FILAMENTOUS FLOWER in gyneocium fusion. Journal of Plant Research, 114:465-469 (Co-first author)

LIST OF FIGURES

LIST OF TABLES

LIST OF ABBREVIATIONS

1D, 2D, 3D	one dimensional, two dimensional, three dimensional
CD	circular dichroism
C.elegans	*caenorhabditis elegans*
CMC	critical micellar concentration
Cpxf	rat complexin I fraction (residues 26-83)
Cpx	rat complexin I
Cryo-EM	Cryo-electron microscopy
Dansyl PE	1,2-dioleoyl-sn-glycero-3-phosphoethanolamine-N-(5-dimethylamino-1-naphthalenesulfonyl)
DLS	dynamic light scattering
DOPS	1,2-dioleoyl-sn-glycero-3-phospho-L-serine
DTT	dithiothreitol
E.coli	*Eschericheria coli*
EDTA	ethylene diamine tetraacedic acid
EGTA	ethylene glycol-bis (β-aminoethyl ether)-tetraacetic acid
FPLC	fast performance liquid chromatography
FRET	fluorescence resonance energy transfer
GST	glutathione S-transferase
HEPES	N-(2-hydroxyethyl) piperizine-N'2-ethanesulphonic acid
HOPS	homotypic fusion and vacuole protein sorting

Hr	hour
HSQC	heteronuclear single quantum coherence spectroscopy
IPTG	isopropyl β-D-thiogalactopyranoside
*K*d	dissociation constant
kDa	kilodalton
LB	luria broth
NBD PE	1,2-dipalmitoyl-sn-glycero-3-phosphoethanolamine-N-(7-nitro-2-1,3-benzoxadiazol-4-yl)
Ni-NTA	nickel-nitrilotriacetic acid
NMR	nuclear magnetic resonance
NSF	N-ethylmaleimide-sensitive factor
OD	optical density
PBS	phosphate buffered saline
PCR	polymerase chain reaction
POPC	1-palmitoyl, 2-oleoyl-sn-glycero-3-phosphocholine
POPE	1-palmitoyl-2-oleoyl-sn-glycero-3-phosphoethanolamine
ppm	part per million
Rho PE	1,2-dioleoyl-sn-glycero-3-phosphoethanolamine-N-(lissamine rhodamine B sulfonyl)
RT	room temperature
SDS-PAGE	sodium dodecyl sulfate- polyacrylamid gel electrophoresis
SM	Sec1/Munc18
rMunc18-1	rat Munc18-1
sMunc18-1	squid Munc18-1

SNAP-25	rat synaptosome associated protein- 25KDa
SNAPs	soluble NSF attachment proteins
SNARE	SNAP receptor
SNC	the C-terminal SNARE motif of rat SNAP25
SNN	the N-terminal SNARE motif of rat SNAP25
Syb2	rat full length synaptobrevin
SyxSN25	co-expressed syntaxin-1 and SNAP-25
Tm	melting temperature
TRIS	tris (hydroxymethyl) aminomethane
t-SNARE	target membrane SNARE
UV	ultraviolet
VAMP	vesicle associated membrane protein
v-SNARE	vesicle SNARE
WT	wild type
β-ME	β-mercaptoethanol
β-OG	octyl-β-D-glucopyranoside

Chapter 1 General Introduction

1.1 The Neurons and Synaptic Vesicle Cycle

The brain is composed of approximately 100 billion neurons that transmit and receive signals. Neurons are all connected, or synapsed to each other to create one of the most complicated structures in which there may be 1,000 trillion synapses (Figure 1.1A). This incredibly complex network of neurons is also the basis for cognition, learning and memory, reasoning and problem solving, even emotion control.

Neurons are specialized cells that process and transmit cellular signals. A typical neuron comprises three parts: the soma or cell body, dendrites, and axon (Kandel *et al.* 1991). The soma is the central part of the neuron and contains the nucleus of the cell, where most protein synthesis occurs. The dendrites of a neuron are cellular extensions with many branches, which can be located on one or both ends of the cell. Dendrites typically branch profusely, getting thinner with each branching, and extending a few hundred micrometres from the soma. The axon is a cable-like extension, reaching long distance and giving rise to hundreds of branches. Unlike dendrites, an axon usually maintains the same diameter as it extends. Moreover, the soma may give rise to numerous dendrites, but to no more than one axon. The axon carries nerve signals away from or back to the soma. Synaptic signals are received by the soma and dendrites; axons conduct the action potential; signals to other neurons are from the synapse, which is the contact junction between the axon terminal of one neuron and a dendrite or soma of another.

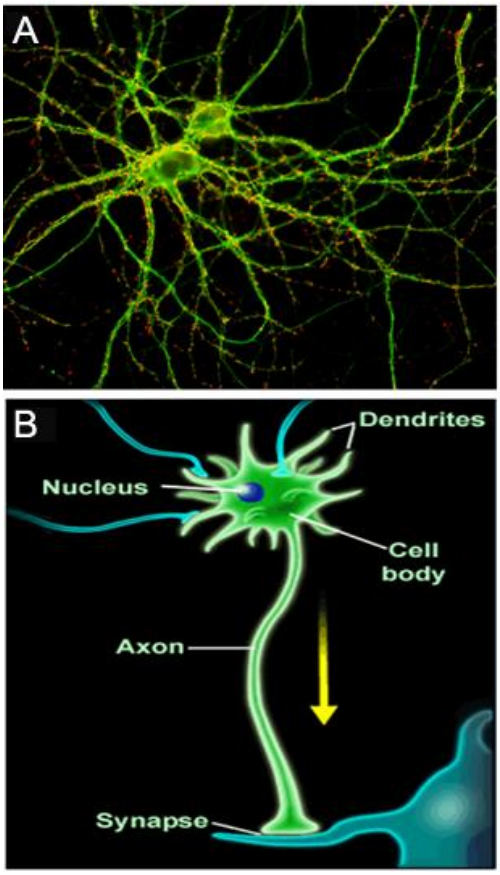

Figure 1.1

Figure 1.1 Neurons and synaptic networks.

(A). Image of a complex network of neurons, with each neuron connecting to thousands of other neurons via synapses. Brain function requires this precisely orchestrated connectivity. Image was taken by Xinran Liu.

(B). A typical neuron has three main parts. The cell body, or soma, is a main cellular space. The soma houses the nucleus, in which the neuron's main genetic information can be found. The axon conducts the action potential. The dendrites receive messages from other neurons. Image was modified from internet (http://www.morphonix.com/software/education/science/brain/game/specimens/neuron_parts.html).

At the synapse, the synaptic vesicles release their contents to the synaptic cleft through fusion with the plasma membrane and signal transmission occurs. Synaptic vesicles are independent functional organelles in the neurons and they undergo a trafficking cycle in the nerve terminal. Synaptic vesicles are first filled with neurotransmitters by active transport and are translocated to the plasma membrane. Then these vesicles dock to a specialized region of the synaptic plasma membrane, the active zone, where they undergo a priming process to form a readily-releasable pool. This priming step involves the formation of a complex between the vesicle and plasma membrane proteins as well as some cytoplasmic proteins. Upon arrival of an action potential, Ca^{2+} influx through the voltage–gated Ca^{2+} channels triggers membrane fusion and releases neurotransmitters into the synaptic cleft. The empty synaptic vesicles undergo endocytosis and are recycled by different pathways, and are refilled with neurotransmitters for another vesicle cycle. The process of neurotransmitter release is crucial for interneuron communication (Südhof 1995; Südhof 2004)

1.2 Proteins Involved in Neurotransmitter Release

The key event in the synaptic vesicle cycle is exocytosis by membrane fusion. The process of membrane fusion is a universal event that happens in all kinds of cells. The molecular machinery for this process is conserved from yeast to neurons (Clary *et al.* 1990; Bennett and Scheller 1993). It is believed that there is a common membrane fusion machinery and mechanism. During the past two decades, a lot of effort has been put into elucidating the mechanism of the fusion. Extensive studies have led to the

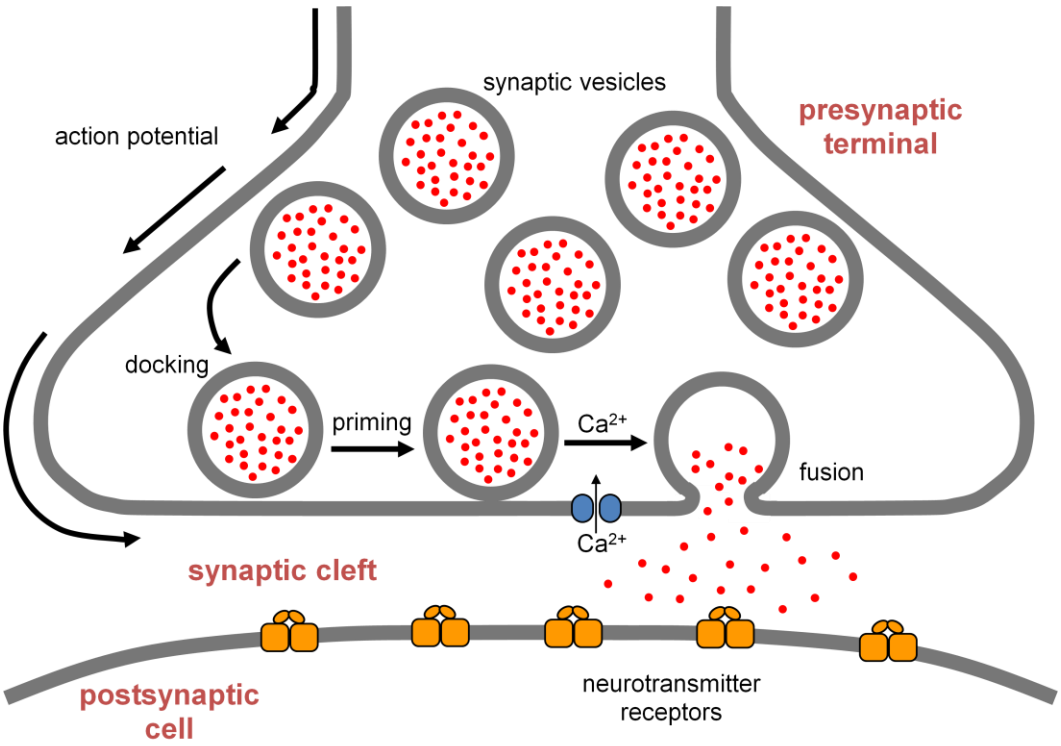

Figure 1.2

Figure 1.2 The synaptic vesicle cycle.

Synaptic vesicles are filled with neurotransmitters. Vesicles dock at the active zone, where they undergo a priming process and reach a fusion ready state. Upon Ca^{2+} influx, the fusion-pore opens and fast fusion occurs. After neurotransmitter release, synaptic vesicles undergo endocytosis and recycle via several pathways.

identification of numerous proteins involved in membrane fusion (Südhof 1995; Augustine *et al.* 1996; Jahn and Südhof 1999; Lin and Scheller 2000). These proteins have homologs in most types of intracellular membrane fusion, including Sec1/Munc18-1(SM) proteins, soluble NSF attachment proteins (SNAPs), the SNAPs receptors (SNAREs), and small G proteins of the Rab3 family. Each fusion pathway requires specific SNAREs and SM proteins. The Ca^{2+} trigged neurotransmitter release at synapses is regulated by the SM protein Munc18-1, the VAMP2/synaptobrevin, and the syntaxin-1 and SNAP-25 (synaptosome associated protein of 25-kDa molecular weight).

1.2.1 SNAREs and SNARE Complex

The general fusion proteins of the neurotransmitter release machinery, at least in part, are the SNAREs. SNAREs are structurally simple, and are characterized by SNARE motifs of approximately 60–70 residues in length, which tend to form a coiled coil structure (Terrian and White 1997; Weimbs *et al.* 1997).

Synaptobrevin is a vesicle-associated membrane protein (VAMP2) with molecular weight of 18 kDa, also called v-SNARE. It consists of a short N-terminal sequence, a SNARE motif, and a C-terminal transmembrane region (Figure 1.3). Synaptobrevin was initially identified as the target of tetanus toxin, which blocks exocytosis by proteolytic cleavage of synaptobrevin (Link *et al.* 1992; Schiavo *et al.* 1992). Mice lacking functional synaptobrevin gene cannot survive after birth, and have a dramatically reduced but not abolished spontaneous and evoked neurotransmitter release

(Schoch *et al.* 2001), while double knockout of synaptobrevin and cellubrevin in chromaffin granules results in fully abolished secretion (Borisovska *et al.* 2005).

Syntaxins belong to a family of membrane integrated t-SNARE proteins participating in exocytosis. Syxtaxin-1 has two isoforms in human, syntaxin-1A and syntaxin-1B, which may function redundantly (Fujiwara *et al.* 2006). In addition to its SNARE motif (also known as the H3 domain), and C-terminal transmembrane region, syntaxin-1 contains a flexible N-terminal sequence, and a three-helix bundle called the Habc domain that is linked to the SNARE motif by a flexible linker (Fernandez *et al.* 1998). The H3 domain binds to both synaptobrevin and SNAP-25 forming the core SNARE complex. The N-terminal Habc domain is stable and can fold independently of the C terminus. Syntaxin-1 adopts two conformations: a closed conformation outside of the SNARE complex in which the Habc domain folds back onto the SNARE motif, and an open conformation in the SNARE complex with a mobile Habc domain (Dulubova *et al.* 1999) (Figure 1.3). This open or closed conformation exists in equilibrium. This closed conformation of syntaxin-1 is believed to be inactive for SNARE complex forming and stabilized by binding of Munc18-1 (Misura *et al.* 2000).

Unlike synaptobrevin and syntaxin-1, SNAP-25 associates with the plasma membrane not through a transmembrane domain, but through palmitoylation of four cysteines in the central region of the molecule. In addition, SNAP-25 contains two SNARE motifs that are separated by the cysteine-rich linker (Figure 1.3). Experimentally,

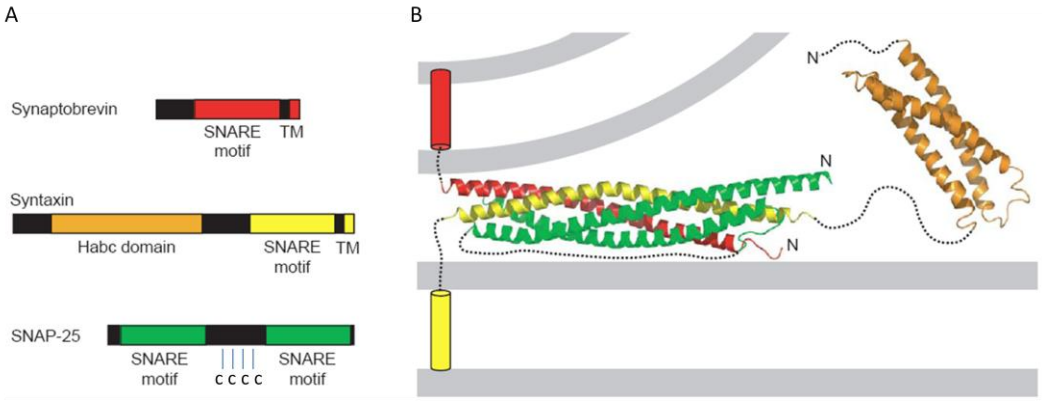

Figure 1.3

Figure 1.3 Domain diagrams of the synaptic SNAREs and structure of the SNARE complex.

(A). Domain architecture diagram of synaptobrevin, syntaxin-1, and SNAP-25. Synaptobrevin consists of a SNARE motif and a transmembrane domain (TM). Syntaxin-1 consists of a Habc domain, a SNARE motif and a transmembrane domain. SNAP-25 consists of two SNARE motifs and a cysteine-rich linker.

(B). Hypothetical model of the trans-SNARE complex in a membrane environment is shown with each of the 4 SNARE motifs: syntaxin-1 (yellow), synaptobrevin (red), the N- (blue) and C (green)-terminal SNARE motifs of SNAP-25, and syntaxin-1 Habc domain (orange). The four SNARE motifs form a parallel bundle and the C-terminal regions of the complex are anchored to the membrane. The diagram uses the crystal structure of the SNARE complex and the NMR structure of the syntaxin-1 Habc domain (Rizo and Südhof 2002).

the four cysteines are often mutated to serines to avoid oxidation. To simplify the experiments, SNARE motif fragments of SNAP-25 are commonly used. Syntaxin-1 and SNAP-25 have a tendency to form 2:1 heterodimer *in vitro*, while co-expression yields a 1:1 heterodimer. SNAP-25 knockout mice undergo normal embryonic development. In neurons cultured from embryonic SNAP-25 knockout mice, evoked exocytosis was not detectable while spontaneous neurotransmission persisted, which might be attributed to a closely related isoform, SNAP-23 (Washbourne *et al.* 2002).

Electron paramagnetic resonance (EPR) studies showed a parallel four-stranded coiled-coil structure of the synaptic SNARE complex (Poirier *et al.* 1998). The crystal structure confirmed an elongated four-helix bundle of about 12 nm in length intertwined by the four SNARE motifs (Sutton *et al.* 1998; Stein *et al.* 2009). In neuronal cells, the synaptobrevin and syntaxin-1 contributes one helix each, while SNAP-25 contributes two helices (Figure 1.3). The SNARE helices are separated from the membrane by linker regions, but the X-ray structure of neuronal SNARE complex with the carboxy-terminal linkers and transmembrane regions showed that assembly proceeds beyond the already known core SNARE complex to form a continuous helical bundle which can extend to the transmembrane helices (Stein *et al.* 2009). Binding of synaptobrevin to pre-formed syntaxin-1-SNAP25 1:1 heterodimer is believed to start at the N terminus of its SNARE motif and then zipper toward the C terminus (Hanson *et al.* 1997; Hanson *et al.* 1997). These findings have led to a hypothetical model that SNAREs proteins spontaneously assemble into a stable four-helix bundle between membranes as a “trans-SNARE complex” and assembly of the SNARE complex directly causes fusion by forcing

membranes closely together as it zippers up (Figure 1.4). Indeed, reconstitution experiments, in which recombinant SNARE proteins were incorporated into separate liposomes, supported that the SNAREs alone could force lipid mixing of two membranes (Weber *et al.* 1998), but the efficiency depends strongly on the protein to lipid ratios and homogeneity of the liposomes, indicating that one or more additional proteins may be required under physiological conditions (Kweon *et al.* 2003; Chen *et al.* 2006).

1.2.2 Munc18-1

SM proteins are highly conserved 60–70kDa polypeptides that are universal indispensible regulators of membrane fusion (Rizo and Südhof 2002; Verhage and Toonen 2007; Südhof and Rothman 2009). The first SM protein identified was UNC-18, which was discovered in genetic screens for uncoordinated phenotypes in C. elegans (Brenner 1974). Deletion of unc-18 results in deficient locomotion and its truncation severely reduces the evoked and spontaneous activity at the ventral nerve cord neuromuscular junction (Brenner 1974; Hosono *et al.* 1992; Weimer *et al.* 2003). Sec1p is the first identified SM protein that has been discovered in genetic screening for secretion defects in yeast (Novick and Schekman 1979; Novick *et al.* 1980). The mammalian homologue of UNC-18, Munc18-1 (also called nSec1 or rbSec1), was identified and linked to synaptic vesicle fusion due to its tight association to syntaxin-1 (Hata *et al.* 1993).

There are three isoforms of Munc18 in mammals. Munc18-1 is brain enriched

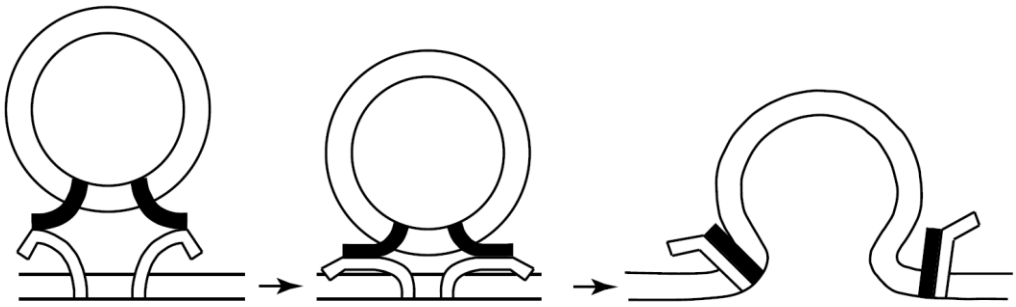

Figure 1.4

Figure 1.4 Model for SNARE-catalyzed membrane fusion.

The t-SNARE anchored in plasma membrane assembles with the v-SNARE anchored in the vesicle membrane to form trans-SNARE complexes. Assembly proceeds from the membrane-distal N terminus toward the membrane-proximal C terminus of the SNAREs. Complete zippering pulls the opposed membrane together and forces them to fuse (Hanson *et al.* 1997).

and regulates both early and late stages of exocytosis (Verhage *et al.* 2000). Munc18-2 is 62% identical to Munc18-1, and is abundant in epithelial cells and regulates vesicle transport to the apical plasma membrane (Tellam *et al.* 1995; Riento *et al.* 1998). It is a Syntaxin-4-binding protein and a key regulator of insulin-stimulated GLUT4 glucose transporting to the cell surface in muscle and adipocytes (Thurmond *et al.* 1998).

Like the SNAREs, SM proteins are crucial for most types of intracellular membrane fusion (Südhof 2004; Carr and Rizo 2010), or even more important than the SNAREs, because Munc18-1 knockout mice die immediately at birth and deletion of Munc18-1 led to a completely abolished neurotransmitter release, either evoked or spontaneous release, throughout development (Verhage *et al.* 2000). The universal requirement for Munc18-1 in vesicle fusion has been recognized for many years through genetic studies. At least three important functions of Munc18-1 have been proposed and supported with substantial experimental evidence: (a) a molecular chaperon for syntaxin-1, allowing both stabilization and appropriate transport of syntaxin-1 to the plasma membrane (Rowe *et al.* 1999; Rowe *et al.* 2001; Medine *et al.* 2007; Han *et al.* 2010). (b) a regulator of docking and priming via promotion of SNARE complex (Voets *et al.* 2001; Toonen *et al.* 2006). (c) a regulator of SNARE-mediated membrane fusion (Shen *et al.* 2007; Deák *et al.* 2009; Rathore *et al.* 2010; Shen *et al.* 2010). These functions of Munc18-1 are associated with diverse modes of interactions between SM proteins and SNAREs proteins.

The first binding mode (Mode 1) involves the closed conformation of syntaxin-1 binding to the arch-shaped Munc18-1 (Figure 1.5). The X-ray structure of the Munc18-

1/syntaxin-1 complex showed that Munc18-1, which has three conserved domains, adopts an arch-shape with a cavity where the syntaxin-1 closed conformation binds (Misura *et al.* 2000). The closed conformation of syntaxin-1 is formed by the SNARE motif helix bound to the Habc domain (Misura *et al.* 2000). This closed conformation of syntaxin-1 has a high affinity for Munc18-1, on the order of 2-20 nM *K*d (Burkhardt *et al.* 2008; Deák *et al.* 2009). The biological relevance of this mode was shown by the finding that Munc18-1 knockdown PC12 cells exhibited decreased expression of syntaxin-1 isoforms and defective trafficking (Voets *et al.* 2001; Arunachalam *et al.* 2008; Han *et al.* 2010). In addition, the expression level of syntaxin-1 was remarkably decreased in Munc18-1-deficient neurons (Verhage *et al.* 2000). These lines of evidences strongly suggested a role of Munc18-1 as a chaperon stabilizing syntaxin-1 and enabling its proper transport to the plasma membrane.

Mode 1 is so far the most extensively studied mode. It plays a key role in vesicle docking in the plasma membrane (Bennett *et al.* 1992; Voets *et al.* 2001; Gulyás-Kovács *et al.* 2007). In Munc18-1 null chromaffin cells, vesicle docking is abolished and it can be rescued by Munc18-1 (Gulyás-Kovács *et al.* 2007). Moreover, vesicle docking correlates with the ability of Munc18-1 to bind to closed syntaxin1. The crystal structure of the Munc18-1/syntaxin-1 complex revealed that the Munc18-1 cradles syntaxin-1 in its closed conformation (Figure 1.5) (Misura *et al.* 2000; Burkhardt *et al.* 2008). In this sense, Munc18-1 has an inhibitory role in sequestering syntaxin-1 and inhibits exocytosis by gating SNARE complex assembly. This is supported by evidence that an open

conformation mutant of syntaxin-1 in mice resulted in reduced binding to Munc18-1 and impaired docking, but dramatic enhancement of vesicle fusion (Gerber *et al.* 2008).

The N-peptide of syntaxin-1 has been shown to be involved in syntaxin-1/Munc18-1 interaction, and it was required for exocytotic membrane fusion (Khvotchev *et al.* 2007). A re-refined Munc18-1/syntaxin-1 complex structure showed syntaxin-1 N-terminal peptide, which connects to the syntaxin-1 Habc helical bundle by an unresolved linker (residues 10–26), binds to the domain 1 of Munc18-1, providing the second binding site for Munc18-1 (Burkhardt *et al.* 2008). In addition, Munc18-3 binds to the N-peptide of syntaxin-4 in isolation (Hu *et al.* 2007; Hu *et al.* 2011). The N-peptide, located at the extreme N terminus of syntaxin-1, is characterized by two or three charged residues followed by a hydrophobic leucine or phenylalanine residue. The N-peptide has been found to bind weakly to a hydrophobic pocket on the surface of cognate SM protein (Burkhardt *et al.* 2008; Smyth *et al.* 2010; Hu *et al.* 2011) (Figure 1.5).

This N-peptide binding mode (Mode 2) is now accepted as a general conserved binding mode across all species. In fact, many yeast SM proteins are known to bind to syntaxin-1 via an N-terminal binding mode. For instance, SM proteins in yeast Golgi transport, Sly1 and Vps45p, bind to cognate syntaxin Tlg2p, which has a closed conformation in isolation, via a short N-terminal peptide (Dulubova *et al.* 2002). Moreover, the yeast ER and Golgi SM protein Sly1p binds to the syntaxins Ufe1p and Sed5p through a short peptide motif at the very N-terminus of Ufe1p and Sed5p (Bracher and Weissenhorn 2002; Yamaguchi *et al.* 2002). This N-peptide binding mechanism may represent the more evolutionarily conserved mode of coupling between syntaxins and SM

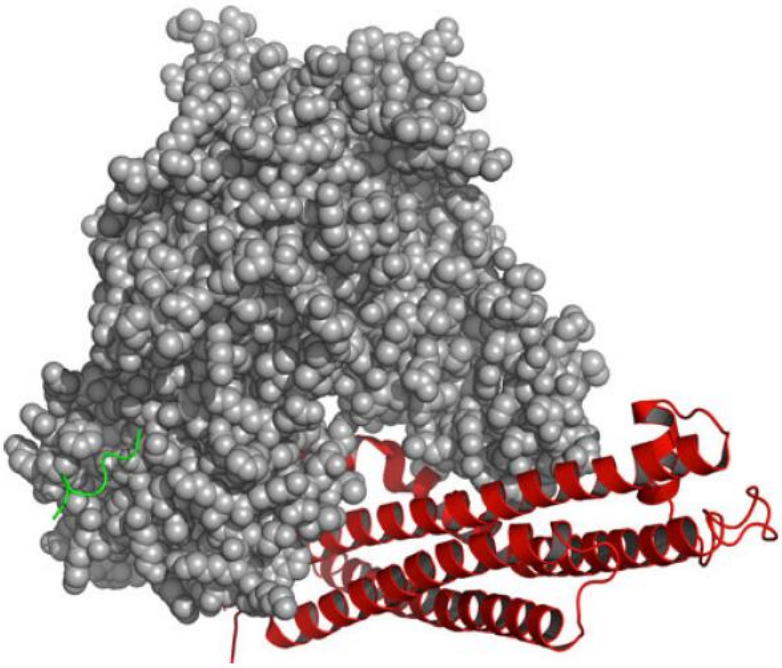

Figure 1.5

Figure 1.5 Re-refined structure of the Munc18-1/syntaxin-1 complex.

The syntaxin-1 N-peptide (green) of syntaxin-1 (red) is bound to a hydrophobic pocket of Munc18-1 (space fill) and is connected to the syntaxin-1 Habc helical bundle by an unresolved linker (residues 10–26). (PDB 3C98) (Burkhardt *et al.* 2008; Smyth *et al.* 2010).

proteins than Mode 1. The biological importance of this binding mode in vivo remains uncertain. Mutations that disrupt the Mode 2 interaction between Sly1 and Sed5, and between Vps45 and Tlg2, show no defects in ER-Golgi or vacuolar trafficking in yeast (Peng and Gallwitz 2004; Togneri *et al.* 2006). However, studies in *C. elegans* illustrated that it is the Mode 2 but not Mode 1 that is essential for UNC-18 function in exocytosis (Johnson *et al.* 2009). Recent *in vitro* reconstitution experiments have revealed a role for Munc18-1 in enhancing SNARE-mediated liposome fusion (Shen *et al.* 2007). This stimulation is eliminated by mutations that impair Mode 2 syntaxin-1 N-peptide binding (Shen *et al.* 2010), suggesting that the N-peptide of syntaxin-1 plays a regulatory role for the Munc18-1/SNARE complex interaction.

A third mode is the binding of SM proteins to SNARE complex four-helix bundle (Figure 1.6). This binding mode is the least extensively studied but probably the most important mode that likely underlies the general function of SM proteins. Yeast SM protein Sec1p binds specifically to the ternary SNARE complex instead of the N-peptide or closed conformation of its cognate syntaxin Sso1p (Togneri *et al.* 2006). Moreover, neuronal SM protein Munc18-1 binds to the SNARE complex four-helix bundle in solution and on the membrane (Shen *et al.* 2007; Diao *et al.* 2010; Xu *et al.* 2010). This Munc18-1–SNARE complex four-helix binding mode is fundamentally important for the mechanism of membrane fusion, since an interaction with the SNARE complex four-helical bundle would explain how SM proteins promote fusion. The biological relevance of the Mode 3 interaction is supported by both *in vitro* biochemistry and *in vivo* evidence. Mutations on yeast Sec1p, which exhibited impaired SNARE complex binding,

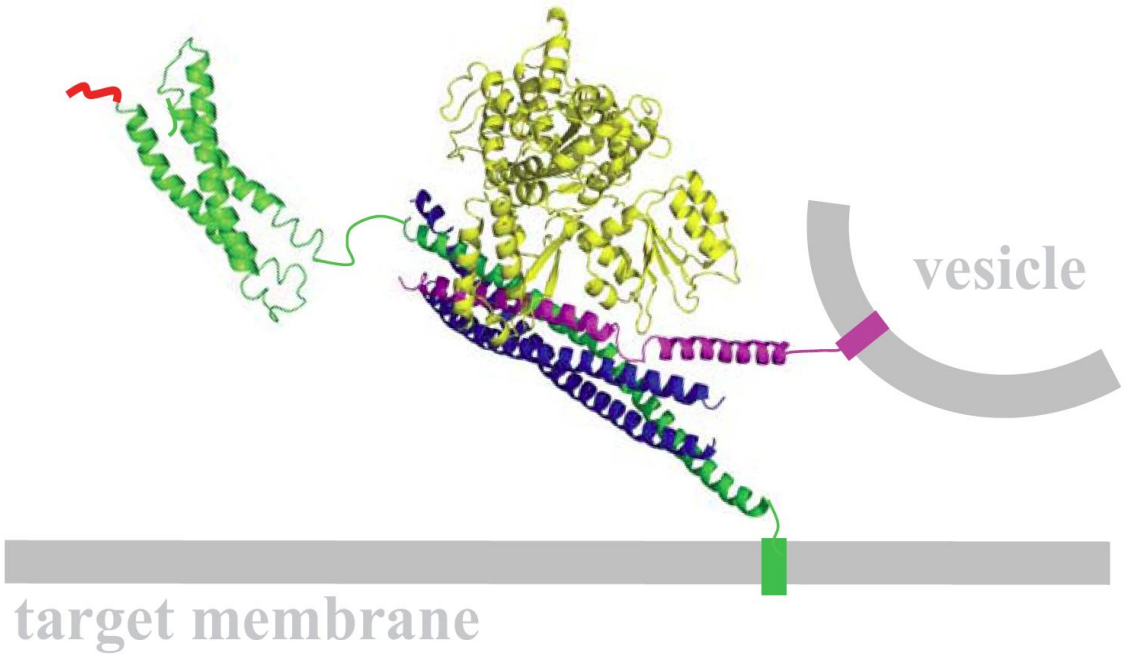

Figure 1.6

Figure 1.6 Model of Mode 3 binding.

Munc18 (yellow) binds to the four-helix bundle of SNARE complex from opposing membranes. Syntaxin-1 (green) Habc domain is flexibly linked to four-helix bundle containing SNAP-25 (blue); synaptobrevin (pink). red, N-peptide (Rathore *et al.* 2010).

led to a range in severity of cell growth and secretion defects. Studies from reconstitution experiments also provided evidence that Munc18-1 can stimulate membrane fusion by binding to the SNARE complex four-helical bundle in the absence of the N-peptide or Habc domain (Diao *et al.* 2010). But other reconstitution experiments suggested that syntaxin-1 N-peptide is dispensable once Munc18-1 has been recruited to the SNARE complex bundle (Rathore *et al.* 2010).

These divergent models raise many questions. If these models are all true, how do the binding modes change? How do the binding modes coordinate and cooperate in membrane fusion? What is the biological relevance of these interactions? The crystal structure of the Munc18-1/SNARE complex is not available yet and several groups are working hard on it. Burkhardt et al. refined the crystal structure of Munc18-1/syntaxin-1 complex including the N-peptide of syntaxin-1 (Burkhardt *et al.* 2008). They conclude that the N-peptide had a role in controlling SNARE complex assembly and Munc18-1-SNARE complex binding is mediated only by the syntaxin-1 Habc domain and the N-terminal sequence (Burkhardt *et al.* 2008). However, NMR and other biochemistry studies suggest that the interaction between Munc18-1 and SNARE complex involves binding to both N-terminal of open syntaxin-1 and four-helix bundle (Dulubova *et al.* 2007; Xu *et al.* 2010). All these evidences imply that the Mode 3 interaction of Munc18-1 with the four-helix SNARE bundle requires Mode 2 N-terminal binding to occur. Although the N-peptide hinders the transition from Munc18/closed syntaxin-1 complex to the Munc18/SNARE complex, Munc13 or other factors in the cell likely facilitate this transition (Guan *et al.* 2008; Weninger *et al.* 2008). Interactions with the N-peptide and

Habc domain could keep Munc18 bound to syntaxin-1 after opening the closed conformation (Dešák *et al.* 2009; Rathore *et al.* 2010). Finally, Munc18 is recruited from N-peptide of syntaxin-1 to the SNARE four-helix bundle to promote fusion, perhaps through diverse transport factors including Rabs, synaptobrevin, etc (Ohya *et al.* 2009; Rathore *et al.* 2010; Weber *et al.* 2010; Wickner 2010; Xu *et al.* 2010).

In addition to playing a key role in synaptic vesicle exocytosis, Munc18-1 and syntaxin-1 have been found to be involved in schizophrenia (SZ), a neurological disorder (Hikita *et al.* 2009; Barakauskas *et al.* 2010; Castillo *et al.* 2010; Gray *et al.* 2010). Thus, understanding the function of Munc18 will not only help to investigate the mechanism of membrane fusion, but also lead to a better understanding of the pathology of SZ and may offer a new drug target for SZ.

1.2.3 Munc13s

The finding of two Munc18/SNARE interaction modes raised important questions. For instance, how are these interaction modes coupled? What is the molecular mechanism underlying the transition of syntaxin-1 from closed conformation when bound to Munc18-1 to the open conformation in the assembled SNARE complex?

It is widely accepted that this transition together with partial SNARE complex formation are crucial steps in synaptic vesicle priming. Apart from Munc18-1, another large protein, Munc13 (rat homolog of Unc13) is known to play key roles in priming. Munc13 is a large protein with three C_2 domains, a C_1 domain, a calmodulin binding site

and a MUN domain (Figure 1.7). Among these diverse domains, the MUN domain is the minimal functional domain in Munc13 (Basu *et al.* 2005; Stevens *et al.* 2005). Genetic evidence showed that Munc13-1 and Munc13-2 double-knockout mice exhibited no primed vesicles and total abrogation of spontaneous and evoked release. MUN domain was sufficient to rescue release in Munc13-1/2 double-knockout *C. elegans* (Basu *et al.* 2005). Moreover, a constitutively open syntaxin-1 LE mutant partially rescued release in UNC-13 nulls in C. elegans, suggesting that UNC-13 and Munc13s play a role in the opening of syntaxin-1. A mechanism underlying the function of Munc13 was suggested in the report from Betz *et al.*, that Munc13 interacts with the N-terminus of syntaxin-1 (Betz *et al.* 1997), suggesting that Munc13 may open syntaxin-1 directly. However, no binding of the MUN domain to syntaxin-1 was observed (Basu *et al.* 2005); instead, the MUN domain interacts weakly with the SNARE complex, Munc18-1 and with the syntaxin-1 SNARE motif (Guan *et al.* 2008; Ma *et al.* 2011). A possible model for MUN domain function has been proposed whereby the MUN domain regulates the transition from the closed syntaxin-1/Munc18-1 complex to the SNARE complex through weak interaction with the syntaxin-1 SNARE motif; then it forms a complex assembly with M18 and SNARE complex to promote membrane fusion (Figure 1.7) (Ma *et al.* 2011), thus playing a key role in synaptic vesicle priming and fusion.

1.2.4 Complexins and Synaptotagmins

Both complexins and synaptotagmins are key regulators for the late steps of synaptic transmission. Complexins are neuron specific proteins with four isoforms and

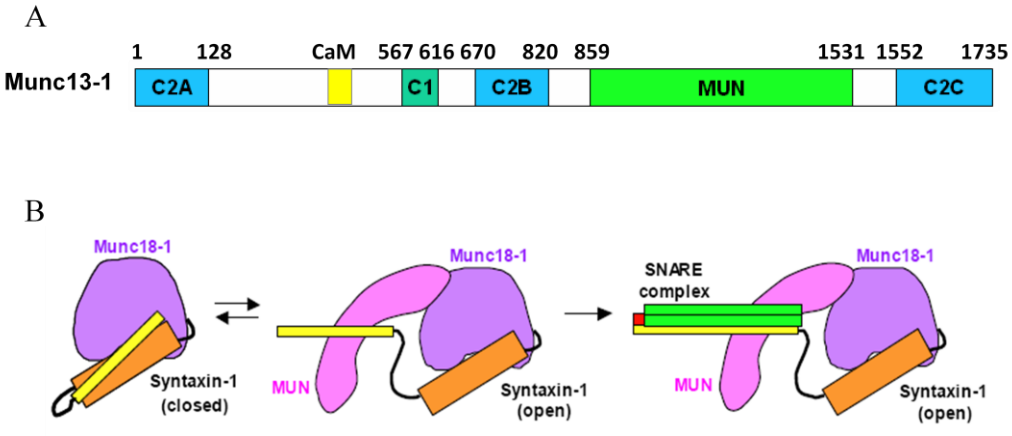

Figure 1.7

Figure 1.7 Domain diagram and functional model of Munc13-1.

(A). Munc13-1 has 1735 residues and several domains. C_2A domain binds to Rim 1. Between C_2A and C_1 domain, there is a calmodulin binding site. C_2B is known to bind Ca^{2+}, MUN domain is the minimal functional domain of Munc13-1. C_2C domain is at the C-terminus.

(B). Syntaxin-1 starts within the complex with Munc18-1 (left panel), then weak MUN/syntaxin-1 SNARE motif interactions lead to a transient state (middle panel), which can lower the energy barrier for the transition and result in SNARE complex assembly (Ma *et al.* 2011).

bind tightly to the SNARE complex (McMahon *et al.* 1995; Reim *et al.* 2005).

Complexin-I is unstructured in isolation and forms a central α helix when binds to the SNARE complex (Figure 1.8) (Chen *et al.* 2002). Crystal structure of the complexin-I/SNARE complex showed that complexin-I binds to the SNARE complex in an anti-parallel fashion, interacting with the interface of synaptobrevin and syntaxin-1 (Chen *et al.* 2002). In the original crystal structure, an accessory α-helix of complexin-I did not make any contact with the SNARE complex and the rest is highly mobile, while later biophysical studies revealed that the N-terminus of complexin-I interacts with the SNARE complex C-terminus (Xue *et al.* 2010).

The function of complexin is complicated. Genetic and cell biology studies showed that complexins may have both facilitatory and inhibitory functions (Rizo and Rosenmund 2008); e.g., complexins null mice died at birth and exhibited a dramatic decrease in neurotransmitter release (Reim *et al.* 2001), which is consistent with *in vitro* data that complexins stabilize the SNARE complex and thus act as facilitators. In contrast, overexpression of complexin results in inhibition of neurotransmitter release (Liu *et al.* 2007), suggesting that complexin acts as an inhibitor of neurotransmitter release.

Synaptotagmins are a large family of integral membrane proteins with a cytoplasmic region that contains two Ca^{2+}-binding motifs (Mackler *et al.* 2002). Sixteen synaptotagmin isoforms have been discovered, and they vary in calcium binding affinities and tissue specificity (Südhof 2002; Glavan *et al.* 2009). Synaptotagmin-I is the Ca^{2+} sensor in neurotransmitter release (Fernandez *et al.* 2001; Carr and Rizo 2010). It is composed of a short N-terminal transmembrane region and two protein kinase C-like

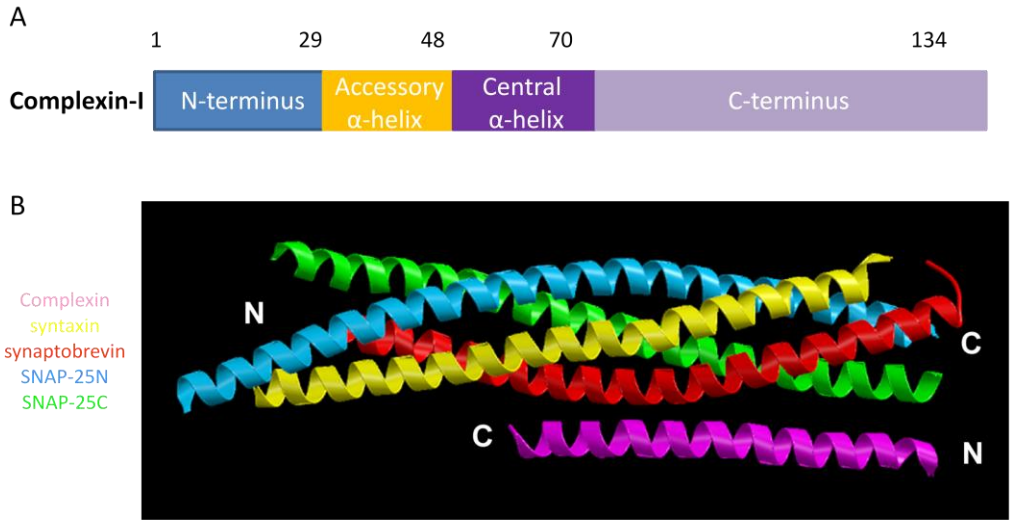

Figure 1.8

Figure 1.8 Structure of the complexin-I/SNARE complex.

(A). Diagram of the distinct regions of Complexin-I. Complexin-I has 134 residues. The first 29 residues are the N-terminal sequence that is required for complexin-I function. Residues 29 to 48 correspond to the inhibitory accessory helix. The SNARE binding central α-helix consists of residues from 49 to 70. The C-terminus of complexin-I corresponds to residues 71-134.

(B). Ribbon diagram of the complexin-I/SNARE complex. Only residues 32-72 of complexin were observable in the crystal structure. Complexin is in pink, syntaxin-1 is in yellow, synaptobrevin is in red, SNAP-25 N-terminal SNARE motif is in blue, SNAP-25 C-terminal SNARE motif is in green (Chen *et al.* 2002).

C_2 domains that are connected by a short flexible linker (Figure 1.9). Both C_2A and C_2B domains adopt a β-sandwich structure with flexible loops emerging from the top and bottom, with Ca^{2+} ions binding exclusively to the top loops (Sutton *et al.* 1995; Shao *et al.* 1998; Fernandez *et al.* 2001). The C_2A domain binds three Ca^{2+} ions (Fernandez-Chacon *et al.* 2002), and the C_2B binds two Ca^{2+} ions (Fernandez *et al.* 2001). Both C_2 domains can bind Ca^{2+} with low affinity, but can bind to Ca^{2+} with high affinity in the presence of phospholipids (Fernandez-Chacon *et al.* 2001). However, Ca^{2+} binding to the C_2A domain is not required for release, whereas Ca^{2+} binding to the C_2B domain is essential for release (Mackler and Reist 2001; Nishiki and Augustine 2004). The C_2B was later shown to be able to cluster liposomes in a calcium-dependent manner, suggesting that the C_2B domain functions by bringing two membranes into close proximity, similar to the SNAREs (Arac *et al.* 2006).

Deletion of synaptotagmins causes precisely the same phenotype as complexins deletion, a loss of Ca^{2+}-triggered release. However fusion was intact, because asynchronous release was unimpaired (DiAntonio *et al.* 1993; Littleton *et al.* 1993; Nonet *et al.* 1993; Geppert *et al.* 1994). In addition, synaptotagmin-I also competes with complexin-I for SNARE complex binding, releasing complexin-I in a Ca^{2+}-dependent manner (Tang *et al.* 2006; Dai *et al.* 2007). However, co-flotation assays have suggested that complexin-I and synaptotagmin-I can bind simultaneously to SNARE complexes (Schaub *et al.* 2006). These results suggested that complexin-I and synaptotagmin-I function in late steps of synaptic vesicle fusion, and they are bound to the SNARE complex after Ca^{2+} influx and then Ca^{2+} induces a rearrangement of interactions that lead

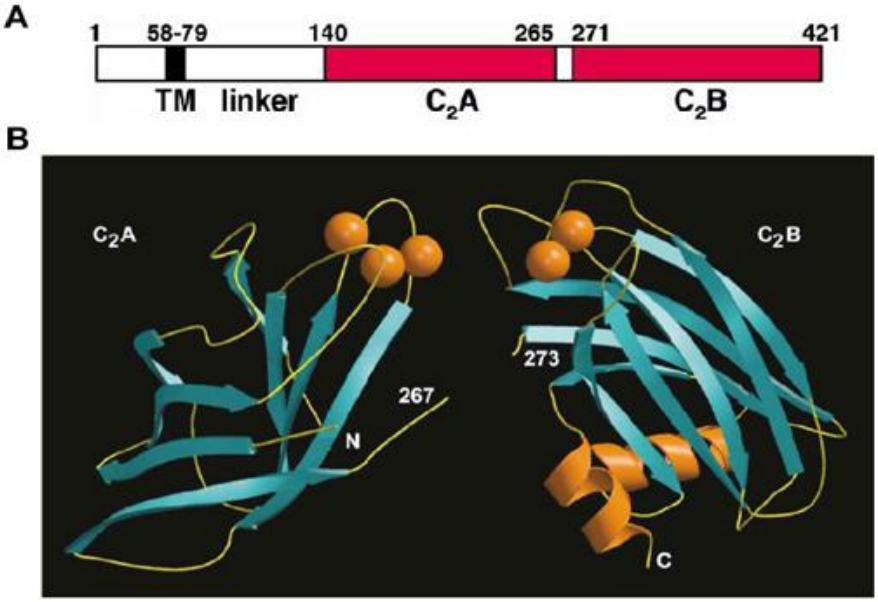

Figure 1.9

Figure 1.9 Structure of synaptotagmin-I.

(A). Domain diagrams of synaptotagmin-I. The C_2A and C_2B domains are colored in red. TM stands for transmembrane region. The residue numbers of the domain boundaries are labeled above the diagram.

(B). Ribbon diagrams of the individual synaptotagmin-I C_2A and C_2B domains. Helices are colored in orange and strands are colored in cyan. Ca^{2+} ions are represented by orange spheres (Sutton et al., 1995; Shao *et al.* 1998; Fernandez et al., 2001).

to fast release (Sudhof 2009, Rizo 2009).

1.3 The Universal Machinery for Synaptic Vesicle Fusion

Previous studies have demonstrated that SNARE proteins play an essential role in intracellular membrane fusion. The X-ray structure of the neuronal SNARE complex showed that, in addition to the core SNARE four-helix bundle, syntaxin-1 and synaptobrevin may form continuous helices throughout their SNARE motifs, linker regions and TMRs (Stein *et al.* 2009). This finding suggests that the energy of SNARE complex formation may be transmitted right into the membrane and that makes the membranes bend toward each other, promoting fusion (McMahon *et al.* 2010). The extent to which the SNAREs pull the opposing membranes close is currently unclear as the rigidity of the linker between the SNARE motif and the transmembrane domain remains unknown. It is possible that the linker region of the SNAREs by itself is not rigid enough to bend the membrane and that the accompanying curvature induced by larger proteins, e.g. SM proteins, may enable the SNARE complex to extend into the membrane and create a bulge in the latter.

On the other hand, reconstitution experiments have shown that SNAREs by themselves are sufficient to drive lipid mixing but the speed observed was extremely slow. However, these earliest studies (Weber *et al.* 1998; Parlati *et al.* 1999) depended strongly on SNARE concentration and local membrane architecture, indicating that one or more additional proteins may be needed under physiological conditions. In fact, genetic deletion of SM proteins blocks exocytosis, suggesting that SM proteins are

universally indispensible (Verhage *et al.* 2000).

SM proteins were bypassed in early reconstituted systems (Weber *et al.* 1998; Parlati *et al.* 1999), while later reconstitution experiments using relatively low SNARE to lipid ratios indeed showed the requirement of Munc18-1 for accelerated membrane fusion (Shen *et al.* 2007; Rathore *et al.* 2010; Shen *et al.* 2010). Exactly how SM proteins cooperate with SNARE complexes for fusion is still unclear as discussed before. SM proteins may be indirectly involved in fusion by helping SNARE complex assembly or directly in fusion through interaction with membranes. *In vitro*, Munc18-1 inhibited SNARE complex formation by sequestering isolated syntaxin-1 (Dulubova *et al.* 1999; Ma *et al.* 2011). But once SNARE complexes are formed and arranged on the membrane, it is possible that SM proteins can prevent the diffusion of SNARE complexes into the space between the membranes (Rizo *et al.* 2006). The HOPS (homotypic fusion and vacuole protein sorting) complex containing the yeast SNAREs and SM protein appears to act in this manner (Stroupe *et al.* 2006).

In sum, the universal fusion machinery may be composed of a SNARE complex containing v-SNARE protein, a t-SNARE complex (syntaxin-1 and SNAP-25 heterodimer), and a bound SM protein. As the trans-SNARE complex zippering towards the membrane to pull membrane closely together, the SM protein cooperates in fusion, either directly or indirectly (Südhof and Rothman 2009; Carr and Rizo 2010). However, it is plausible that additional proteins also form part of the core fusion machinery, including Rab proteins, Munc13s, complexins, and synaptotagmins (Figure 1.10) (Rizo and Rosenmund 2008).

The importance of Munc18-1 and the SNAREs for membrane fusion is well established, but there are still many questions need to be answered to understand the function of Munc18-1 in neurotransmitter release and membrane fusion. For instance, how the functions of Munc18-1 and SNARE complex are coupled? Whether the interaction between Munc18-1 and the SNARE complex is biologically relevant? Is Munc18-1 involved directly in the fusion? To address these questions, first, it is crucial to determine which of the steps leading to release depends on this interaction. We designed mutations in Munc18-1 that selectively impair binding to SNARE complexes while still retaining tight binding to closed syntaxin-1, and we found they have different abilities to rescue neurotransmitter release in Munc18-1 KO neurons. Importantly, these mutations disrupt the synaptic vesicle priming without altering the efficiency of release of primed vesicles. Moreover, I gave clear evidence that Munc18-1 binds directly to the SNARE motif of synaptobrevin and to the SNARE four-helix bundle with similar affinity and that these interactions involve the same cavity of Munc18-1 where closed syntaxin-1 binds. The Munc18-1 binding site was mapped to the membrane-proximal region of the synaptobrevin, which would place Munc18-1 right at the site where membrane fusion occurs. To study whether Munc18-1 is involved in membrane fusion directly, I reconstituted the SNAREs to liposomes and did lipid mixing assays with Munc18-1. I found that Munc18-1 causes lipid mixing even in the absence of SNAREs. Biochemistry studies showed that it was the denaturation of Munc18-1 that cause membrane lipid mixing in the absence of SNARE proteins. Hence, caution should be taken when interpreting the results of lipid mixing assays, and one should ensure that the results are not due, at least in part, to protein denaturation.

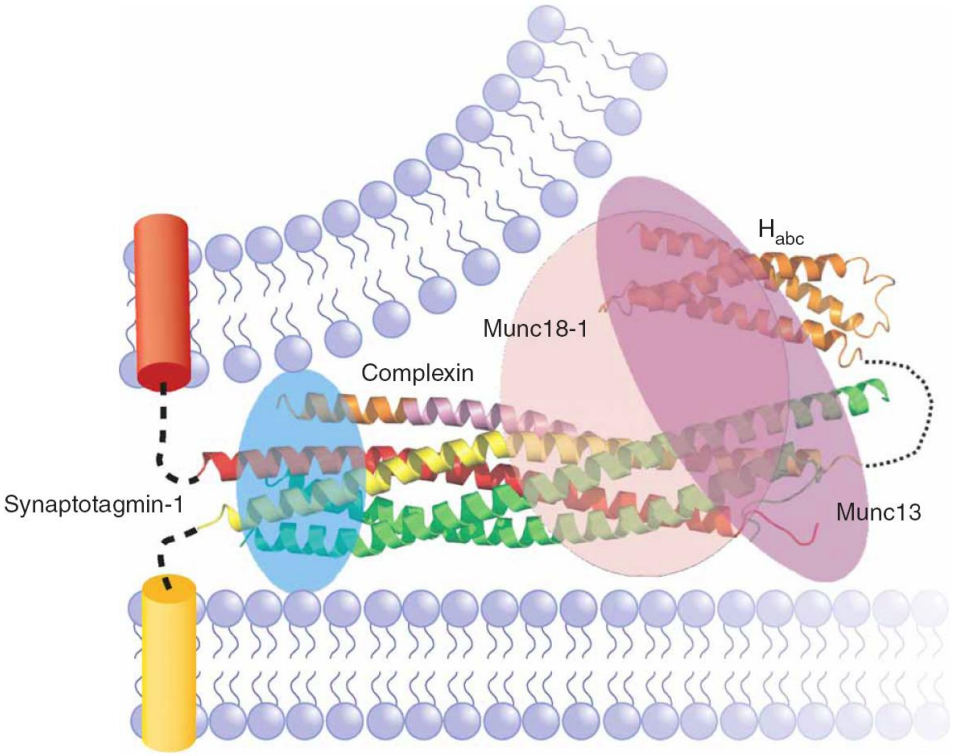

Figure 1.10

Figure 1.10 Diagram of the universal fusion machinery.

SNARE complex and bound Munc18-1, Munc13, complexin and synaptotagmin-1 form part of the core fusion machinery (Rizo and Rosenmund 2008).

Chapter 2 Munc18-1 Binding to the Neuronal SNARE Complex Controls Synaptic Vesicle Priming

2.1 Introduction

The machinery that regulates synaptic vesicle fusion is conserved in most types of intracellular membrane traffic. The core machinery for fusion includes proteins from the Sec1/Munc18 (SM) and SNARE families (Rizo and Südhof 2002; Toonen and Verhage 2003; Jahn and Scheller 2006). The SNARE proteins form tight four-helix bundles called SNARE complexes that bring the two membranes to close proximity (Hanson *et al.* 1997). Assembly of these complexes is key for all steps in membrane fusion (Brunger 2005; Rizo and Rosenmund 2008).

The function of SM proteins is much less clear. Munc18-1 is the neuronal SM family member which binds to the closed conformation of syntaxin-1, but this feature is not generally conserved in syntaxins from ER or yeast (Misura *et al.* 2000; Dulubova *et al.* 2001; Bracher and Weissenhorn 2002; Dulubova *et al.* 2002; Yamaguchi *et al.* 2002; Dulubova *et al.* 2003). Munc18-1 also binds to the open syntaxin-1 when it forms the SNARE complex with other SNARE proteins. (Dulubova *et al.* 2007; Shen *et al.* 2007).

The importance of Munc18-1 and the SNAREs for neurotransmitter release is well recognized, but it is still unclear how their functions are coupled and we are still far from understanding how Munc18-1/SNARE complex interactions control release. The interaction between Munc18-1 and the closed conformation of syntaxin-1 (Hata *et al.*

1993; Dulubova *et al.* 1999) stabilizes both proteins and controls SNARE complex formation by sequestering syntaxin-1 in a closed conformation (Verhage *et al.* 2000; Gerber *et al.* 2008). But this binding mode does not appear to be general. In fact, Munc18-1 binding to SNARE complexes containing open syntaxin-1 does seem to be universal (Carr *et al.* 1999; Grote *et al.* 2000; Yamaguchi *et al.* 2002; Collins *et al.* 2005; Khvotchev *et al.* 2007; Shen *et al.* 2007). Moreover, recent studies provided evidence for the physiological relevance of SM-protein/SNARE complex interactions (Khvotchev *et al.* 2007; Shen *et al.* 2007). However, the function of Munc18-1/open syntaxin-1 interactions in release was unknown, and it was unclear which steps leading to neurotransmitter release depend on these interactions.

In order to provide some fundamental insights into these questions, it is crucial to determine which steps in fusion depend on binding of Munc18-1 to open syntaxin-1. Moreover, to unravel whether Munc18-1 competes for SNARE complex binding with complexins is particularly important, since it is well established that these small soluble proteins function at the last step of Ca^{2+}-triggered release (Reim *et al.* 2001; Tang *et al.* 2006), and they are generally believed to be bound to the SNARE complex before Ca^{2+} influx (Rizo and Rosenmund 2008). I and the collaborators from the Südhof lab addressed these questions using a combination of biophysical experiments and a Munc18-1 knockout rescue approach. We have designed mutations in Munc18-1 to disrupt binding to SNARE complexes containing open syntaxin-1, while retaining tight binding to closed syntaxin-1. Then we tested the ability of mutants to rescue survival and neurotransmitter release in Munc18-1 knockout neurons.

2.2 Material and Methods

2.2.1 Recombinant Protein DNA Constructs

Bacterial expression vectors to express full-length rat Munc18-1, rat syntaxin-1A(2-253 or 2-243) (abbreviated as Syx), rat synaptobrevin-2(29-93) (abbreviated as Syb), human SNAP-25(11-82 and 141-203; abbreviated as SNN and SNC), and rat complexin(26-83) (abbreviated as Cpx) as GST-fusion proteins were available in the lab. Point mutants of Munc18-1(E59K, K63E and E66A) were generated from the WT constructs using the QuickChange site-directed mutagenesis kit (Stratagene) and custom-designed primers, and were verified by sequencing.

2.2.2 Preparation of Recombinant Proteins

These constructs were transformed into *Escherichia coli* BL21 (DE3) cells for expression and stored in glycerol stocks (40% glycerol) at -80 ℃.

The expression and purification of four SNARE proteins are similar except minor differences such as the induction temperature, elution buffer, further purification methods, etc. (table 2.1). One colony was picked into 50 ml of LB (w/ 100 μg/ml ampicillin) and incubated in a shaker at 250 rpm overnight at 37 ℃. The next day, 15 ml of the overnight culture were transferred to 1 L LB media (w/ 100 μg/ml ampicillin). The flask was incubated at 37 ℃ shaker for 2-2.5 hr till OD_{600} reached 0.8-0.9. Then the temperature was lowered to 25 ℃ (for SNN, SNC, Syb) or 20 ℃ (for Syx and Munc18-1), 0.4 mM IPTG (isopropyl β-D-thiogalactopyranoside, from Sigma) was added into each 1 L

culture to induce protein expression. After the addition of IPTG, the cultures were incubated at 25 ℃ or 20 ℃ overnight.

For proteins with isotopic labeling, a similar growth and expression strategy was used except using M9 minimal media instead of LB. 1L M9 minimal media contains 6.8 g Na_2HPO_4, 3.0 g KH_2PO_4, 0.5 g NaCl, 2.0 mM $MgSO_4$, 100 μM $CaCl_2$, 1.0 g NH_4Cl and 4.0 g D-(+)-glucose. For NMR experiments requiring ^{15}N labeled protein, $^{15}NH_4Cl$ was used instead of the standard NH_4Cl.

The cells were then harvested by centrifugation at 4000 rpm for 30 minutes in a swinging bucket rotor (Beckman Instruments) and the pellets were re-suspended in 30 ml PBS buffer containing 2 mM EDTA, 2 mM EGTA, 1 mM AEBSF, and 10 μl/ml sigma inhibitor cocktail (Sigma). The cell suspension was then frozen in liquid nitrogen and could be stored at -80 ℃ for further purification. The frozen cell suspension was thawed in a room-temperature water bath and passed through a high pressure homogenizer (Emulsiflex C-5, Avestin Inc.) at 10,000 psi for 3 to 4 times. The lysate was then centrifuged at 20,000 rpm in a JA-20 rotor (Beckman Instruments) for 30 minutes. The supernatant was passed through a 0.45 μm syringe filter and mixed with 1 ml slurry of prewashed glutathione sepharose beads (Amersham Pharmacia Biotech.), and rotated for overnight at 4 ℃ or 2 hr at room temperature to allow the GST-fusion protein to binds to the glutathione beads. In the case of purification of Syx(2-253) and Syx(191-253), a 4 ml slurry of glutathione beads was used to obtain a much higher yield. To prewash the Sepharose 4B beads, 50 ml H_2O was added to 1 ml slurry and centrifuged at 800 rpm for 10 minutes to get rid of residual ethanol. 50 ml PBS were then used to replace the H_2O.

The mixture was then run through a gravity flow chromatography column (Bio-Rad), allowing most of the non-binding proteins to flow through. To remove non-specifically bound proteins, the beads were then successively washed with 100 ml PBS containing 1% triton X-100, 1 M NaCl, and PBS. A Benzonase treatment was optional to remove protein-bound DNA. In the case of SNARE proteins, beads were washed with Benzonase buffer (50 mM Tris pH 8.0, 2 mM $MgCl_2$) and then incubated for 1 hr at room temperature with 10 units/ml Benzonase to digest bound DNA. After Benzonase treatment, the beads were washed with PBS. The beads were then equilibrated with thrombin cleavage buffer (50 mM Tris pH 8.0, 150 mM NaCl, 2.5 mM $CaCl_2$) and then incubated with 3-5 units of thrombin for two hours at room temperature to release protein from its GST tag.

The flow through was collected and further purified through a Superdex 75 HiLoad 16/60 size exclusion chromatography column (Amersham Pharmacia Biotech.). In the cases of Syx(2-253, 2-243), an ion exchange chromatography step was required before gel filtration (Source Q). Briefly, a linear gradient of salt (0-1 M NaCl) was used to elute the protein from a Source Q or Source S column. Protein inhibitors containing 1 mM 1:100 Sigma Inhibitor cocktail, 1 mM AEBSF, 2 mM EDTA, 2 mM EGTA, and 2 mM TCEP were added after the protein concentration was assessed by UV^{280}. Proteins were divided into aliquots, frozen in liquid nitrogen, and stored at -80 ℃. A typical yield was 3-5 mgs per liter of culture. In the case of M9 media, the yield was a little lower.

The expression and purification for Cpx or Cpx(26-83) (referred to as Cpxf) were similar to those for the SNARE motifs as described. After thrombin cleavage treatment,

Cpx was eluted in 20 mM sodium acetate buffer pH 4.5, and was further purified by ion exchange chromatography (Source S). A linear gradient of salt (0-1 M NaCl, pH 5.5) was used to elute the Cpx from the Source S column. Cpx was further purified by size exclusion chromatography column (Superdex 75, abbreviated as S75) and the purity of the fractions were assessed by SDS-PAGE and Coomassie blue staining.

	Induction Temperature	Elution buffer	Column for further purification
SNN	25 ℃	PBS buffer	Superdex75
SNC	25 ℃	PBS buffer	Superdex75
Syb(29-93)	25 ℃	PBS buffer	Superdex75
Syx(2-243, 2-253)	20 ℃	50 mM Tris pH 8.0,	Source Q, Superdex75
Munc18-1	25 ℃	50 mM Tris pH 8.0,	Source Q, Superdex200
Cpx, Cpxf	25 ℃	50 mM NaAc pH 5.5	Source S, Superdex75

Table 2.1 Specific information for purification of each SNARE motif, Cpx and Munc18-1.

2.2.3 Isothermal Titration Calorimetry (ITC) Experiments

ITC experiments were performed using a VP-ITC (GE Healthcare) calorimeter at 20 ℃ as described in the previous chapter. WT or mutant Munc18-1s and Syx(2-243) were changed to the same buffer (PBS, pH 7.4) by gel filtration on a Superdex 200 column. The titration of Syx(2-243) or SNARE complex with different Munc18-1 was

performed by 35×8 μL injections of 100-150 μM Syx(2-243) or SNARE complex at 3-min intervals into a 1.8 ml sample cell containing 5-10 μM WT or mutant Munc18-1s. After polynomial baseline correction to remove a slight drift of the initial data points, the data were fitted using a single-site binding model with MicroCal Origin™ software for ITC version 5.0 (GE Healthcare).

2.2.4 ^{15}N-edited 1D NMR (Nuclear Magnetic Resonance) Experiments

All NMR spectra were acquired at 25 ℃ on INOVA600 spectrometers (INOVA600; Varian) in a buffer containing 20 mM sodium phosphate, pH 7.1, 150 mM NaCl, and 2 mM DTT. Complexin(26-83) was labeled with ^{15}N and Munc18-1 was labeled with ^{13}C. ^{13}C-labeled Syx(2-243) was assembled into SNARE complex with other SNARE motifs (referred to as ^{13}C-labeled SNARE complex for simplicity), and was purified by ion exchange and size exclusion chromatography columns sequentially to remove the free Syx(2-243). For the titration experiments, samples contained 2 μM ^{13}C-labeled SNARE complex and the desired concentration of unlabeled WT or mutant Munc18-1s; a separate sample was prepared for each concentration. The first trace of ^{1}H-^{13}C or ^{1}H-^{15}N HSQC was acquired and all data were processed using NMRPipe and visualized using the program NMRViewJ. The titration data were fit to a single-site binding model using SigmaPlot (SPSS, Inc).

2.2.5 Gel Filtration Binding Assays

Purified 5 μM Munc18-1, 7.5 μM full length complexin or complexin(26-83) fragment, and 5 μM SNARE complex that was formed with Syx(2-253), Syb(29-93), SNN, and SNC were loaded onto a Superdex S200 (10/300GL) singly in 400 μl of 20 mM Tris, pH 7.4, and 120 mM NaCl. 400 μl samples containing 5 μM Munc18-1 and 5 μM SNARE complexes were incubated on ice for 30 minutes, then injected onto the column. A combination of 5 μM SNARE complex and 7.5 μM complexin or complexin(26-83) were incubated in the presence or absence of 5 μM Munc18-1 and applied to a Superdex S200 column. Data were analyzed by UNICORN 5.01 (Amersham Biosciences).

2.3 Results

2.3.1 Design of Mutations to Distinguish Munc18-1/SNARE Interactions

The crystal structure of the Munc18-1/syntaxin-1 complex revealed that Munc18-1 has an arch shape with a central cavity region where the syntaxin-1 closed conformation binds (Misura *et al.* 2000) (Figure 2.1A). The N-terminal domain of Munc18-1 (in cyan in Figure 2.1A) plays a key role in the interaction, making extensive contacts with the Habc domain and the SNARE motif of syntaxin-1 (in orange and yellow, respectively, in Figure 2.1A). The syntaxin-1 N-terminal sequence was not observable in the initial crystal structure, but also participates in binding (Khvotchev *et al.* 2007; Burkhardt *et al.* 2008).

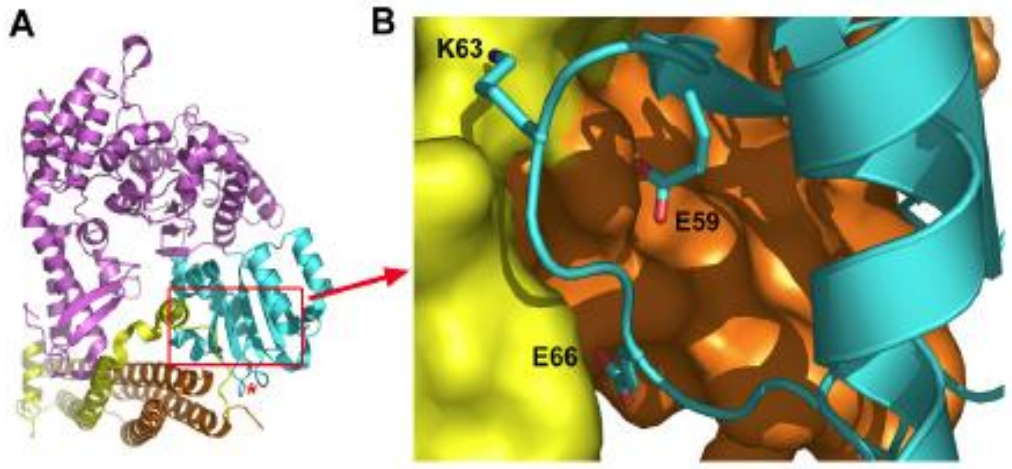

Figure 2.1

Figure 2.1 Design of mutations to disrupt Munc18-1/SNARE interactions.

(A). Ribbon diagram of the Munc18-1/syntaxin-1 complex. The N-terminal domain of Munc18-1 is colored in cyan and the other parts are in purple. Syntaxin-1 is in orange (Habc domain) and yellow (linker and SNARE motif). The red star indicates the position where cerulean was inserted for later rescue experiments.

(B). A close up of the interface showing the mutated residues.

Although no high-resolution structure of the Munc18-1/SNARE complex is available, NMR data showed that formation of the complex involves the syntaxin-1 N-terminal sequence and Habc domain, as well as the four-helix bundle formed by the SNARE motifs (Dulubova *et al.* 2007). These observations suggest that the interactions of Munc18-1 with the syntaxin-1 C-terminus must change drastically in the transition between the two complexes, whereas interactions with the N-terminal sequence and Habc domain may involve similar residues in both complexes. However, the energetic contributions of individual interactions to binding are likely to change during the transition between the two complexes due to the syntaxin-1 C-terminal rearrangements, particularly if the interactions involve residues near the interface between the Habc domain and SNARE motif in the closed conformation. Hence, replacing residues near this interface is likely to have differential disruptive effects on binding of Munc18-1 to syntaxin-1 or the SNARE complex. Based on these considerations, three residues on the Munc18-1 N-terminal domain that contact the syntaxin-1 Habc domain (E59), the SNARE motif (K63), or both (E66) (Fig. 2.1B), were selected for mutagenesis. Three point mutants of Munc18-1 bearing substitutions in one of these three residues were prepared. Two of the substitutions (E59K and K63E) were charge reversals to try to enhance their disruptive effects, while the third (E66A) only neutralized the charge, aiming for more moderate effects.

2.3.2 ITC Analysis of Binding of WT and Mutant Munc18-1 to Syntaxin-1

The effects of the three mutations on the binary Munc18-1/syntaxin-1 interaction were investigated by isothermal titration calorimetry (ITC) (Fig. 2.2). For this purpose, I

used a syntaxin-1 fragment encompassing residues 2-243, which include all the sequences that make contact with Munc18-1 in the crystal structure of the binary complex. I also tried using a slightly longer fragment, Syx(2-253), to perform ITC and yielded comparable but less consistent results due to the tendency of this fragment to oligomerize (Chen *et al.* 2008). Triplicate repeated experiments with Syx(2-243) and the WT or mutants Munc18-1 yielded the following average *K*d values and standard deviations: WT, 7.5 ± 2.7 nM; E59K, 12.0 ± 5.6 nM; K63E, 20.5 ± 11.7 nM; E66A, 11.3 ± 4.1 nM. The *K*d measured for WT Munc18-1 and Syx(2-243) was comparable to the 10-20 nM *K*d values measured previously by other methods (Pevsner *et al.* 1994; Khvotchev *et al.* 2007) and the 2.7 nM *K*d value reported in a recent ITC study (Burkhardt *et al.* 2008). The differences between these values can be attributed to differences in experimental conditions and/or the protein fragments used, or likely to intrinsic difficulties in obtaining accurate measurements for such high affinities, which also underlie the relatively large standard deviations in our measurements. Despite these difficulties, it was clear from our ITC data that the three Munc18-1 mutants retain tight binding to syntaxin-1. Each of the mutations did appear to impair the binary interaction slightly, particularly the K63E mutation, but none of the differences between the *K*d values measured for WT Munc18-1 and the mutants was statistically significant.

2.3.3 NMR Analysis of Binding of WT and Mutant Munc18-1 to the SNARE Complex

ITC experiments with WT Munc18-1 and the SNARE complex yielded very small binding enthalpies (Figure 2.3) (Burkhardt *et al.* 2008), which suggest that

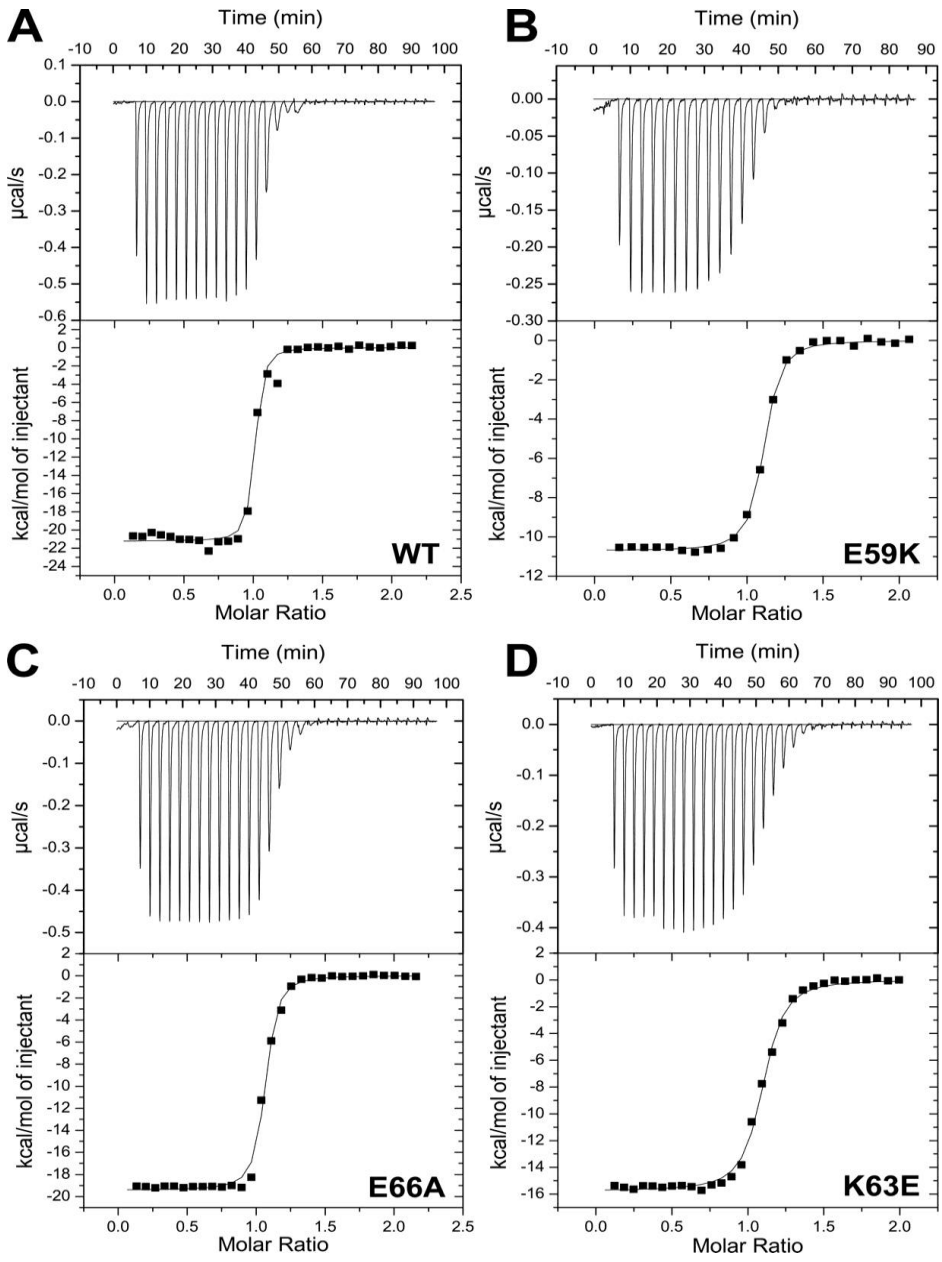
A
Time (min)
µcal/s
kcal/mol of injectant
Molar Ratio
WT
B
Time (min)
µcal/s
kcal/mol of injectant
Molar Ratio
E59K
C
Time (min)
µcal/s
kcal/mol of injectant
Molar Ratio
E66A
D
Time (min)
µcal/s
kcal/mol of injectant
Molar Ratio
K63E

Figure 2.2

Figure 2.2 ITC analysis of binding of WT and mutant Munc18-1 to syntaxin-1.

Illustrative examples of the ITC data obtained for binding of WT Munc18-1 (A) and E59K (B), E66A (C) and K63E (D) Munc18-1 mutants to syntaxin-1(2-243) are shown. A polynomial baseline correction was applied to remove a slight drift in the initial points of each titration before fitting the data to a single-site binding model. This correction did not substantially alter the *K*d values obtained.

The interaction is entropically driven and hinders quantitative comparisons by ITC. To measure the effects of the mutations in Munc18-1 on its interaction with open syntaxin-1 within the SNARE complex, I turned to an NMR method that we used previously to demonstrate this interaction (Dulubova *et al.* 2007). The method was based on the observation of a decrease in the intensity of the strongest methyl resonance (SMR) in one dimensional (1D) ^{13}C-edited ^{1}H-NMR spectra of a ^{13}C-labeled protein (or complex) upon binding to an unlabeled protein as a result of the broadening caused by formation of a larger species (Arac *et al.* 2003).

To apply this method to study Munc18-1/SNARE complex binding, I prepared SNARE complexes containing ^{13}C-labeled syntaxin-1, which were referred to as ^{13}C-labeled SNARE complex for simplicity. Addition of 2.5 μM WT Munc18-1 induced a moderate but reproducible decrease in the SMR intensity of 2 μM ^{13}C-labeled SNARE complex (Figure 2.4A), which reflected formation of the Munc18-1/SNARE complex assembly. I measured the decrease in the SMR intensity of the ^{13}C-labeled SNARE complex as a function of WT Munc18-1 concentration (Figure 2.4B) in multiple titration experiments, obtaining a *K*d of 266 ±41 nM. This value is consistent with the *K*ds of 100-300 nM that we estimated previously (Dulubova *et al.* 2007). The K63E Munc18-1 mutant had a similar affinity as WT Munc18-1, and the E66A mutant had a lower affinity (Figure 2.4A). Titrations with the Munc18-1 mutants and SNARE complex yielded a *K*d of 310 ±82 nM for K63E, which is not significantly different from WT, and a *K*d of 1.61 ±0.35 μM for E66A that reveals a considerable disruption of Munc18-1 binding to the SNARE complex. Interestingly, the E59K mutant did not significantly decrease the SMR

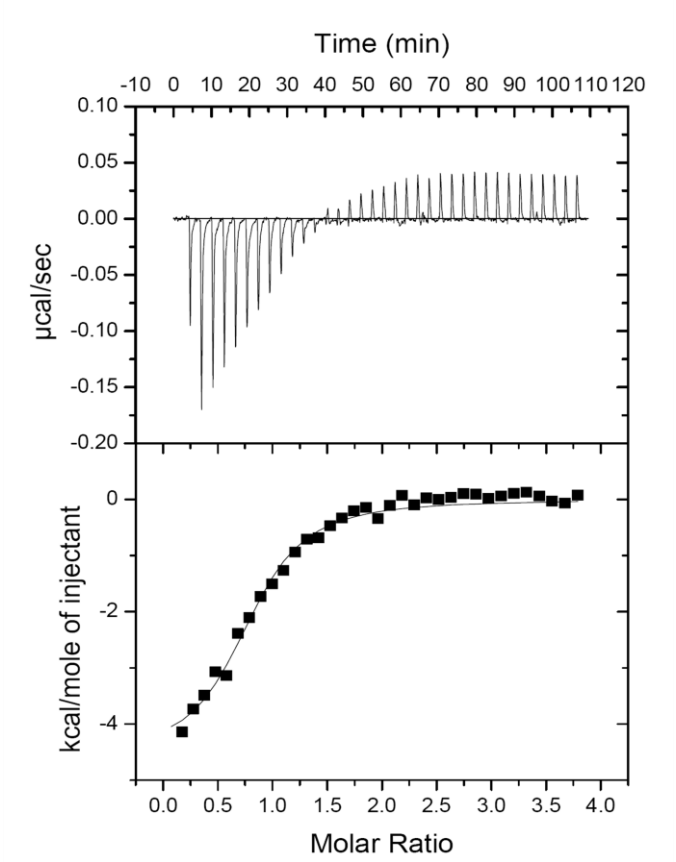

Figure 2.3

Figure 2.3 ITC analysis of binding of WT Munc18-1 to SNARE complex.

SNARE complex contains Syx(2-243), Syb(29-93), SNN, and SNC. The *K*d value is around 900 nM. Upper panels, raw data obtained from 35 injections, 8 µl each of SNARE complex. Lower panel, integrated curve showing experimental points.

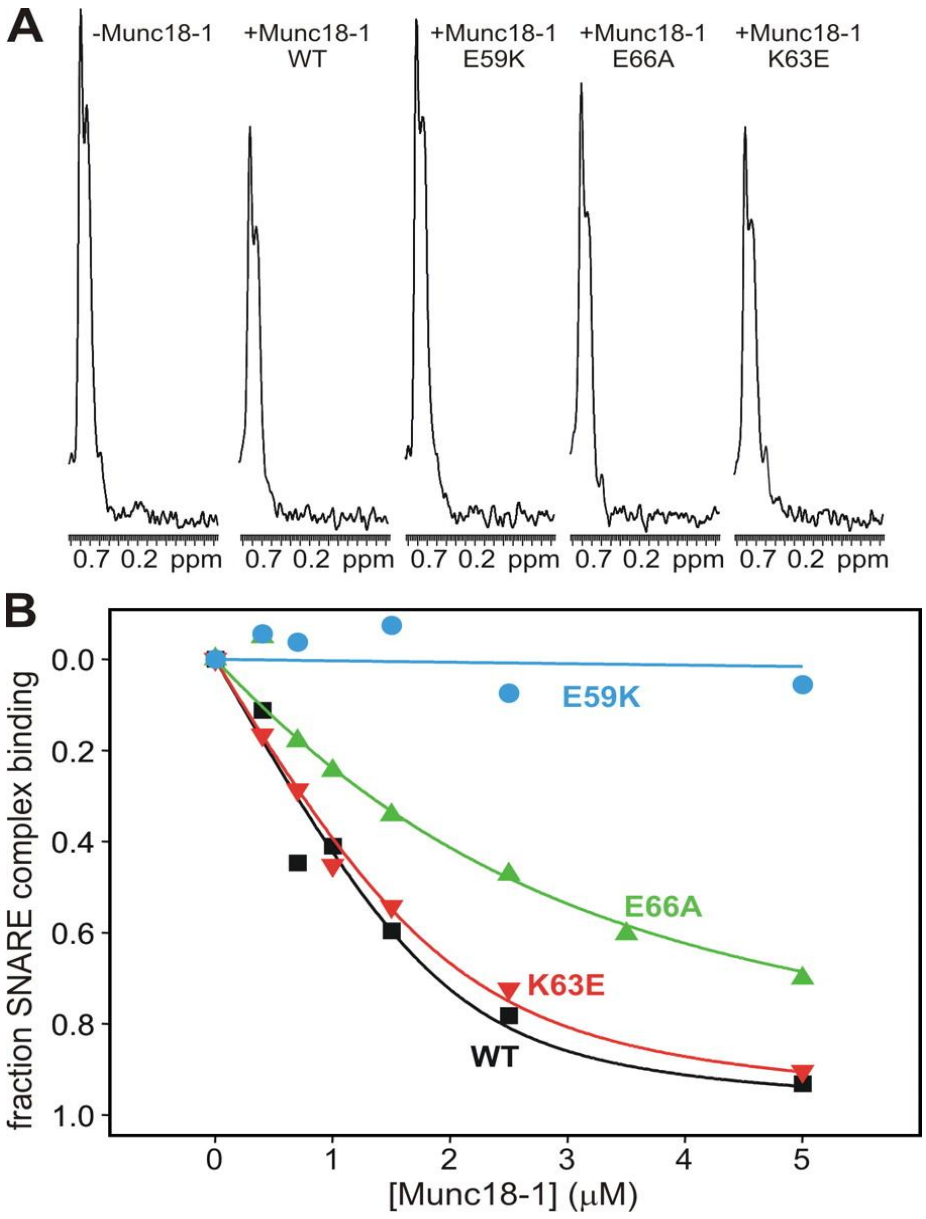
A
-Munc18-1
+Munc18-1 WT
+Munc18-1 E59K
+Munc18-1 E66A
+Munc18-1 K63E
0.7 0.2 ppm
B
fraction SNARE complex binding
0.0
0.2
0.4
0.6
0.8
1.0
E59K
E66A
K63E
WT
0
1
2
3
4
5
[Munc18-1] (μM)

Figure 2.4

Figure 2.4 Munc18-1 point mutations had different effects on binding to the SNARE complex.

(A). Sample traces of the methyl regions of 1D ^{13}C-edited ^{1}H-NMR spectra of 2 μM ^{13}C-labeled SNARE complex in the absence or presence of 2.5 μM unlabeled WT or mutant Munc18-1s.

(B). Binding curves obtained from the SMR intensities observed in 1D ^{13}C-edited ^{1}H-NMR spectra of titrations of 2 μM SNARE complex containing uniformly ^{13}C-labeled syntaxin-1(2-243) in the presence of increasing amounts of unlabeled WT or mutant Munc18-1s. The data were fit to a standard single-site binding model and normalized to % binding using as limit values the initial intensity in the absence of Munc18-1 (0% binding) and the intensity extrapolated to infinite Munc18-1 concentration (100% binding).

intensity of the ^{13}C-labeled SNARE complex (Figure 2.4A). Titrations with the E59K mutant consistently showed that this mutation strongly impairs SNARE complex binding, although there appeared to be some binding at the higher concentrations (Figure 2.4B); based on the sensitivity of the method, we estimated a *K*d of >30 μM for this mutant.

Hence, these results showed that the three mutations in Munc18-1 had markedly different effects on SNARE complex binding, and that two of them (E66A and E59K) disrupted more strongly this interaction than the binary interaction with the syntaxin-1 closed conformation.

2.3.4 Rescue of Survival and Synaptic Release in Munc18-1 Knockout Neurons

Munc18-1 KO mice experiments were made by our collaborators from the Südhof lab. Munc18-1 knockout mice die immediately at birth and exhibit a total abrogation of spontaneous, hypertonic sucrose-induced and Ca^{2+}-triggered neurotransmitter release (Verhage *et al.* 2000). To explore whether Munc18-1 could rescue release in neurons from these mice by overexpression of WT Munc18-1, primary cortical cultures from mouse embryos at E 16.5 day were selected. During the first week in vitro, Munc18-1 deficient neurons exhibited apparently normal neurite outgrowth and synapse formation as judged by immunocytochemistry and electron microscopy. Subsequently, neurons from Munc18-1 knockout mice degenerated rapidly, and cultures did not survive more than 10 days in vitro (DIV) (Figure 2.5). To overcome this problem, we used lentiviral expression of Munc18-1. To visualize the expressed Munc18-1 to make it easier to monitor the levels of wild-type and mutant Munc18-1, we tagged

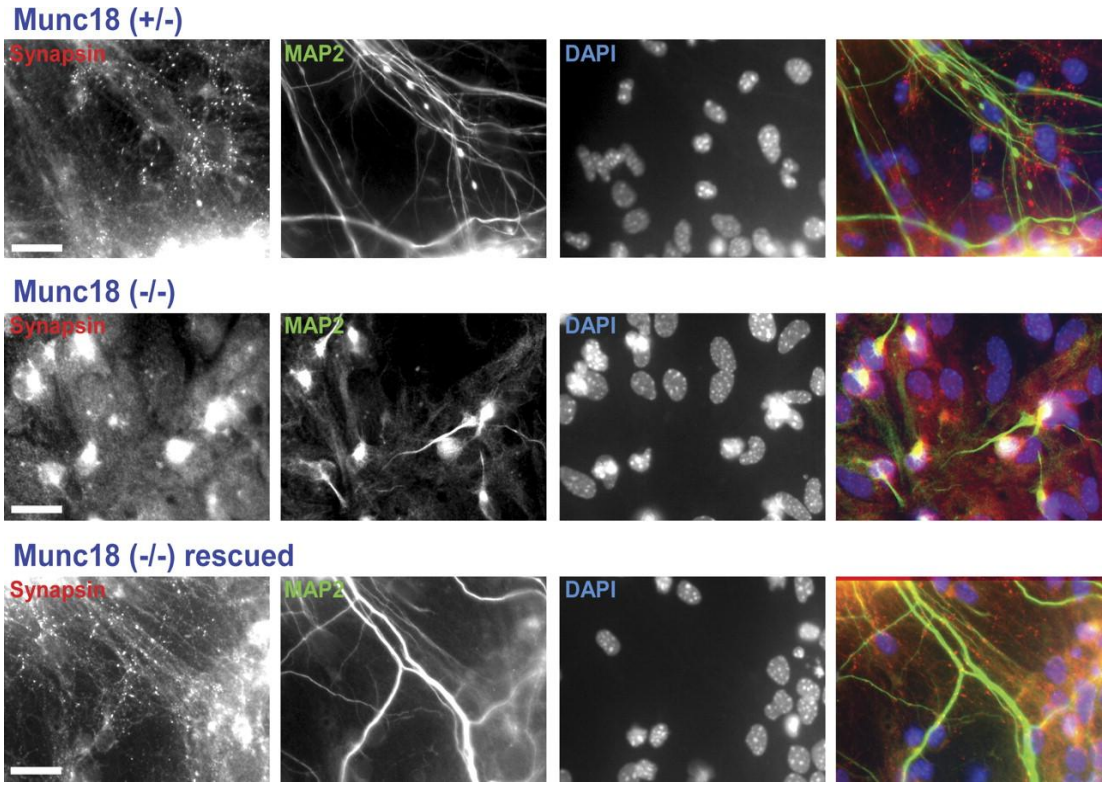

Figure 2.5

Figure 2.5 Rescue of neuronal survival in Munc18-1 knockout neurons by Munc18-1 expression.

Representative images of cortical synapses from littermate heterozygotes (upper row), homozygote knockouts for Munc18-1 (middle row) or Munc18-1 knockouts infected with Munc18-1-containing lentivirus (lower row). Cells were maintained in culture for 11 days before labeled with antibodies against the presynaptic marker synapsin (first column from the left), the neurofilament marker MAP2 (second column) and the nuclear DAPI marker (third column). The last column shows the combined image of the three labeling procedures, with colors that match the relevant labels in the other columns. Scale bars: 20 μM.

Munc18-1 with the cerulean-variant of GFP. We initially explored a C-terminal cerulean-fusion protein and three fusion proteins where cerulean was inserted into loops of Munc18-1. The three loops were chosen in exposed surface locations of Munc18-1 that, based on the crystal structure of the Munc18-1/syntaxin-1 complex (Misura *et al.* 2000), were close to syntaxin-1 (for future FRET studies in vivo) and were predicted to be able to harbor insertion of cerulean without disrupting folding and/or binding. Although no systematic studies were performed, preliminary experiments indicated that insertion of cerulean between residues 24 and 25 (referred to as Munc18-1-24-cerulean; see red star in Figure 2.1A), allowed efficient rescue of the survival and the neurotransmitter release phenotype in Munc18-1 deficient neurons (Figure 2.6), and that the rescue was better than that observed with the other fusion proteins. Therefore, we performed all of our functional experiments with this cerulean-fusion protein of Munc18-1.

We infected cultured Munc18-1 deficient neurons at DIV 1 with lentiviruses expressing wild-type or E59K, E66A, or K63E mutant Munc18-1 that was fused to cerulean. The survival and morphology of the neurons and expression levels were monitored using fluorescence microscopy at DIV 11. All Munc18-1 fusion proteins rescued neuronal survival, and there was no significant difference between the number of synapses in WT neurons and in neurons rescued with WT or mutant Munc18-1 proteins (Figure 2.7). Similar expression levels were observed for the WT and mutant Munc18-1 proteins as monitored from cerulean fluorescence intensities (Figure 2.8A), although Western blots indicated lower levels of E59K mutant (25-37% compared to WT; Figure 2.8B). The reason for this discrepancy is unclear, but these data suggest that the

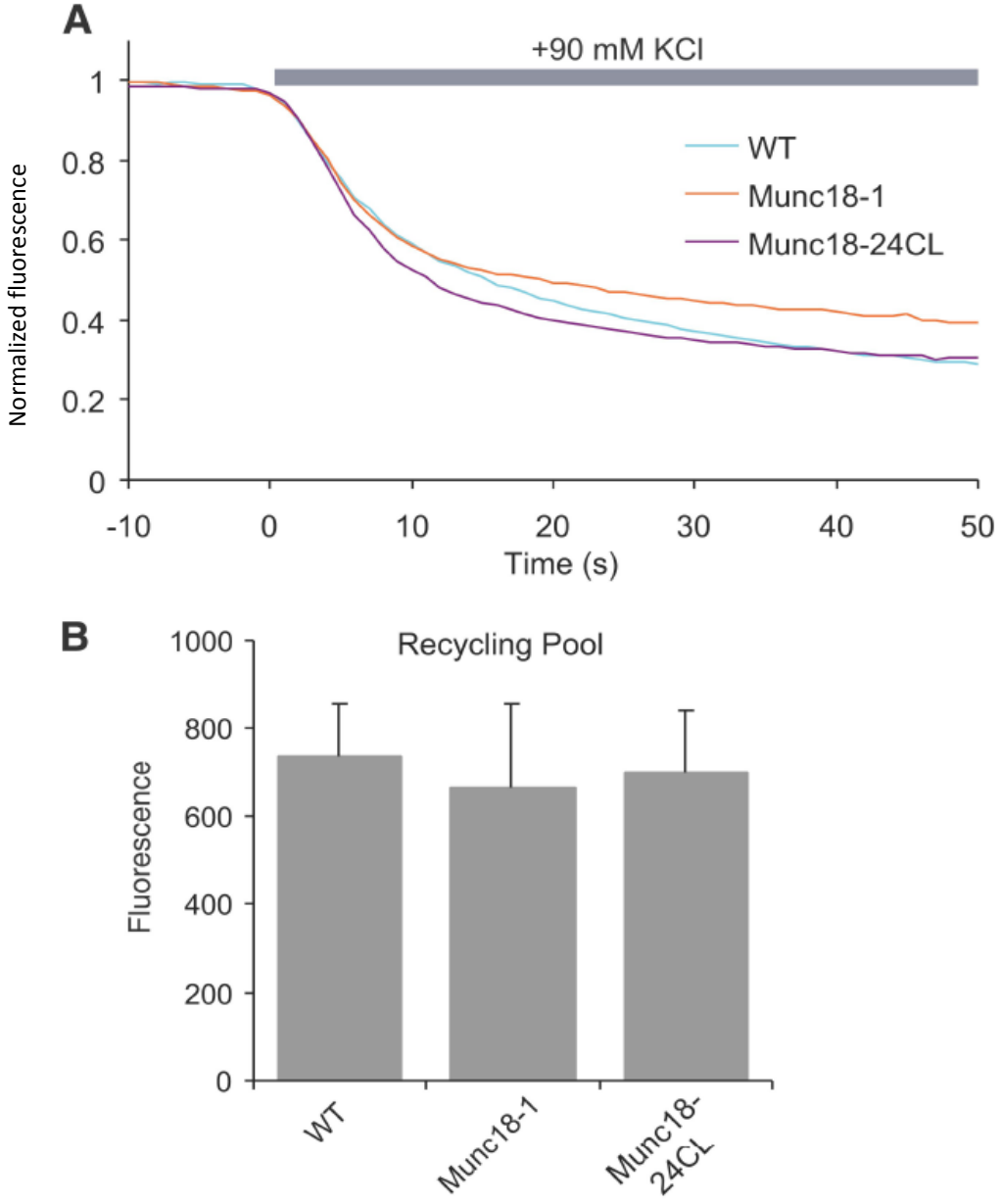
A
+90 mM KCl
Normalized fluorescence
1
0.8
0.6
0.4
0.2
0
-10
0
10
20
30
40
50
Time (s)
WT
Munc18-1
Munc18-24CL
B
Recycling Pool
Fluorescence
1000
800
600
400
200
0
WT
Munc18-1
Munc18-24CL

Figure 2.6

Figure 2.6 Comparison of calcium dependent synaptic release from WT neurons and Munc18-1 KO neurons rescued with WT Munc18-1 or Munc18-1-24-cerulean.

(A). Average destaining curves during high potassium induced depolarization. Fluorescence of FM2-10 dye was normalized to the beginning value right before the stimulation (WT control, n=9 cells; Munc18-1 rescue, n=3 cells; Munc18-1-24-cerulean rescue, n=6 cells).

(B). Bar graph depicting the average size of recycling synaptic pools for WT synapses and synapses rescued with WT Munc-18-1 or Munc18-1-24-cerulean. Same experiments as on panel (A).

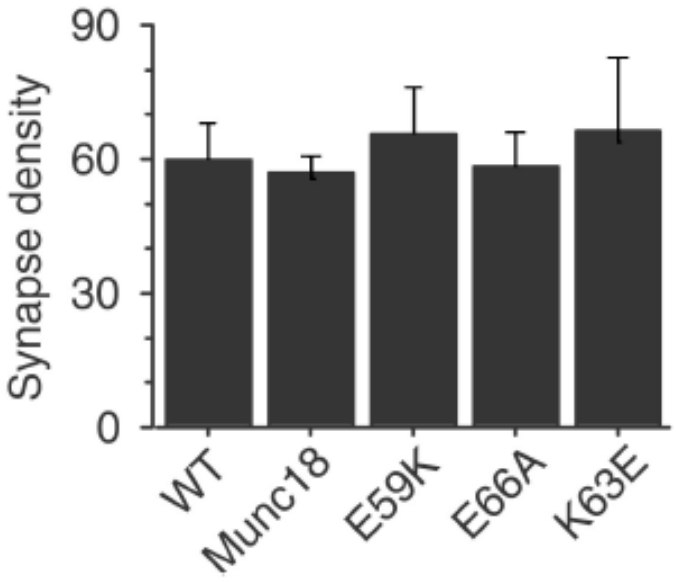

Figure 2.7

Figure 2.7 WT and mutant Munc18-1s rescued synaptic density in Munc18-1 deficient cortical cultures.

Synapses were labeled by 200 μM FM2-10 during 47 mM KCl stimulation for 90 seconds, washed and recorded. Number of synapses was estimated from 50x50 micrometer sections of fluorescence images offline. Sections (n=22-50) were analyzed from four independent cultures. Note that no difference is statistically significant.

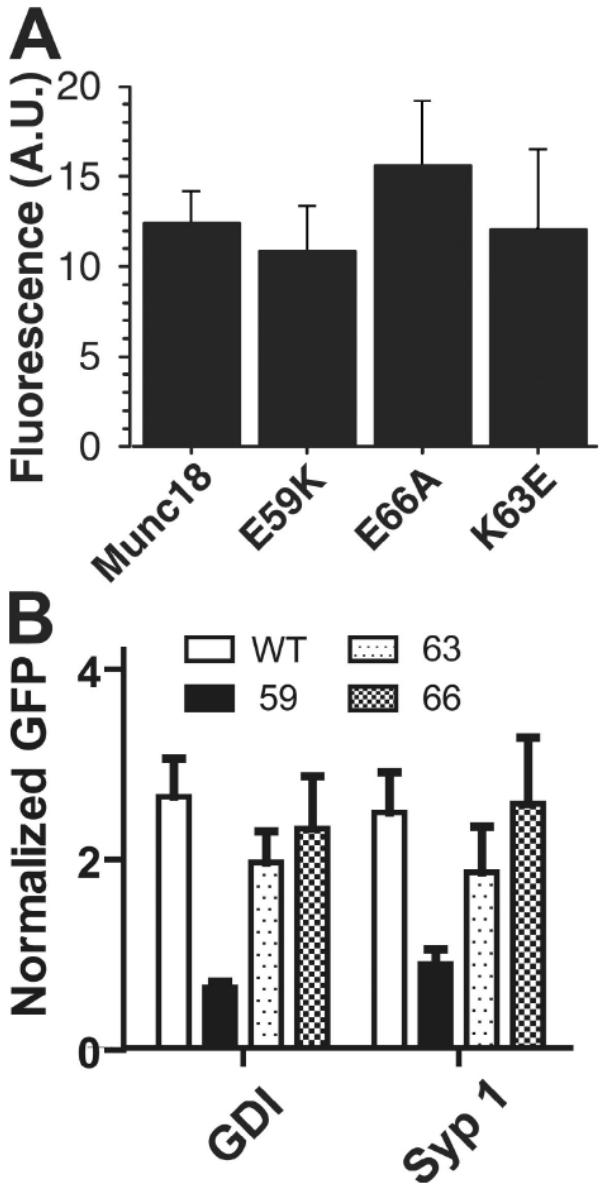
A
Fluorescence (A.U.)
20
15
10
5
0
Munc18
E59K
E66A
K63E
B
Normalized GFP
WT
63
59
66
4
2
0
GDI
Syp 1

Figure 2.8

Figure 2.8 Expression levels of WT and mutant Munc18-1s as monitored by fluorescence microscopy.

(A). Quantification by fluorescence microscopy. Fluorescence of cerulean was recorded and compared in synapses infected with WT Munc18-1–24-cerulean (n = 8) or Munc18-1–24-cerulean with the E59K (n = 6), E66A (n = 5), or K63E (n = 5) mutation. Fluorescence intensity acquired on a 200-ms acquisition time is depicted in arbitrary units (A.U.). No difference is statistically significant.

(B). Quantification from Western blots. High density hippocampal neurons from Munc18-1 KO mice were infected with WT Munc18-1–24-cerulean or Munc18-1–24-cerulean with the E59K, E66A, or K63E mutation. Cerulean levels were quantified 2–3 wk after infection by phosphoimaging of Western blots performed with GFP antibodies and iodinated secondary antibodies. The data were normalized to the levels of the general marker GDP dissociation inhibitor (GDI) or the neuronal marker Syp1, which were also quantified from Western blots of the same cultures. Data are shown as means ± SEMs.

electrophysiological results described below for this mutant need to be interpreted with caution.

Next, patch-clamp recordings were utilized to test whether the cerulean-fused WT Munc18-1 rescues neurotransmitter release in Munc18-1 knockout neurons. As expected, no evoked or spontaneous activity was observed in knockout cultures at DIV 6-7, when there are still some surviving neurons, which confirmed previous findings (Verhage *et al.* 2000), while spontaneous and evoked neurotransmitter release were restored by lentiviral expression of wild-type Munc18-1 as monitored by recordings at DIV 12-18 (Figure 2.9). Similarly, release stimulated at higher frequencies (10 Hz; Figure 2.10) or by hyperosmotic sucrose (Figure 2.11) was rescued by wild-type Munc18-1. These results showed that lentiviral expression of wild-type Munc18-1 was efficient enough to confer wild-type electrophysiological responses on Munc18-1 deficient neurons.

2.3.5 Mutations in Munc18-1 Impair Vesicle Priming

We next investigated the ability of the three mutations in Munc18-1 to rescue neurotransmitter release. We first examined spontaneous release (minis), and found that the E59K-mutation dramatically decreased the mini frequency (~90%), but had no effect on their amplitude (Figure. 2.9A,B). The E66A-mutation also significantly decreased the mini frequency (more than 60%), but to a lesser extent than the E59K-mutation, whereas the K63E-mutation had no significant effect. Hence, the impairment of spontaneous release caused by the Munc18-1 mutations mirrored the effects of these mutations on

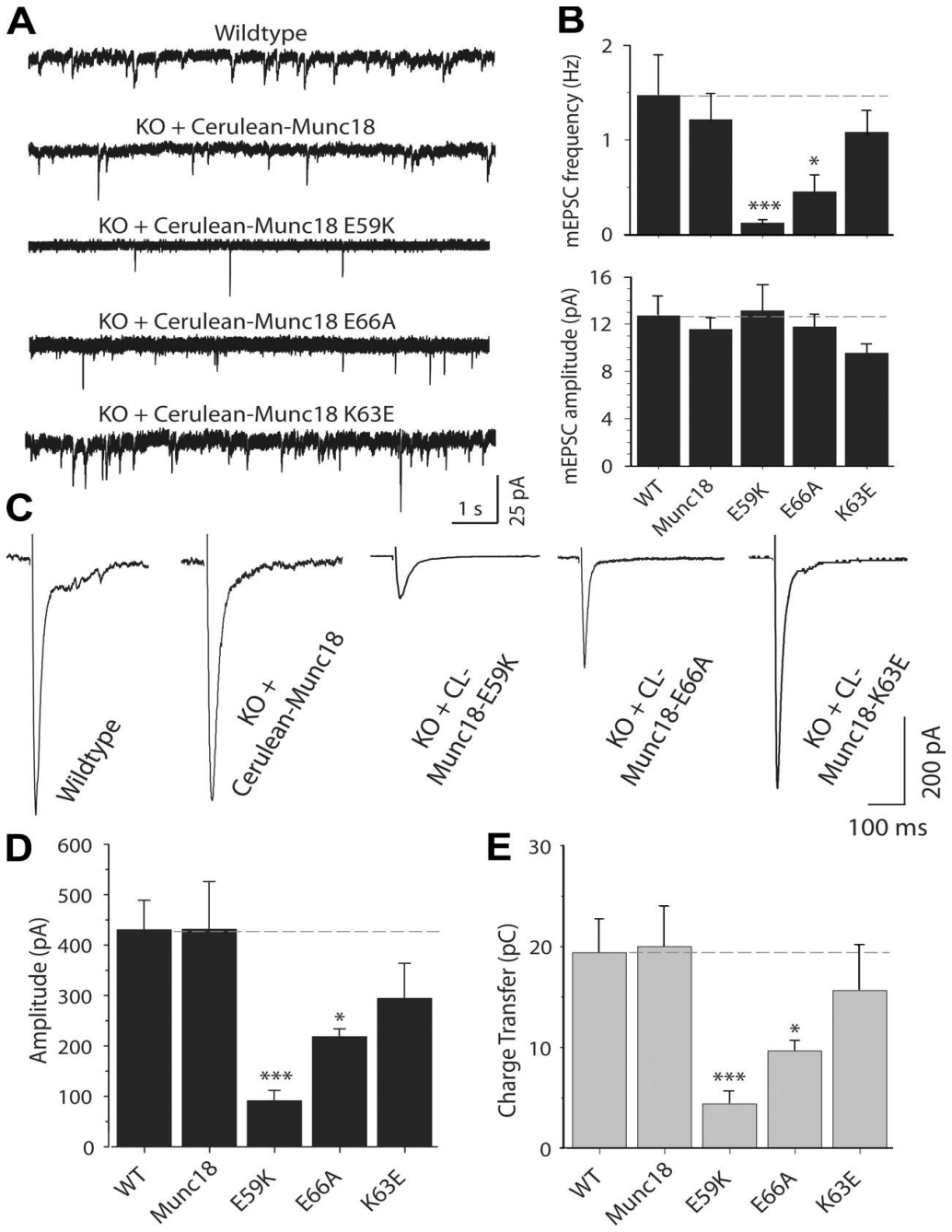
A
Wildtype
KO + Cerulean-Munc18
KO + Cerulean-Munc18 E59K
KO + Cerulean-Munc18 E66A
KO + Cerulean-Munc18 K63E
1 s
25 pA
B
mEPSC frequency (Hz)
mEPSC amplitude (pA)
WT
Munc18
E59K
E66A
K63E
C
Wildtype
KO + Cerulean-Munc18
KO + CL-Munc18-E59K
KO + CL-Munc18-E66A
KO + CL-Munc18-K63E
200 pA
100 ms
D
Amplitude (pA)
E
Charge Transfer (pC)

Figure 2.9

Figure 2.9 Synaptic release depends on Munc18-1 binding to the SNARE complex.

(A). Analysis of spontaneous synaptic release upon rescue with WT and mutant Munc18-1s. Representative ten second segments from 10 minute-long traces of spontaneous excitatory synaptic activity, recorded at a holding potential of –70 mV in the presence of 1 μM tetrodotoxin and 50 μM picrotoxin.

(B). Bar diagram describing the frequency (upper panel) and amplitude (lower panel) of spontaneous release (WT n=13; munc18 n=19, E59K n=10, K63E and E66A n=9)**.**

(C). Representative traces of field stimulation (at 0.4 Hz) evoked excitatory responses from neurons of WT (n=14) or Munc18-1 KO infected with WT (n=9), E59K (n=7), E66A (n=16) or K63E (n=11) Munc18-1-24-cerulean. Note that only the first 400 ms of the traces are shown for clarity.

(D). Bar diagram summarizing the amplitudes of evoked responses for cultures rescued with the WT Munc18-1 and different Munc18-1 mutants.

(E). Synaptic responses characterized as the amount of transferred charge. Asterisks in the bar diagrams mark statistical significance of the difference between the WT and mutant rescues (* $P < 0.05$; *** $P < 0.005$).

Munc18-1/SNARE complex binding.

We then measured the effects of the Munc18-1 mutations on evoked neurotransmitter release (Figure 2.9C-E). Again, the E59K-mutation severely impaired release (~80%). The E66A mutation caused a considerable impairment of release (50%), and the K63E mutation had no statistically significant effect, although there was a trend for less release. Note that the finding that the E66A mutation markedly impairs spontaneous and evoked release, while the K63E mutation has little or no effect, clearly correlates with the effects of these mutations on SNARE complex binding. The E59K mutant data further extends this correlation, although we cannot rule out the possibility that the disruption of release caused by this mutation arises in part from decreased protein levels.

The possible reasons for the decrease in evoked release that was caused by the mutations could be a reduction in the size of the readily-releasable pool (RRP) of vesicles, and/or in the vesicular release probability. To distinguish between these possibilities, we first analyzed release probability in evoked responses at 10 Hz stimulation frequency. In these experiments, a reduced release probability is expected to lead to synaptic facilitation. The effects of the mutations on the amplitude of the first response of the train paralleled those observed at low frequency stimulation but, importantly, all mutants exhibited strong synaptic depression during the stimulus train (Figure 2.10). Then we determined the size of the RRP by measuring synaptic response to 0.5 M hypertonic sucrose. We found that the E59K-mutation decreased the size of the RRP dramatically (~76% decrease), whereas the E66A mutation had a smaller effect (~50% decrease). And

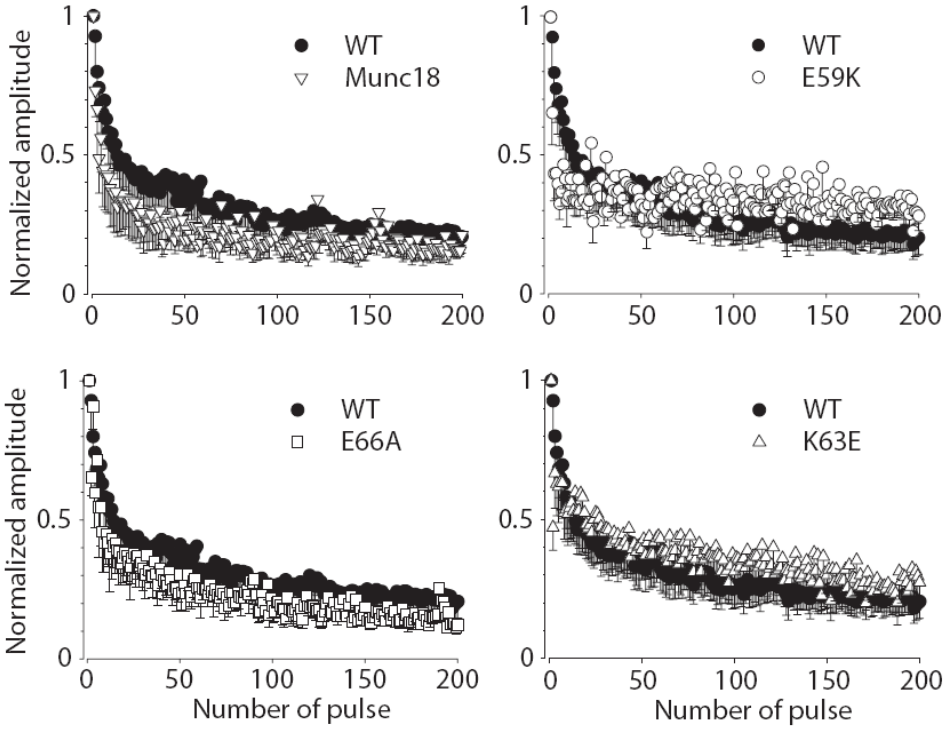

Figure 2.10

Figure 2.10 Synaptic depression with Munc18 mutants.

Relative evoked current amplitudes during 10 Hz field stimulation. Evoked postsynaptic excitatory currents were normalized to the amplitude of the first response in the train (WT n=8, Munc18 and E59K n=5; E66A n=4 and K63E n=3). Note the strong synaptic depression for all Munc18-1 variants tested.

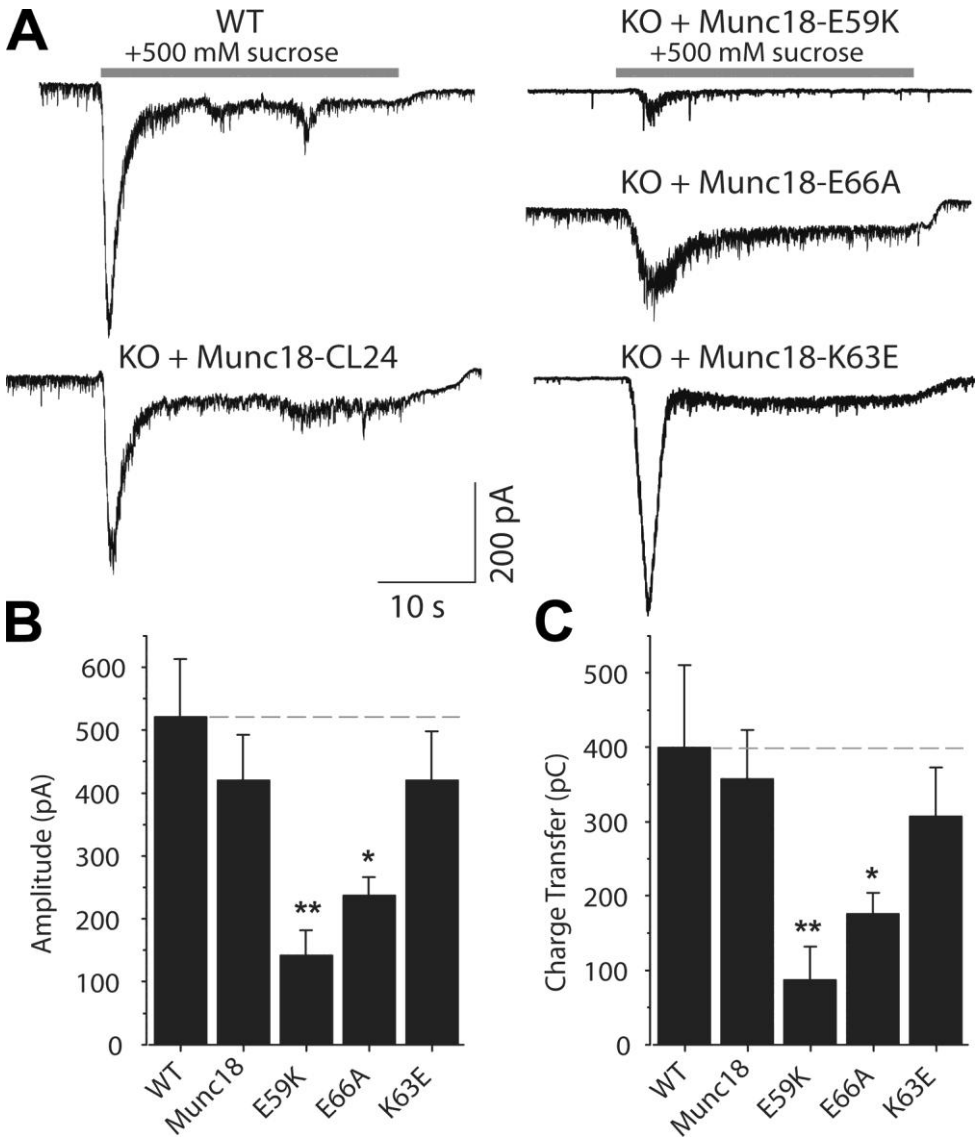
A
WT
+500 mM sucrose
KO + Munc18-E59K
+500 mM sucrose
KO + Munc18-E66A
KO + Munc18-CL24
KO + Munc18-K63E
200 pA
10 s
B
Amplitude (pA)
600
500
400
300
200
100
0
**
*
WT
Munc18
E59K
E66A
K63E
C
Charge Transfer (pC)
500
400
300
200
100
0
**
*
WT
Munc18
E59K
E66A
K63E

Figure 2.11

Figure 2.11 Munc18-1 binding to the SNARE complex is critical for release readiness of synaptic vesicles.

(A). Representative traces of synaptic excitatory responses to hypertonic solution (+500 mM sucrose to the bath) in WT neurons from littermate controls and Munc18-1 KO neurons rescued with lentivirus expressing WT Munc18-1-24 cerulean or Munc18-1-24-cerulean with the E59K, K63E or E66A mutations.

(B). Bar diagram depicting the amplitudes of responses to hypertonic sucrose solution for WT cultures or Munc18-1 knockout cultures rescued with the WT and mutant Munc18-1s (WT n=5; Munc18-1, K63E and E66A n=8; E59K n=5).

(C). Readily releasable synaptic excitatory transmission characterized as the amount of charge transfer induced by hypertonic sucrose. Asterisks in the bar diagrams mark statistical significance of the difference between the WT and mutant rescues (* $P < 0.05$; ** $P < 0.01$).

the K63E mutation caused no significant effect (Figure 2.11). Thus, the effects of the mutations on the RRP were parallel with those observed in the spontaneous and evoked responses (Figure 2.9), as well as in the Munc18-1/SNARE complex binding assays (Figure 2.4). Correspondingly, the ratio between the synaptic charge transfer in evoked release (Figure 2.9E) and the sucrose-induced charge transfer (Figure 2.11C) was very similar for the WT and mutant Munc18-1 rescue (Figure 2.12), suggesting that, for the vesicles that are primed, Ca^{2+} triggering of fusion is normal. These results showed that the impairment in release caused by the Munc18-1 mutations occurs at the synaptic vesicle priming step and suggest that the interaction of Munc18-1 with the Habc domain in open syntaxin-1 is critical for this step but not for the downstream events that lead to release.

2.3.6 A Munc18-1/SNARE/Complexin Macromolecular Assembly

A fundamental question to understand the mechanism of Munc18-1 in neurotransmitter release is to characterize the relation between its interaction with SNARE complex and other binding modes (Südhof 2004; Brunger 2005). Does Munc18-1 only participate in the vesicle priming step? Or is Munc18-1 crucial for all states that lead to neurotransmitter release? Complexins function at the Ca^{2+}-triggering step of release (Reim *et al.* 2001) and they are generally believed to be bound to the SNARE complex before Ca^{2+} influx (Rizo and Rosenmund 2008). If Munc18-1 and complexin can bind simultaneously to the SNARE complex, this finding would suggest that Munc18-1 is bound to the SNAREs within the release-ready state that results after vesicle

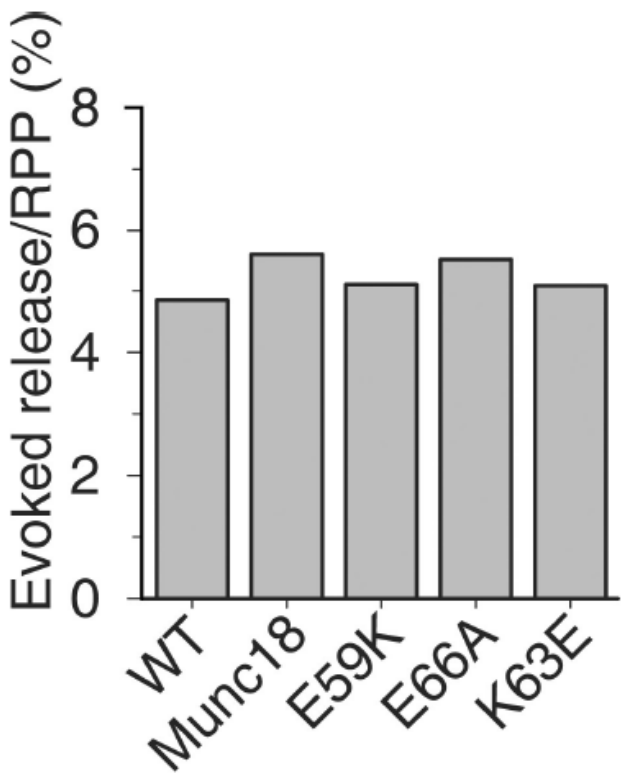

Figure 2.12

Figure 2.12 The Munc18-1 mutations cause parallel decreases in evoked release and RRP.

The bar diagram shows the ratios between the mean synaptic charge transfer with a single action potential (Figure 2.9E) and the mean synaptic charge transfer caused by hypertonic sucrose (Figure 2.12 C) in WT neurons and Munc18-1 KO neurons rescued with the WT Munc18-1–24-cerulean or Munc18-1–24-cerulean bearing the E59K, K63E, or E66A mutation.

priming.

To address this question, I first used the same 1D ^{13}C-edited ^{1}H-NMR assays (Arac *et al.* 2003; Dulubova *et al.* 2005) as the previous NMR experiments (Figure 2.4). Thus, the SMR intensity of 1D ^{13}C-edited ^{1}H-NMR spectra of 2 μM Munc18-1 (65kDa) was considerably reduced in the presence of 2 μM unlabeled SNARE complex (55 kDa), revealing formation of the Munc18-1/SNARE complex assembly as expected (Figure 2.13A). If complexin (16 kDa) bound simultaneously to the Munc18-1/SNARE complex assembly, the SMR intensity of Munc18-1 would have no change or even exhibit a further decrease. If complexin displaced Munc18-1 from the SNARE complex, the SMR intensity would have been restored to that of isolated Munc18-1. When I added 2 μM ^{15}N-labeled complexin-1 (16 kDa) to the mixture of 2 μM Munc18-1 and 2 μM SNARE complex, the SMR intensity of Munc18-1 dropped a little bit more (Figure 2.13A), which can be attributed to binding of complexin-1 to the Munc18-1/SNARE complex assembly. The formation of a Munc18-1/SNARE complex/complexin macromolecular assembly was confirmed by 1D ^{15}N-edited ^{1}H-NMR spectra of 2 μM ^{15}N-labeled complexin-1 (Figure 2.13B). Many complexin-1 signals in these spectra are broadened beyond detection upon SNARE complex binding and are still not observable upon addition of Munc18-1, showing that Munc18-1 does not displace complexin-1 from the SNARE complex. Signals that remain observable correspond to the flexible regions in complexin-1, regardless of the presence or absence of Munc18-1. Note in particular that the spectra containing ^{13}C-labeled Munc18-1, unlabeled SNARE complex and ^{15}N-labeled complexin-1 (right panels in Figure 2.13A, B) was acquired on the same sample and

unambiguously demonstrate that Munc18-1 and complexin-1 can bind simultaneously to the SNARE complex.

To confirm this conclusion by a different method, I used gel filtration experiments (Figure 2.14). Molecules are separated on gel-filtration chromatography, based on their molecular mass or, more precisely, their Stokes radius. A mixture of complexin-1 and SNARE complex co-eluted earlier than those of separate samples of complexin-1 and SNARE complex, as expected from the high affinity of their interaction (McMahon *et al.* 1995). Similar results were obtained with samples of Munc18-1 and SNARE complex, as described earlier (Dulubova *et al.* 2007). Importantly, in the presence of complexin-1, Munc18-1/SNARE complex assembly eluted even faster and co-eluted at smaller volumes (Figure 2.14A), reflecting that complexin-1 binds to this assembly. It is worth noting that the elution of the SNARE complex is shifted to smaller volumes by complexin-1 than by Munc18-1 despite the much smaller size of complexin-1. This difference can be attributed, first, to the formation of a more compact structure in the SNARE complex and Munc18-1 due to interactions of Munc18-1 with both the four-helix bundle and the N-terminal region of syntaxin-1 (Dulubova *et al.* 2007), and second, to the fact that complexin-1 contains large unfolded regions even after SNARE complex binding (Pabst *et al.* 2000). To rule out the possibility that the co-elution of Munc18-1 with complexin-1 and the SNARE complex came out faster might arise from binding of Munc18-1 to these unfolded regions of complexin-1, I performed additional gel filtration experiments with a shorter complexin-1 fragment (residues 26-83). Upon SNARE complex binding, this region becomes structured (Pabst *et al.* 2000; Chen *et al.* 2002).

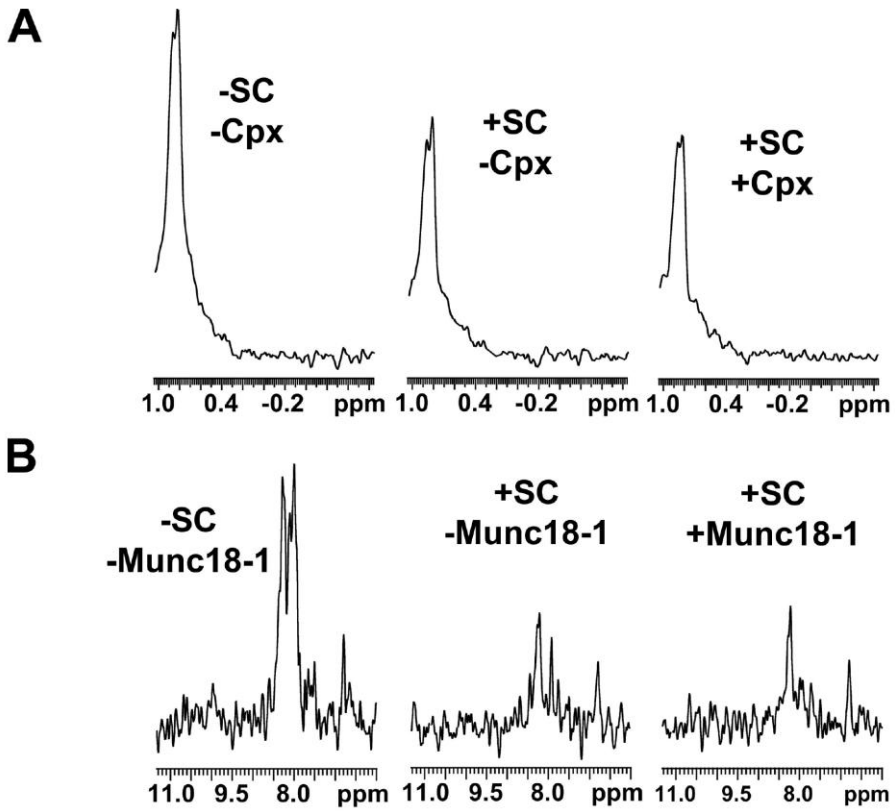

Figure 2.13

Figure 2.13 Munc18-1 and complexin-1 bind simultaneously to the SNARE complex.

(A). Sample traces of the methyl regions of 1D ^{13}C-edited ^{1}H-NMR spectra of 2 μM Munc18-1 in the absence or presence of 2 μM unlabeled SNARE complex or 2 μM unlabeled SNARE complex plus 2 μM ^{15}N-labeled complexin-1.

(B). Sample traces of 1D ^{15}N-edited ^{1}H-NMR spectra of 2 μM ^{15}N-labeled complexin-1 in the absence or presence of 2 μM unlabeled SNARE complex or 2 μM unlabeled SNARE complex plus 2 μM ^{13}C-labeled Munc18-1. The spectra on the right of panels (A) and (B) were acquired with the same sample.

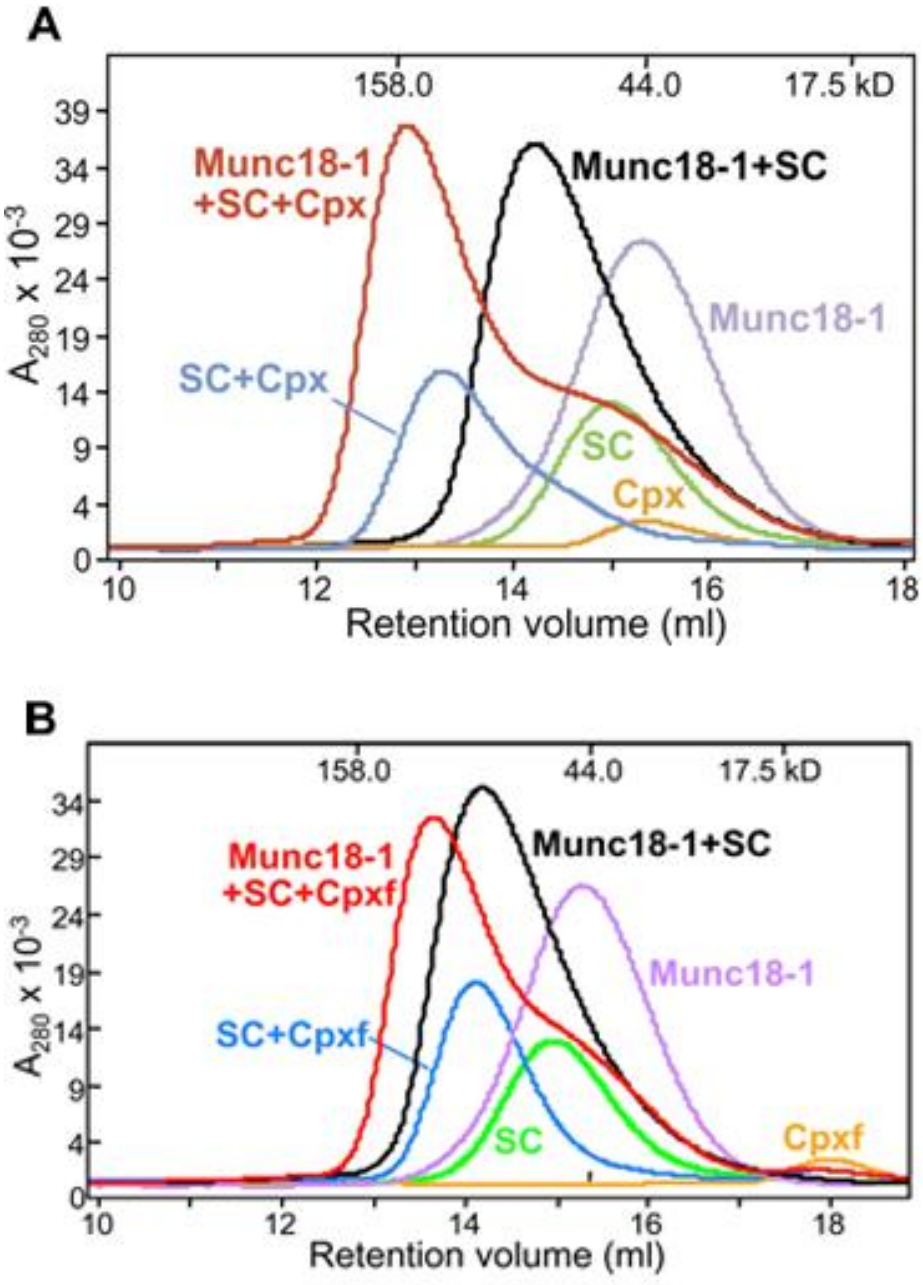
A
158.0
44.0
17.5 kD
Munc18-1
+SC+Cpx
Munc18-1+SC
Munc18-1
SC+Cpx
SC
Cpx
A280 x 10-3
Retention volume (ml)
B
158.0
44.0
17.5 kD
Munc18-1
+SC+Cpxf
Munc18-1+SC
Munc18-1
SC+Cpxf
SC
Cpxf
A280 x 10-3
Retention volume (ml)

Figure 2.14

Figure 2.14 Munc18-1 and complexin-1 can bind simultaneously to the SNARE complex.

Gel filtration on Superdex S200 (10/300GL) of Munc18-1, complexin-1, SNARE complex, and mixtures of the SNARE complex with Munc18-1, complexin (A) or complexin-1(26-83) (labeled Cpxf, B), or both. The SNARE complexes used for all these experiments contained Syx(2-253), Syb(29-93), SNN and SNC.

Analogous results were obtained with this fragment (Figure 2.14B), confirming again the formation of a Munc18-1/SNARE/complexin assembly.

2.4 Discussion

The importance of Munc18-1 and the SNAREs for neurotransmitter release is well established, but it is still unclear how their functions are coupled. The binary interaction initially identified between Munc18-1 and the closed conformation of syntaxin-1 (Hata *et al.* 1993; Dulubova *et al.* 1999), which stabilizes both proteins and gates the entry of syntaxin-1 into SNARE complexes (Verhage *et al.* 2000; Gerber *et al.* 2008), does not appear to be general and may have emerged to meet specific requirements of regulated secretion. Munc18-1 binding to SNARE complexes containing open syntaxin-1 does seem to be universal (Dulubova *et al.* 2007; Shen *et al.* 2007; Rodkey *et al.* 2008), and functional data provided evidence for the physiological relevance of SM-protein/SNARE complex interactions in diverse systems (Carr *et al.* 1999; Grote *et al.* 2000; Yamaguchi *et al.* 2002; Collins *et al.* 2005; Khvotchev *et al.* 2007; Shen *et al.* 2007). However, the point of action of Munc18-1/open syntaxin-1 interactions in release was unknown, and the relation between these interactions and those of the SNAREs with other key proteins such as complexins was unclear. Our data now provide fundamental insights into these questions, showing that binding of Munc18-1 to the Habc domain of open syntaxin-1 is critical for synaptic vesicle priming but not for the release step, and that Munc18-1 and complexin-1 can bind simultaneously to the SNARE complex.

The development of a strategy to rescue survival and neurotransmitter release in neurons from Munc18-1 knockout mice, which is strongly hindered by the deleterious effects arising from deletion of this protein, was key for this study. In addition, we wanted to perform the rescue with fluorescently tagged Munc18-1 to ensure that we could monitor the proper localization of the expressed protein. After extensive efforts, we overcame these difficulties by identifying a Munc18-1/cerulean fusion that rescues the Munc18-1 deficiency phenotype when expressed with a lentivirus, which allowed us to study the functional effects of the three Munc18-1 mutations with the precision of electrophysiology, and correlate them with our in vitro binding data.

Although the energetic contributions of individual residues to protein-protein interactions are difficult to predict from three-dimensional structures, the observed biochemical effects of the Munc18-1 mutations can be rationalized according to general knowledge on the energetics of protein-protein interactions and to the model used to design these mutations. In this model, the syntaxin-1 SNARE motif contributes strongly to the binary interaction with Munc18-1, but needs to be released upon formation of the Munc18-1/SNARE complex assembly, leading to a different interaction of Munc18-1 with the four-helix bundle (Figure 2.15A). In contrast, the Habc domain-Munc18-1 interface is likely similar in both complexes (Khvotchev *et al*. 2007). The latter assumption implies that, in the Munc18-1/SNARE complex assembly, E59 contacts the Habc domain extensively, E66 makes fewer contacts, and K63 does not interact with the Habc domain (in the binary complex E66 is between the Habc domain and the SNARE motif, while K63 only contacts the SNARE motif; Figure 2.1); this prediction correlates

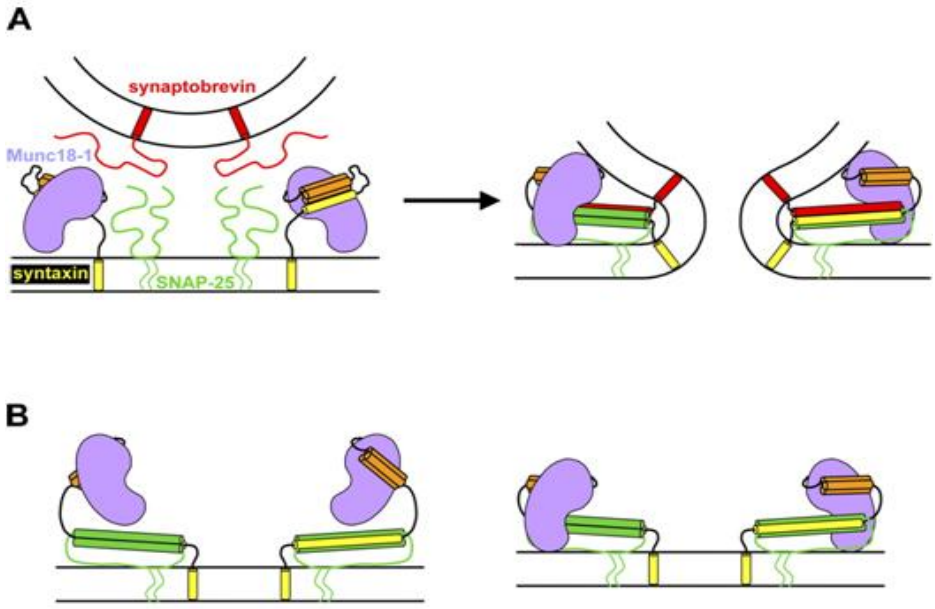

Figure 2.15

Figure 2.15 Models of potential interactions between Munc18-1 and SNAREs.

(A). Diagrams of the binary complex between Munc18-1 and closed syntaxin-1 (left) and the Munc18-1/SNARE complex assembly (right). Munc18-1 is purple, synaptobrevin is red, SNAP-25 is green and syntaxin-1 is orange (Habc domain) and yellow (SNARE motif and transmembrane region). The model of the binary complex is based on its crystal structure (Misura *et al.* 2000; Burkhardt *et al.* 2008). The model of the Munc18-1/SNARE complex assemblies is based on NMR data suggesting a multifaceted interaction (Rizo *et al.* 2006; Dulubova *et al.* 2007).

(B). Models of potential interactions between Munc18-1 and open syntaxin-1 within syntaxin-1/SNAP-25 heterodimers. The model on the left is based on the finding that Munc18-1 can bind to the isolated syntaxin-1 N-terminal region (Khvotchev et al., 2007;Burkhardt et al., 2008), while the model on the right incorporates, in addition, interactions with the SNARE motifs (Weninger *et al.* 2008).

very well with the relative impairments in Munc18-1/SNARE complex binding caused by the E59K and E66A mutations, and the lack of an effect by the K63E mutation. A key prediction of the model was that, because of the proximity of E59, K63 and E66 to the Habc domain-SNARE motif interface in the binary Munc18-1/syntaxin-1 complex, and because of the large rearrangement of the syntaxin-1 SNARE motif upon formation of the Munc18-1/SNARE complex assembly, the energetic contributions of these residues to binding would be different in the two complexes. The different effects of the mutations on the binary Munc18-1/syntaxin-1 interaction compared to those caused on Munc18-1/SNARE complex binding agree with this prediction. It is not surprising that none of the mutations strongly reduced Munc18-1 binding to syntaxin-1, given the adaptability of protein-protein interfaces upon introduction of point mutations (Atwell *et al.* 1997), particularly for complexes of high affinity and involving large interfaces such as that in the Munc18-1/syntaxin-1 complex [more than 4,000 Å of buried surface area; see (Misura *et al.* 2000; Burkhardt *et al.* 2008)]. Although not reaching statistical significance, the K63E mutation did appear to have an effect on Munc18-1/syntaxin-1 binding, consistent with the notion that interactions with the SNARE motif contribute strongly to the affinity of the binary complex; such contribution likely facilitates toleration of the E59K and E66A mutations.

The considerable impairment of Ca^{2+}-evoked, sucrose-induced and spontaneous release caused by the E66A mutation, and the little functional consequences of the K63E mutation (Figures 2.9, 2.11), correlate very well with the effects of these mutations on binding of Munc18-1 to SNARE complexes containing open syntaxin-1, but not with

their effects on binding of Munc18-1 to closed syntaxin-1 (Figure 2.2). Although the functional data obtained for the E59K mutant needs to be interpreted with caution, the data appear to extend the correlation between impairment of release and disruption of Munc18-1/SNARE complex binding, but not Munc18-1/syntaxin-1 binding. Note that the expression of this mutant is sufficient to rescue survival in Munc18-1 KO neurons, and that decreased Munc18-1 levels in syntaxin-1B LE mutant mice lead to a much more moderate decrease in the RRP (Gerber *et al.* 2008) than that caused by the E59K mutation (Figure 2.11C). Hence, it seems likely that the strong impairment of release caused by this mutation arises at least in part from disruption of the interaction between Munc18-1 and open syntaxin-1. Importantly, the decreases in spontaneous and Ca^{2+}-evoked release caused by the E66A and E59K mutations mirror the corresponding RRP reductions. This finding is in sharp contrast with the phenotype observed in the syntaxin-1 LE mutant mice, where the RRP decreased (likely because of the lower protein levels), but spontaneous release and release of primed vesicles were enhanced (Gerber *et al.* 2008). Since the LE mutation impairs Munc18-1 binding to closed syntaxin-1 but not to SNARE complexes (Gerber *et al.* 2008), this contrast further supports the conclusion that the functional effects of the E66A and E59K mutations arise from disruption of interactions of Munc18-1 with open syntaxin-1, rather than closed syntaxin-1.

Synaptic vesicle docking was not affected in Munc18-1 knockout mice (Verhage *et al.* 2000). Hence, it is unlikely that the E66A and E59K mutations alter docking. This observation, together with the finding that these mutations cause parallel decreases in spontaneous, sucrose-induced and Ca^{2+}-triggered release, resulting in evoked release/RRP

ratios that are similar to WT (Figure 2.12), strongly suggest that the mutations selectively disrupt synaptic vesicle priming, but not the downstream events that lead to evoked release. Immediate questions that arise are: do Munc18-1/SNARE interactions play any role after priming? And, does Munc18-1 form part of the macromolecular complex that results after priming and is poised for Ca^{2+}-triggered release? As a first step to address these questions, we examined whether complexin-1 and Munc18-1 compete for SNARE complex binding. Complexins play a role in the Ca^{2+}-triggering step of release (Reim *et al.* 2001) and bind tightly to SNARE complexes (McMahon *et al.* 1995), interacting with the SNARE four-helix bundle (Chen *et al.* 2002). These observations strongly suggest that complexins are key components of the primed macromolecular assembly that is ready for release (Rizo and Rosenmund 2008), and our demonstration that Munc18-1 and complexin-1 can bind simultaneously to the SNARE complex suggest that Munc18-1 likely forms part of this assembly as well. Structural studies will be required to characterize in detail the resulting Munc18-1/SNARE/complexin assembly, but it is noteworthy that Munc18-1 binding barely shifts the elution profile of the complexin-1-SNARE complex despite doubling its molecular mass (Figure 2.14). This observation suggests that such binding leads to a more compact shape due to interactions of Munc18-1 with both the N-terminal region of syntaxin-1 and the four-helix bundle, as proposed for the Munc18-1/SNARE complex assembly (Dulubova *et al.* 2007) (Figure 2.15A, right panel).

In contrast, a recent study concluded that binding of Munc18-1 to the SNARE complex involves interactions with only the syntaxin-1 N-terminal region (residues 1-

179), based on the similar affinities of Munc18-1 for the SNARE complex and Syx(1-179) (Burkhardt *et al.* 2008). However, this conclusion ignores the possibility that the energy gained from Munc18-1/four-helix bundle interactions may be offset by release of interactions contributing to the affinity of Munc18-1 for Syx(1-179) (e.g. involving the syntaxin-1 linker region), and abundant evidence has demonstrated interactions of Munc18-1 with the SNARE motifs (Dulubova *et al.* 2007; Shen *et al.* 2007; Rodkey *et al.* 2008; Weninger *et al.* 2008). Nevertheless, the similar affinities suggest that there is little cooperativity between interactions of Munc18-1 with the four-helix bundle and the syntaxin-1 N-terminal region. Conversely, Munc18-1/membrane interactions seem to cooperate with binding to the four-helix bundle, as the syntaxin-1 N-terminal region is required for binding of Munc18-1 to soluble SNARE complexes, but not for binding to membrane-anchored SNARE complexes (Shen *et al.* 2007).

These observations, together with our data, suggest a model whereby synaptic vesicle priming involves opening of syntaxin-1, and binding of Munc18-1 to the syntaxin-1 Habc domain is critical for the opening reaction, but not for downstream events leading to release. In this model, transition from the Munc18-1/closed syntaxin-1 complex to the Munc18-1/SNARE complex assembly (Figure 2.15A) involves a series of intermediate states. Thus, release of the SNARE motif from closed syntaxin-1 to bind to SNAP-25 [likely assisted by Munc13-1 (Guan *et al.* 2008; Weninger *et al.* 2008)] may involve a transient state where Munc18-1 is only interacting with the syntaxin-1 N-terminal region (Figure 2.15B, left panel). This interaction might keep Munc18-1 near the site of action to facilitate the establishment of new interactions with the syntaxin-

1/SNAP-25 SNARE motifs (Figure 2.15B, right panel), forming an acceptor complex for synaptobrevin binding. The resulting Munc18-1/SNARE complex assembly (Figure 2.15A, right panel) may involve cooperative interactions of Munc18-1 with the four-helix bundle and one or both membranes, which might be key for membrane fusion but might shift the energetic balance so that the interactions of Munc18-1 with the syntaxin-1 N-terminal region become dispensable. These features can explain why binding of Munc18-1 to the Habc domain of open syntaxin-1 is crucial for priming but not for the downstream events leading to fusion. The existence of the proposed intermediate states is supported by the finding that Munc18-1 can bind to isolated syntaxin-1 N-terminal fragments (Khvotchev *et al.* 2007; Burkhardt *et al.* 2008) and to syntaxin-1-SNAP-25 heterodimers (Guan *et al.* 2008; Weninger *et al.* 2008). The hypothesis that Munc18-1 binds to the four-helix bundle and the two apposed membranes correlates with the role proposed for the HOPS complex (which includes the Munc18-1 homologue Vps33p) in discriminating trans from *cis*-SNARE complexes in yeast vacuolar fusion (Starai *et al.* 2008). Our model is also consistent with evidence suggesting that Munc18-1 plays multiple roles in the different steps that lead to release (Gulyás-Kovács *et al.* 2007), but, clearly, further research will be required to test this model and to elucidate how the function of Munc18-1 is coupled to those of other SNARE-binding proteins such as complexins, Munc13s and synaptotagmin-1.

Chapter 3 Binding of Munc18-1 to Synaptobrevin and to the SNARE Four-Helix Bundle

3.1 Introduction

SNAREs proteins play an essential role in mediating membrane fusion as discussed in chapter one. Munc18-1, which is also crucial for accurate docking, priming, and fusion steps of neurotransmitter release, binds both closed syntaxin-1 in isolation and open syxtaxin-1 in the SNARE complex (Hata *et al.* 1993; Dulubova *et al.* 2007; Carr and Rizo 2010). Several lines of evidence suggest that formation of Munc18-1-SNARE complex assemblies might underlie the key functional importance of SM proteins, as predicted in a model in which the core fusion machinery is formed by SM protein-SNARE complex assemblies rather than SNARE complexes alone (Rizo *et al.* 2006; Dulubova *et al.* 2007). The model predicted a direct role for Munc18-1 in membrane fusion (Rizo and Südhof 2002). It emerged from the realization that Munc18-1-SNARE complex assemblies might be much more efficient than SNARE complexes alone in exerting mechanical force on the membranes to induce fusion (Rizo *et al.* 2006). Munc18-1 binding to the four-helix bundle formed by the SNARE motifs of syntaxin-1, SNAP-25, and synaptobrevin (below termed the SNARE four-helix bundle or mcc) is a central aspect of this model. Some data suggested that Munc18-1 indeed binds to the SNARE four-helix bundle (Dulubova *et al.* 2007; Shen *et al.* 2007), and the stimulation of SNARE-dependent lipid mixing caused by Munc18-1 in reconstitution assays appeared to depend on Munc18-1-synaptobrevin interactions (Shen *et al.* 2007). However,

there was no direct evidence showing Munc18-1 binds to synaptobrevin in this study. Hence, it is still unclear whether Munc18-1 indeed binds to synaptobrevin and to the SNARE four-helix bundle, and what is the importance of these kinds of binding.

To address these questions, I used a combination of biophysical and biochemical approaches including fluorescence resonance energy transfer (FRET) assays, isothermal titration calorimetry (ITC), ^{1}H-^{15}N heteronuclear single quantum coherence (HSQC), and chemical cross-linking. We demonstrate that Munc18-1 binds directly to the SNARE motif of synaptobrevin and to the SNARE four-helix bundle with an affinity in the low micromolar range. Our data suggest that these interactions involve the same cavity of Munc18-1 involved in binding to the syntaxin-1 closed conformation and map the Munc18-1 binding site on synaptobrevin to the very C-terminus of its SNARE motif. These results suggest that synaptobrevin binding places Munc18-1 right at the site of membrane fusion and that Munc18-1 may indeed have a direct role in fusion in cooperation with the SNAREs.

3.2 Material and Methods

3.2.1 Recombinant Protein DNA Constructs

Bacterial expression vectors to express full-length rat Munc18-1, rat syntaxin-1A(2-253), rat syntaxin-1A(2-180), and to the SNARE motifs of syntaxin-1A(191-253), rat synaptobrevin-2(29-93, 29-96, 49-96 or 1-96), and human SNAP-25(11-82 and 141-203) as GST-fusion proteins were available in the lab. These constructs were made by

Evghenii Kovrigin, a former postdoctoral fellow in our laboratory. A vector to express full-length squid Munc18-1 as a His-tagged protein was a gift from W. Weissenhorn laboratory (Bracher *et al.* 2000).

Mutations of Munc18-1(K125C and K308C), syntaxin-1A(2-253)(D27C), synaptobrevin(1-96)(S61C), synaptobrevin(29-96)(S61C), and synaptobrevin(29-96)(S61C) were generated from the WT constructs using the QuickChange site-directed mutagenesis kit (Stratagene) and custom designed primers, and verified by sequencing.

3.2.2 Protein Expression and Purification

The expression and purification for recombinant proteins were similar to those described in the previous chapter.

3.2.3 Assembly and Purification of SNARE four-helix Bundles and SNARE Complexes

Minimal core complexes were formed with the four SNARE motifs, including syntaxin-1A(191-253), synaptobrevin(29-93 or 1-96), SNAP-25(11-82), SNAP-25(141-203), by overnight incubation at 4 ℃. The molar ratio of the four fragments is 1:1:1:1. The assembled mini-core complexes were purified by extensive concentration/dilution with a Millipore concentrator (10 kDa cutoff) to remove unassembled fragments.

In the case of SNARE complexes using syntaxin-1A(2-253), SNARE complexes were assembled using about 40-50 μM syntaxin-1A(2-253) and about 1.5 molar excess of

all the other SNAREs. The assembled SNARE complexes were purified from unassembled fragments by ion-exchange chromatography on Source Q column followed by size-exclusion chromatography on S200 Superdex column. Note that the complexes are SDS resistant, the purity of complexes was judged by SDS-PAGE and Coomassie blue staining.

3.2.4 Isothermal Titration Calorimetry (ITC) Experiments

ITC experiments were performed using a VP-ITC (MicroCal, Northhampton, MA) calorimeter at 20 ℃. Squid Munc18 and synaptobrevin(49-96) or synaptobrevin(77-96) were dialyzed in 20 mM HEPES (pH 7.4) and 100 mM KCl. The titration of synaptobrevin(49-96) or synaptobrevin(77-96) with squid Munc18 was performed by 35×8 μl injections of 0.4mM synaptobrevin(49-96) or 0.5 mM synaptobrevin(77-96) solution at 3-min intervals into a 1.8 ml sample cell containing 20 μM squid Munc18. The data were fitted with a nonlinear least squares routine using a single-site binding model with MicroCal Origin^{TM} software for ITC version 5.0.

3.2.5 Fluorescence Resonance Energy Transfer (FRET) Assays

Single cysteine mutations of Munc18-1(K125C and K308C) were purified and labeled with *N*-(2-aminoethyl) maleimide BODIPY-FL (Molecular Probes) as a donor fluorescence probe in 20 mM HEPES (pH 7.4) and 100 mM KCl. Specific labeling of residue 125 or 308 was verified by trypsin digestion followed by mass spectrometry (MS). Synaptobrevin(1-96)(S61C) was labeled with tetramethylrhodamine-5-iodoacetamide

dihydroiodide (Molecular Probes) as a fluorescence acceptor probe. Syntaxin-1A(2-253 D27C C145S) was labeled with Texas Red C5-bromoacetamide or tetramethylrhodamine-5-iodoacetamide dihydroiodide (Molecular Probes) as a fluorescence acceptor probe as well. The labeling reaction was carried out by adding 10-15-fold molar excess of fluorescence probe to a solution of 100 μM purified protein. The reaction was shielded from light and allowed to proceed overnight at 4 ℃. 10 mM DTT was added to stop the reaction. Unreacted fluorescence was removed using a PD-10 desalting column followed by gel filtration. The labeling efficiency of the fluorescence was calculated by dividing the moles of fluorescence by the moles of protein. Amounts of dye and protein were determined using a UV-Vis spectrophotometer (HP) and comparing the absorbance of the dye at 550 nm (Rho), 595 nm (TR) or 510 nm (BP) to the absorbance at 280 nm (protein). Labeling efficiency was between 85-100%.

Fluorescence emission spectra were acquired on a PTI fluorimeter with excitation at 465 nm and detection of emission from 480 to 680 nm, using 50-100 nM BODIPY-FL-labeled Munc18-1 dissolved in 20 mM HEPES (pH 7.4) and 100 mM KCl, and variable concentration of SNARE complexes or fragments.

3.2.6 Chemical Cross-linking Experiment

17 μM rat Munc18-1 and 1x or 5x synaptobrevin(29-96) were incubated with 5 mM 1-ethyl-3-[3-dimethylaminopropyl]carbodiimide (EDC) or 1 mM Bis(sulfosuccinimidyl)suberate (BS3) for 1 hr at room temperature and the reaction was

quenched with quench buffer (25 mM Tris, pH8.0) for 15 minutes. Samples of 18 μg of protein were loaded on SDS gels for PAGE and LC-MS/MS analysis.

3.2.7 ^{1}H-^{15}N Heteronuclear Single Quantum Coherence (HSQC) Experiments

Samples for ^{1}H-^{15}N HSQC spectra were prepared using M9 minimal media containing uniform ^{15}N labeling. ^{1}H-^{15}N HSQC spectra were acquired with 40 μM synaptobrevin(29-96) in the absence and presence of 40 μM squid Munc18-1 in 20 mM HEPES (pH 7.4) and 120 mM KCl.

3.3 Results

3.3.1 Munc18-1 Binds to Syntaxin-1 and to the SNARE Complex

To directly test for diverse types of Munc18-1/SNARE interactions using FRET, I prepared two single mutants of rat Munc18-1 in which residue 125 or 308 was mutated to cysteine and labeled them with BODIPY-FL as a donor fluorescence probe. Specific labeling of residue 125 or 308 was verified by trypsin digestion and mass spectrometry (MS), and was favored by the fact that these side chains are highly exposed to the solvent, whereas the native cysteine side chains of wild type (WT) Munc18-1 are buried. I refer to the labeled Munc18-1 proteins as Munc18-125-BP and Munc18-308-BP. I also introduced a single cysteine mutation at residue 27 of the cytoplasmic region of syntaxin-1(2-253), where the only native cysteine (residue 145) was mutated to serine, and at residue 61 of the cytoplasmic region of synaptobrevin(1-96), where a serine was mutated

to a cysteine. These cysteine mutants were then labeled with Rhodamine or Texas Red as fluorescence acceptor probes. I refer to the labeled proteins as syntaxin-27-Rho or –TR and synaptobrevin-61-Rho or TR, respectively. Representative experiments with one probe or the other are shown below, but the nature of the probe did not alter the results observed.

To test the labeled protein in a well-characterized interaction, I first tested Munc18-1-syntaxin-1 binding. I observed a high FRET efficiency (E > 70%) between Munc18-125-BP and syntaxin-27-Rho (Figure 3.1A), as expected from the proximity of residue 125 of Munc18-1 to residue 27 of syntaxin-1 in the crystal structure of the Munc18-1/syntaxin-1 complex [~ 23Å (Misura *et al.* 2000)] and assuming a Forster radius of 50Å. Titrations with variable syntaxin-27-Rho concentrations yielded saturable dose-response curves (Figures 3.1 A,B) and an approximate dissociation constant (Kd) of 5 nM, consistent with the low nanomolar affinity between Munc18-1 and closed syntaxin-1 measured previously by diverse methods (Khvotchev *et al.* 2007; Burkhardt *et al.* 2008; Deák *et al.* 2009). Similar results were obtained with Munc18-308-BP (Figure 3.2), although the FRET efficiency was lower because residue 308 of Munc18-1 is farther than residue 125 from residue 27 of syntaxin-1.

I also analyzed binding of a SNARE complex containing syntaxin-27-TR or -Rho to Munc18-125-BP or Munc18-308-BP. I observed FRET efficiencies similar to those observed with isolated syntaxin-27-Rho or –TR, as expected if Habc domain occupies a similar position upon binding of syntaxin-1 or the SNARE complex to Munc18-1 (Khvotchev *et al.* 2007; Burkhardt *et al.* 2008; Deák *et al.* 2009). Titrations with different

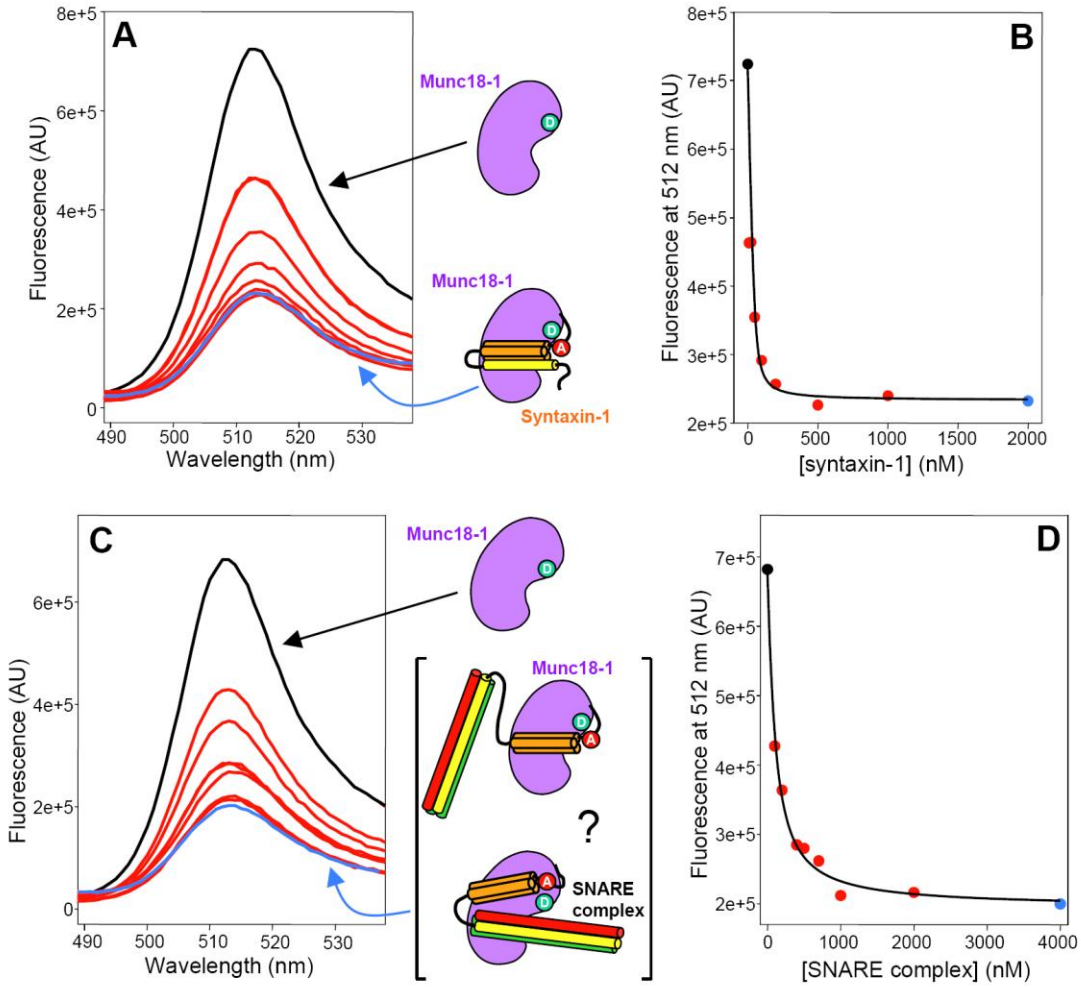
A
Fluorescence (AU)
Wavelength (nm)
Munc18-1
Munc18-1
Syntaxin-1
B
Fluorescence at 512 nm (AU)
[syntaxin-1] (nM)
C
Munc18-1
Munc18-1
?
SNARE complex
Fluorescence (AU)
Wavelength (nm)
D
Fluorescence at 512 nm (AU)
[SNARE complex] (nM)

Figure 3.1

Figure 3.1 Binding of Munc18-1 to closed syntaxin-1 and neuronal SNARE complex monitored by FRET.

(A and C) Emission fluorescence spectra of 50 nM Munc18-125-BP and variable concentrations of syntaxin-27-Rho (A) or the SNARE complex containing syntaxin-27-TR (C). The SNARE complex was formed with syntaxin-27-Rho, and the SNARE motifs of synaptobrevin and SNAP-25. The diagrams next to the spectra represent Munc18-1 (purple) with a donor fluorescence probe (green), syntaxin-1(2-253) (SNARE motif, yellow; Habc domain, orange) labeled with an acceptor fluorescence probe (red), and SNARE complexes containing syntaxin-1(2-253), synaptobrevin (red) and SNAP-25 (green). In the bracket, two different types of Munc18-1/SNARE complex assemblies are represented.

(B and D) Plots of the fluorescence emission intensity at 512 nm as function of syntaxin-27-Rho concentration (B) and SNARE complex concentration (D), derived from the spectra shown in panels A and C, respectively. The data were fit to a standard single binding site model.

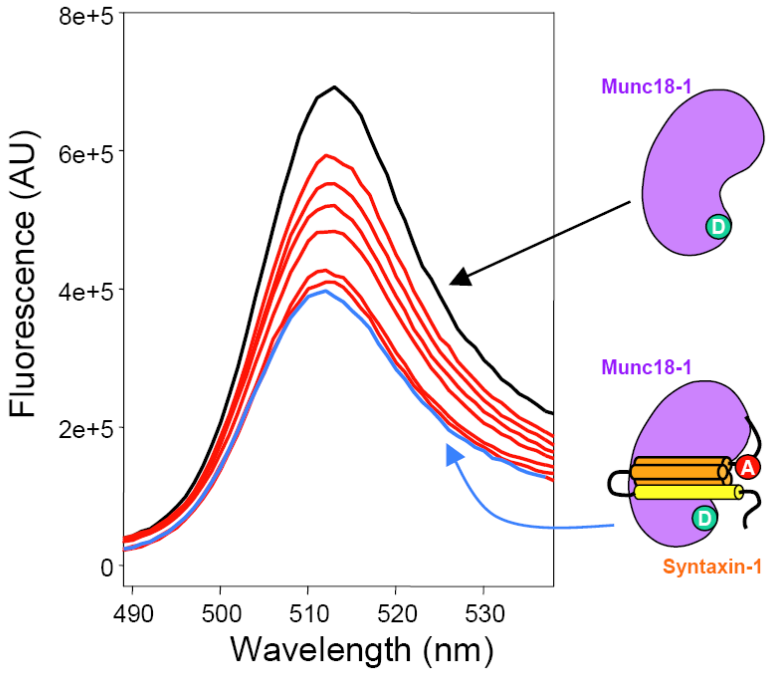

Figure 3.2

Figure 3.2 Binding of Munc18-1 to closed syntaxin-1 monitored by FRET using Munc18-308-BP.

The left panel shows emission fluorescence spectra of 50 nM Munc18-308-BP and variable concentrations of syntaxin-27-Rho. The diagrams next to the spectra represent Munc18-1 (purple) with a donor fluorescence probe (green) and syntaxin-1(2-253) (SNARE motif, yellow; Habc domain orange) labeled with an acceptor fluorescence probe (red). Note that the FRET efficiency (E ~ 40%) is lower than that observed with the BP label at residue 125 of Munc18-1 (Fig. 2.1 A) because residue 308 of Munc18-1 is farther from residue 27of syntaxin-1 (ca. 56 Å) in the syntaxin-1/Munc18-1 complex.

SNARE complex concentrations yielded saturable binding curves with a *K*d of ~ 100 nM (Figures 3.1C,D), comparable to those determined previously by NMR spectroscopy (Dulubova *et al.* 2007; Deák *et al.* 2009). Hence, all these data showed that the fluorescently labeled mutants exhibit interactions analogous to those between the WT proteins.

3.3.2 Munc18-1 Binds to Synaptobrevin and to the SNARE Four-Helix Bundle

The similarity in the FRET efficiencies observed for binding of Munc18-1 to either syntaxin-1 or the SNARE complex were consistent with the notion that the interactions of the syntaxin-1 N-terminal region with Munc18-1 are similar in the context of the binary syntaxin-1/Munc18-1 complex and the quaternary Munc18-1/SNARE complex assemblies (Dulubova *et al.* 2007; Burkhardt *et al.* 2008; Deák *et al.* 2009). However, these data did not clarify whether the SNARE four-helix bundle interacts directly with Munc18-1 in these assemblies (Figure 3.1). To test whether the four-helix bundle can directly bind to Munc18-1, I used minimal SNARE complexes containing synaptobrevin-61-Rho and lacking the syntaxin-1 N-terminal region (i.e. using a syntaxin-1 fragment 191-253 rather than 2-253). Importantly, these complexes exhibited substantial FRET with Munc18-308-BP and less efficient FRET with Munc18-125-BP (Figure 3.3A). In titration experiments, I was unable to reach complete saturation because of limited availability of the fluorescently-labeled SNARE four-helix bundles, but the data could be fit well with a standard protein-ligand binding equation (Figure

3.3B), yielding estimated *K*d values of 6 μM. Hence, these results demonstrate that Munc18-1 binds to the SNARE four-helix bundle with low micromolar affinity.

I also tested for binding of isolated synaptobrevin-61-Rho to Munc18-308-BP, and observed even more efficient FRET (Figure 3.3C). Titrations with different synaptobrevin-61-Rho concentrations (Figure 3.3D) also yielded *K*d values on the order of 6 μM. This similarity in affinities suggested that analogous residues mediate the interactions of Munc18-1 with synaptobrevin and with the SNARE four-helix bundle, and hence that synaptobrevin is largely responsible for binding of the SNARE four-helix bundle to Munc18-1. The observation that the FRET efficiency was higher for the Munc18-308-BP/synaptobrevin-61-Rho interaction (Figures 3.3A,C) was not inconsistent with this conclusion, since isolated synaptobrevin is known to be highly flexible (Hazzard *et al.* 1999). Therefore, if the region of synaptobrevin containing residue 61 remains flexible upon Munc18-1 binding, such flexibility can yield a range of distances between the donor and acceptor probes, and the r^{-6} dependence of the FRET efficiency is expected to yield ensemble-averaged values that are strongly biased in favor of the shorter distances.

Note also that addition of 50 μM unlabeled synaptobrevin(1-96) led to a considerable decrease in the efficiency of FRET between Munc18-1 and the SNARE four-helix bundle containing synatobrevin-61-Rho (Figure 3.4A), showing that synaptobrevin and the SNARE four-helix bundle compete for Munc18-1 binding and strongly supporting the conclusion that both interactions involve similar binding sites.

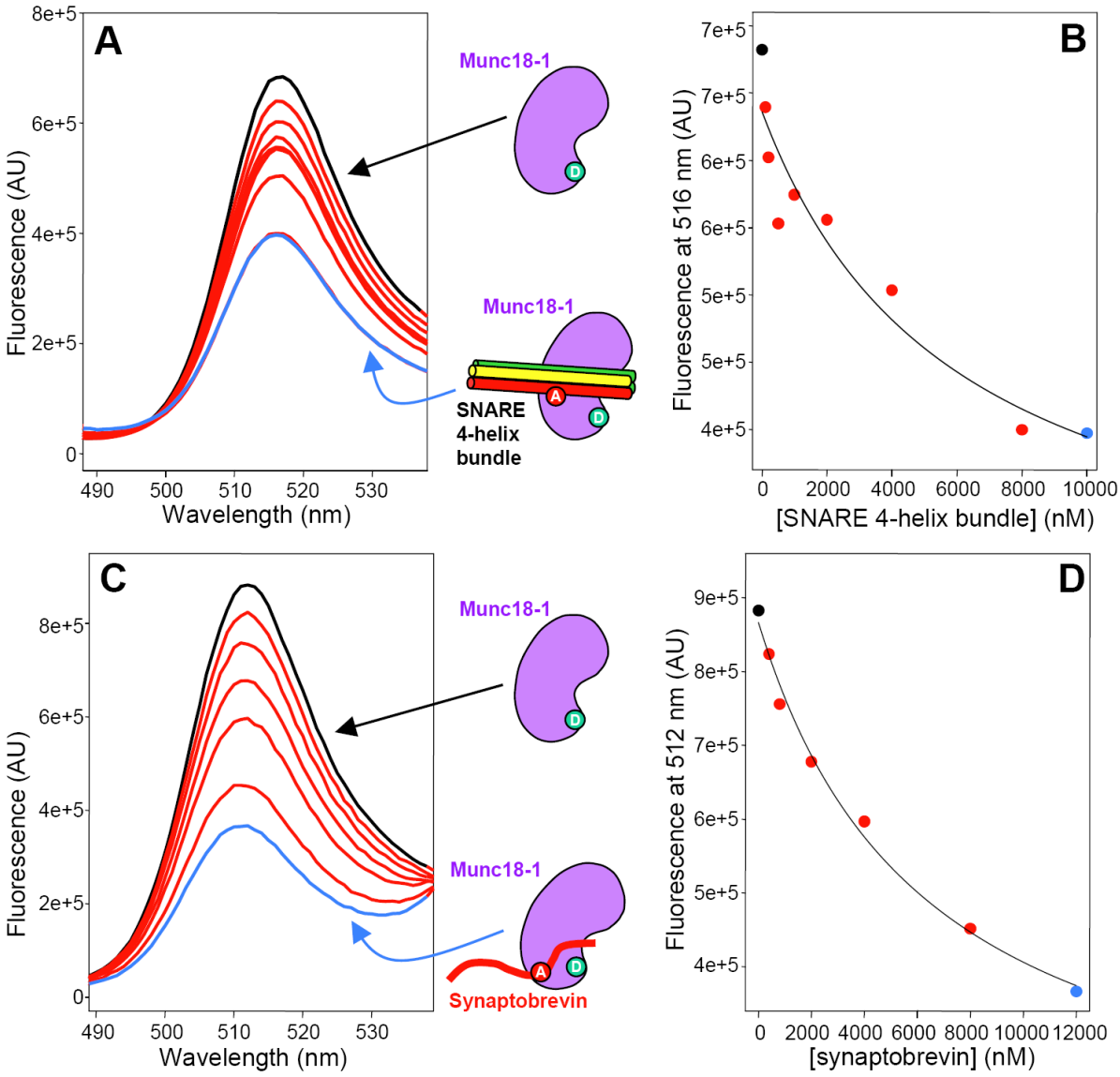
A
Fluorescence (AU)
Wavelength (nm)
Munc18-1
SNARE
4-helix
bundle
B
Fluorescence at 516 nm (AU)
[SNARE 4-helix bundle] (nM)
C
Fluorescence (AU)
Wavelength (nm)
Munc18-1
Synaptobrevin
D
Fluorescence at 512 nm (AU)
[synaptobrevin] (nM)

Figure 3.3

Figure 3.3 Munc18-1 binds to synaptobrevin and the SNARE four-helix bundle.

(A and C). Emission fluorescence spectra of 50 nM Munc18-308-BP and variable concentrations of synaptobrevin-61-Rho (C) or the SNARE four-helix bundle containing synaptobrevin-61-TR and the SNARE motifs of syntaxin-1 and SNAP-25 (A). The diagrams next to the spectra represent Munc18-1 (purple) with a donor fluorescence probe (green), synaptobrevin(1-96) (red) with an acceptor fluorescence (red), and SNARE four-helix bundles containing the labeled synaptobrevin(1-96) (red) and the SNARE motifs of syntaxin-1 (yellow) and SNAP-25 (green).

(B and D) Plots of the fluorescence emission intensity at 512 nm as a function of synaptobrevin-61-Rho concentration (D) or SNARE complex concentration (B), derived from the spectra shown in panels A and C, respectively. The data were fit to a standard single binding site model.

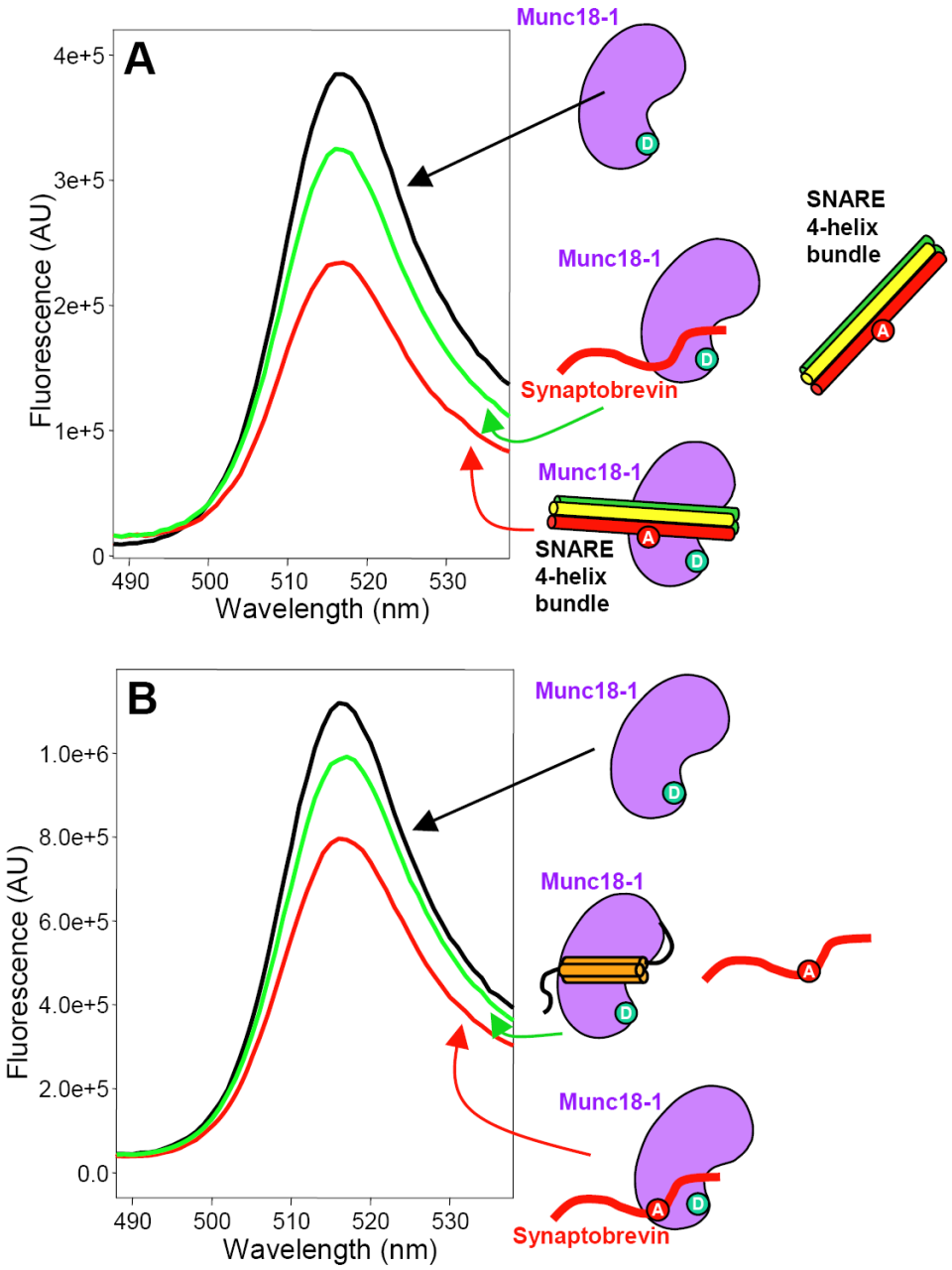
A
Fluorescence (AU)
4e+5
3e+5
2e+5
1e+5
0
490
500
510
520
530
Wavelength (nm)
Munc18-1
SNARE
4-helix
bundle
Munc18-1
Synaptobrevin
Munc18-1
SNARE
4-helix
bundle
B
Fluorescence (AU)
1.0e+6
8.0e+5
6.0e+5
4.0e+5
2.0e+5
0.0
490
500
510
520
530
Wavelength (nm)
Munc18-1
Munc18-1
Munc18-1
Synaptobrevin

Figure 3.4

Figure 3.4 Competition of the SNARE four-helix bundle and the syntaxin-1 N-terminal region with synaptobrevin for Munc18-1 binding.

(A). The left panel shows emission fluorescence spectra of 50 nM Munc18-308-BP alone (black) or in the presence of 10 μM SNARE four-helix bundle containing synaptobrevin-61-TR and the SNARE motifs of syntaxin-1 and SNAP-25, before (red) or after (green) addition of 50 μM synaptobrevin.

(B). The left panel shows emission fluorescence spectra of 50 nM Munc18-308-BP alone (black) or in the presence of 10 μM synatobrevin-61-Rho before (red) or after (green) addition of 30 μM syntaxin-1 N-terminal region (residues 1-180). The diagrams next to the spectra represent Munc18-1 (purple) with a donor fluorescence probe (green), synaptobrevin(1-96) (red) with or without an acceptor probe (red), SNARE four-helix bundles containing synaptobrevin(1-96) (red) with an acceptor fluorescence probe (red) plus the SNARE motifs of syntaxin-1 (yellow) and SNAP-25 (green), and the syntaxin-1 N-terminal region (Habc domain in orange).

3.3.3 The Syntaxin-1 N-terminal Region Competes for the SNARE Four-Helix Bundle

The syntaxin-1 closed conformation consists of a four-helix bundle formed by the Habc domain and the SNARE motif (Misura *et al.* 2000). Hence, it is natural to speculate that the SNARE four-helix bundle may bind to the same cavity of Munc18-1 as the syntaxin-1 closed conformation. Since the Habc domain likely remains bound at the same site when the SNARE complex interacts with Munc18-1 (Deák *et al.* 2009), this domain might hinder binding of the SNARE four-helix bundle to Munc18-1.

To test this hypothesis, I first performed FRET experiments with Munc18-308-BP and the SNARE four-helix bundle containing synaptobrevin-61-Rho or TR. Efficient FRET was observed when excess (10 μM) SNARE four-helix bundle was added to 50 nM Munc18-308-BP, but most of the FRET was lost when 10 μM syntaxin-1 N-terminal region (residues 1-180) was present (Figure 3.5A). Moreover, I observed no FRET between Munc18-308-BP and the SNARE complex containing the syntaxin-1 N-terminal region and synaptobrevin-61-Rho or TR (Figure 3.5B). Although we could not rule out the possibility that these results arise from conformational changes, the data strongly support the hypothesis that the syntaxin-1 N-terminal region and the SNARE four-helix bundle compete for binding to the same Munc18-1 cavity. The syntaxin-1 N-terminal region also decreased the efficiency of FRET between synaptobrevin-61-Rho and Munc18-308-BP (Figure 3.4B), again suggesting that the same Munc18-1 cavity binds to synaptobrevin.

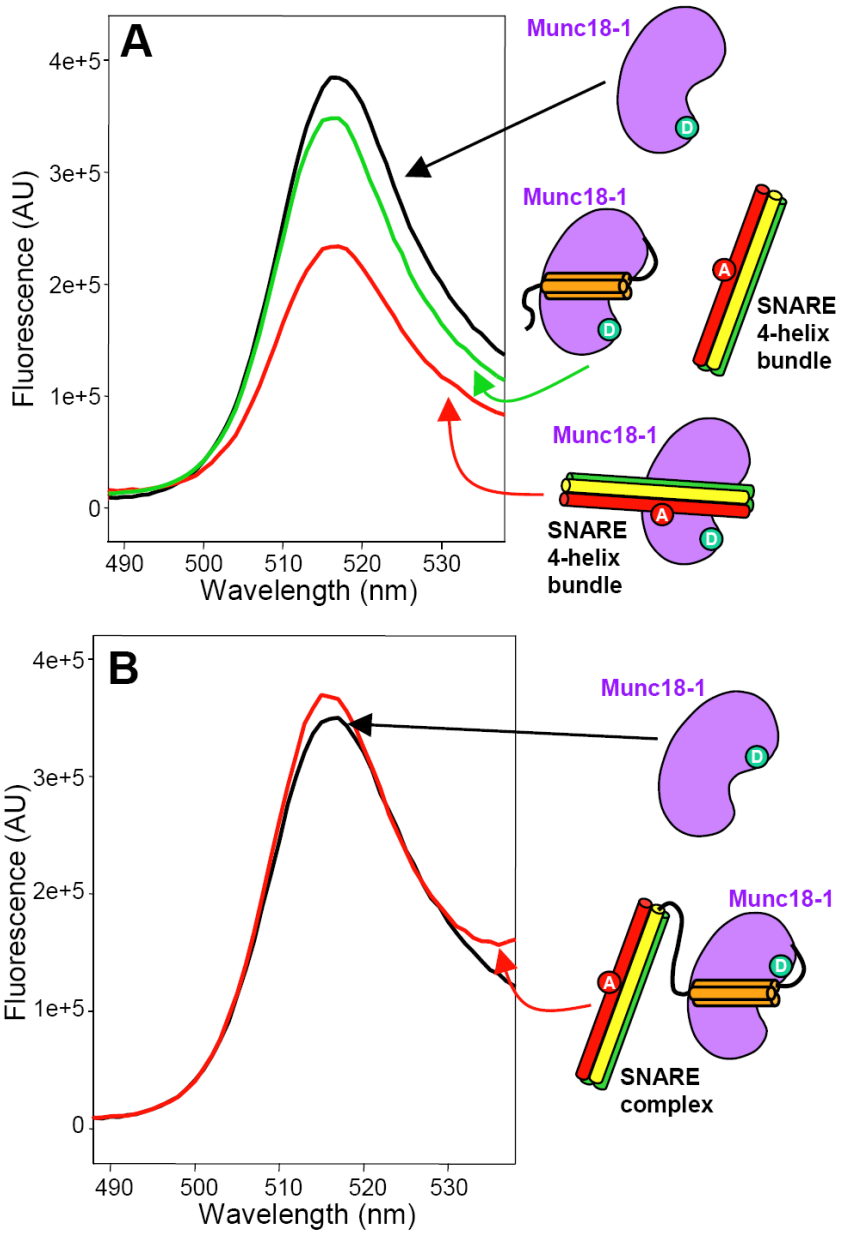
A
Fluorescence (AU)
4e+5
3e+5
2e+5
1e+5
0
490
500
510
520
530
Wavelength (nm)
Munc18-1
D
Munc18-1
D
A
SNARE
4-helix
bundle
Munc18-1
A
D
SNARE
4-helix
bundle
B
Fluorescence (AU)
4e+5
3e+5
2e+5
1e+5
0
490
500
510
520
530
Wavelength (nm)
Munc18-1
D
Munc18-1
A
D
SNARE
complex

Figure 3.5

Figure 3.5 The N-Terminal region of syntaxin-1 competes with the SNARE four-helix bundle for Munc18-1 binding.

(A). Emission fluorescence spectra of 50 nM Munc18-308-BP alone (black) or in the presence of 10 μM SNARE four-helix bundle containing synaptobrevin-61-TR and the SNARE motifs of syntaxin-1 and SNAP-25, before (red) or after (green) addition of 10 μM syntaxin-1 N-terminal region (residues 1−180). The diagrams next to the spectra represent Munc18-1 (purple) with a donor fluorescence probe (green), the syntaxin-1 N-terminal region (Habc domain colored orange), and SNARE four-helix bundles containing labeled synaptobrevin(1−96) (red) with an acceptor fluorescence probe (red) and the SNARE motifs of syntaxin-1 (yellow) and SNAP-25 (green).

(B). Emission fluorescence spectra of 50 nM Munc18-308-BP alone (black) or in the presence of 20 μM SNARE complex formed with synaptobrevin-61-Rho, syntaxin(2−253), and the SNARE motifs of SNAP-25.

3.3.4 Munc18-1 Binds to the C-terminus of the Synaptobrevin SNARE Motif

To gain further insights into the residues involved in Munc18-1/synaptobrevin binding, Lijing Su, a student in the Rizo laboratory who has been also involved in this project, performed chemical cross-linking experiments between WT Munc18-1 and a synaptobrevin fragment spanning its SNARE motif (residues 29-96). No cross-linking was observed when she used EDC, an agent that links carboxyl groups to primary amines, even when an excess of synaptobrevin(29-96) was used in the reaction (Figure 3.6A). However, efficient cross-linking was observed upon addition of BS3, an agent that cross-links primary amines with primary amines (see red arrow in Figure 3.6A). Trypsin digestion of the cross-linked product and MASS analysis revealed one peptide containing a sequence from synaptobrevin (KYWWK, residues 87-91) cross-linked to a sequence from Munc18-1 (KMPQYQK, residues 333-339). Mapping of the sequence to the three-dimensional structure of Munc18-1/syntaxin-1 complex showed that residues 333-339 of Munc18-1 indeed located in the cavity that binds to closed syntaxin-1A (Figure 3.6B). Intriguingly, residues 87-91 of synaptobrevin were at the very C-terminus of the SNARE motif (Figure 3.6B), which was adjacent to the synaptic vesicle membrane. This finding could be fundamentally important for the mechanism of membrane fusion, since an interaction with the C-terminus of the synaptobrevin SNARE motif would place Munc18-1 right at the site where membrane fusion occurs.

To investigate the Munc18-1 binding site on synaptobrevin by a different method, I used NMR spectroscopy. I first acquired ^{1}H-^{15}N heteronuclear single quantum coherence (HSQC) spectra of 5 μM ^{15}N-labeled synaptobrevin(29-96) in the presence and

absence of 6 μM rat Munc18-1. While the spectra suggested that rat Munc18-1 indeed binds to the C-terminus of synaptobrevin(29-96), obtaining high-quality data was hindered by the insolubility of rat Munc18-1 at the concentrations required for these NMR experiments. To solve this problem, Lijing turned to squid Munc18-1 (sMunc18-1), which shares a high sequence identity (66.4%) with rat Munc18-1 and is more stable and soluble [note that this better behavior allowed crystallization of isolated sMunc18-1 (Bracher *et al.* 2000)].

Gel filtration experiments showed that sMunc18-1 co-elutes with mammalian syntaxin-1 and the SNARE complex (Figure 3.7), indicating that sMunc18-1 binds tightly to the mammalian SNAREs like rat Munc18-1. Moreover, we were able to obtain ^{1}H-^{15}N HSQC spectra of 40 μM synaptobrevin(29-96) in the absence and presence of sMunc18-1. Since synaptobrevin is unstructured (Hazzard *et al.* 1999), binding to a large protein such as sMunc18-1 was expected to lead to selective broadening of the cross-peaks from the sequences involved in binding, while regions that do not participate in the interaction were expected to remain flexible and still yield observable cross-peaks. Indeed, we observed that addition of sMunc18-1 caused broadening of some synaptobrevin(29-96) cross-peaks, while many others were unaffected (Figure 3.8A). Importantly, the majority of broadened cross-peaks correspond to the region encompassing residues 75-95 of synaptobrevin (Figure 3.8A) at the very C-terminus of its SNARE motif (Figure 3.8B), in correlation with the cross-linking results obtained with rat Munc18-1.Note that the binding region does not include residues 60-70, which were previously suggested to mediate Munc18-1-synaptobrevin interactions (Shen et al., 2007), although we can not

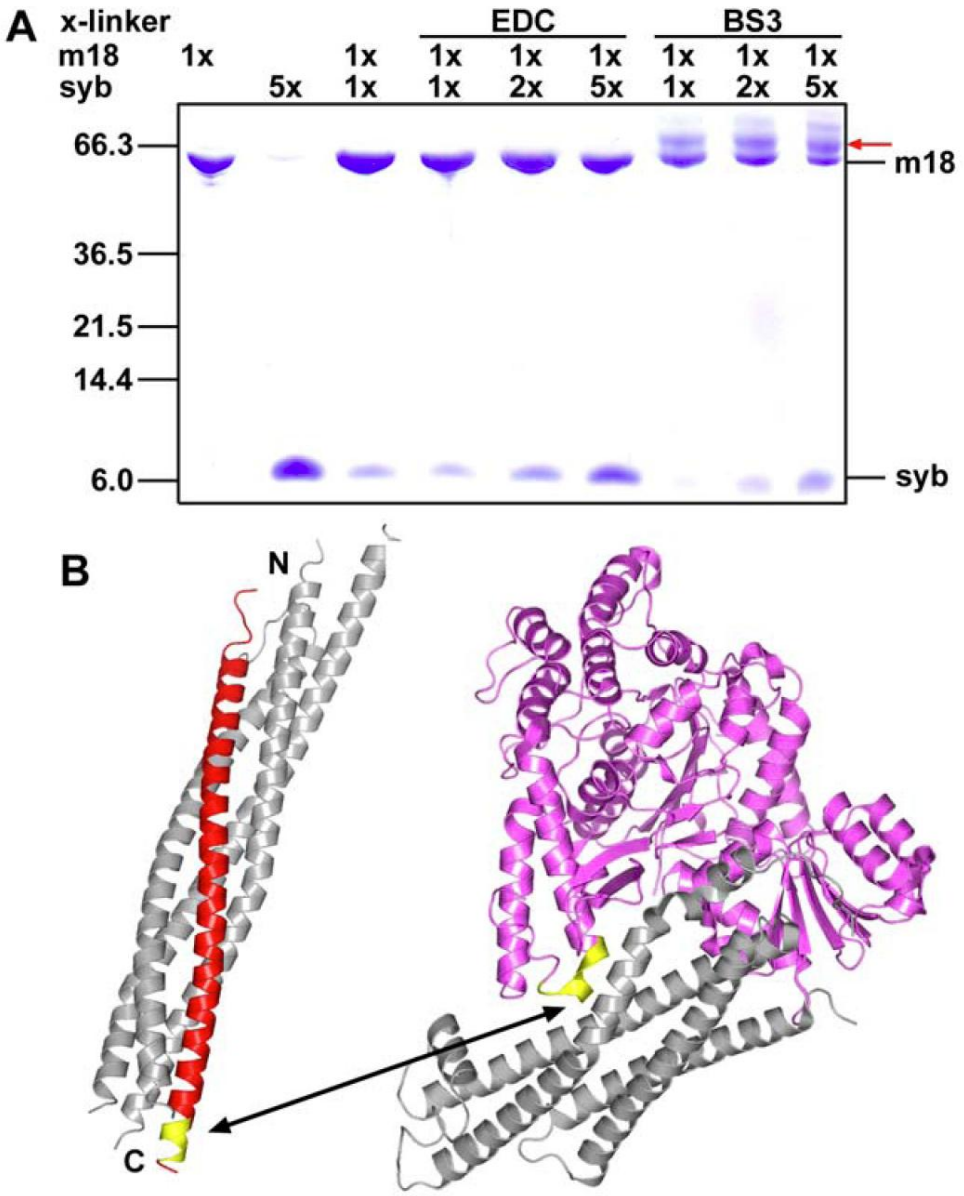
A
x-linker
EDC
BS3
m18
1x
1x
1x
1x
1x
1x
1x
1x
syb
5x
1x
1x
2x
5x
2x
5x
66.3
36.5
21.5
14.4
6.0
m18
syb
B
N
C

Figure 3.6

Figure 3.6 Cross-linking of synaptobrevin and Munc18-1.

(A). SDS−PAGE of samples containing synaptobrevin(29-96), Munc18-1, or both after cross-linking with EDC or BS3. The relative concentrations of both proteins are indicated above the lanes. The positions of molecular mass markers are indicated at the left. The red arrow at the right indicates the position of the cross-linked product.

(B). Ribbon diagrams of the crystal structure of the SNARE complex (Sutton 1998) and the Munc18-1−syntaxin-1 complex (Misura et al., 2000) with synaptobrevin colored red and Munc18-1 colored purple (other proteins colored gray). The sequences of synaptobrevin and Munc18-1 that were cross-linked are colored yellow.

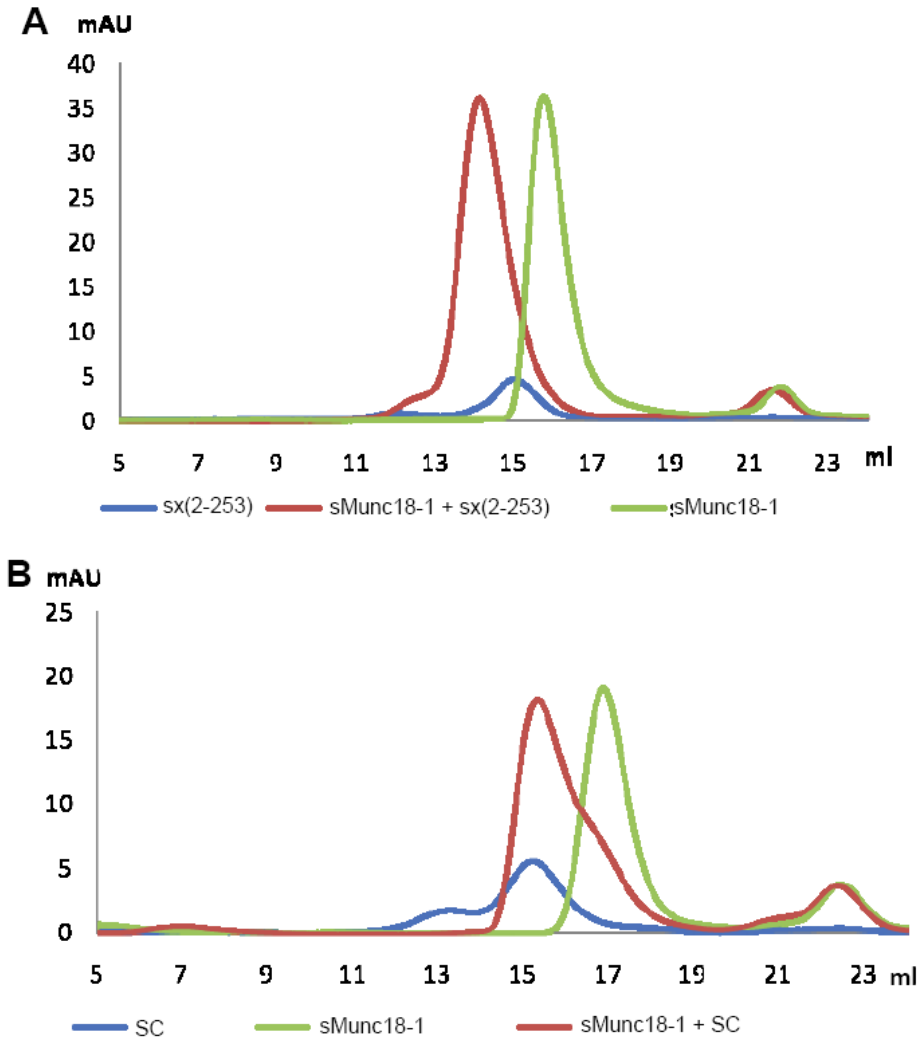
A
mAU
40
35
30
25
20
15
10
5
0
5
7
9
11
13
15
17
19
21
23
ml
sx(2-253)
sMunc18-1 + sx(2-253)
sMunc18-1
B
mAU
25
20
15
10
5
0
5
7
9
11
13
15
17
19
21
23
ml
SC
sMunc18-1
sMunc18-1 + SC

Figure 3.7

Figure 3.7 sMunc18-1 binds to mammalian syntaxin-1 and SNARE complex.

Gel filtration profiles on Superdex 200 10/30HR (Amersham) of sMunc18-1 alone (green) or mixed with rat syntaxin-1(2-253) (red, panel A) or SNARE complex formed with rat syntaxin-1(2-253) and the SNARE motifs of rat synaptobrevin and human SNAP-25 (red, panel B). In blue are shown the controls with rat syntaxin-1(2-253) alone (A) or SNARE complex alone (B). The shifts in the elution profiles of sMunc18-1 observed in both cases demonstrate binding to the mammalian syntaxin-1 and SNARE complex.

rule out the possibility that this region might contribute to Munc18-1-SNARE four-helix bundle interactions.

To further confirm our conclusions, we obtained a synthetic peptide corresponding to residues 77-96 of synaptobrevin, and acquired ^{1}H NMR spectra of the peptide alone, sMunc18-1 alone, and a mixture of the peptide and sMunc18-1, comparing the intensities in the methyl region of the spectra before and after applying a Carr−Purcell−Meiboom−Gill (CPMG) pulse sequence for 100 ms. The stronger T_2 relaxation of the peptide in the presence of sMunc18-1 showed that the peptide binds to sMun18-1 (Figure 3.9). Finally, we also compared the affinity of sMunc18-1 for a fragment containing the C-terminal half of the synaptobrevin SNARE motif (residues 49-96) and the synaptobrevin(77-96) peptide using ITC, obtaining *K*d values of 13.3 and 13.5 μM, respectively (Figure 3.8C,D). These values are comparable to the *K*d values obtained by FRET for binding of rat Munc18-1 to synaptobrevin(1-96) and the SNARE four-helix bundle (Figure 3.3), and their similarity confirms that the C-terminus of the SNARE motif is responsible for synaptobrevin-binding to Munc18-1.

3.3.5 Mutations in the Synaptobrevin SNARE Motif Disrupt the Binding to Munc18-1

To disrupt the binding of rat Munc18-1, I made double mutations on synaptobrevin(29-96) based on HSQC spectra and cross-linking results. Residues 86 and 87 are mutated to residues with opposite charge to glutamic acid, referred to as synaptobrevin(29-96) R86EK87E. In another mutant, residues 83 and 86 are mutated to

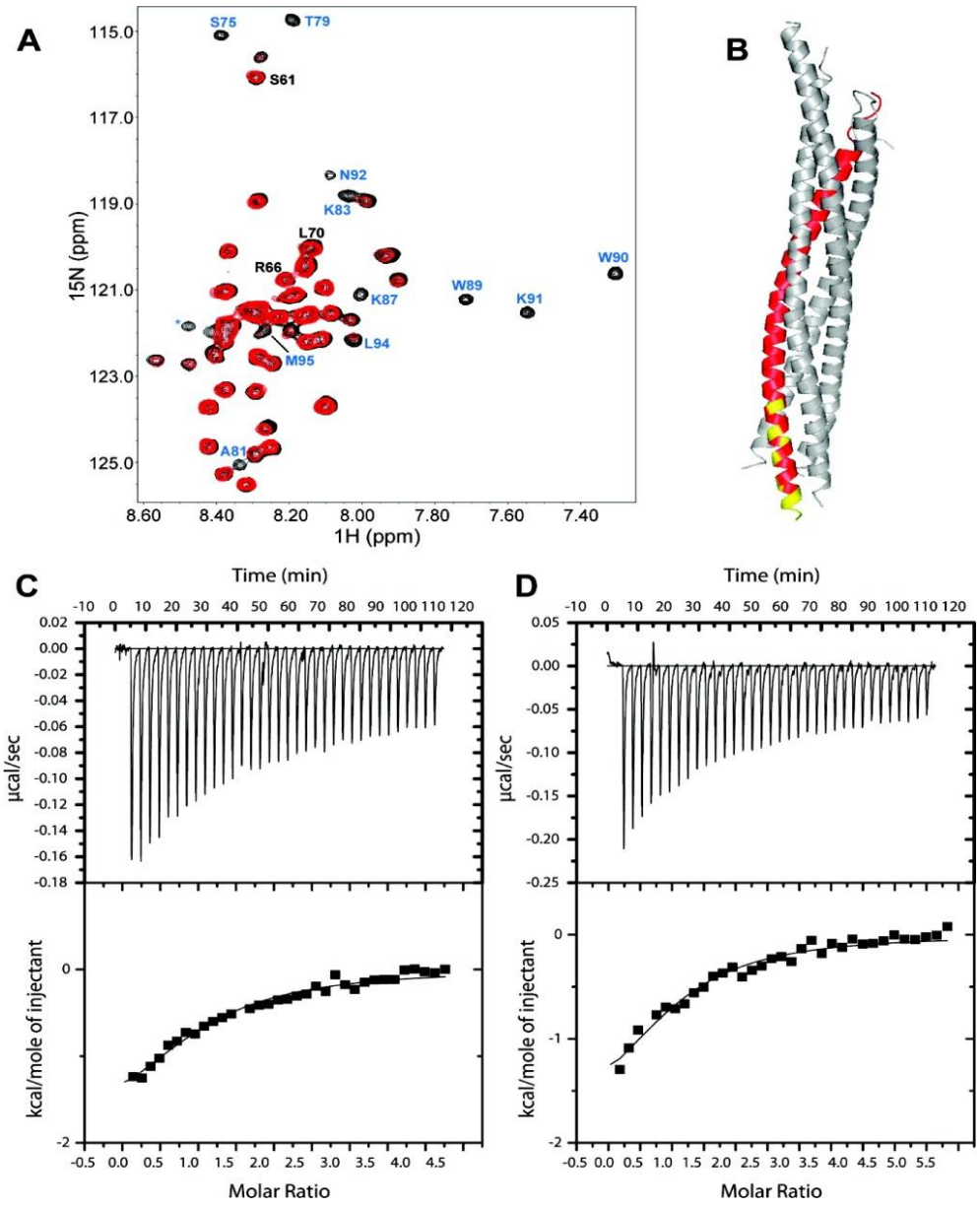
A
S75
T79
S61
N92
K83
L70
R66
K87
W89
K91
W90
L94
M95
A81
15N (ppm)
1H (ppm)
B
C
Time (min)
µcal/sec
kcal/mole of injectant
Molar Ratio
D
Time (min)
µcal/sec
kcal/mole of injectant
Molar Ratio

Figure 3.8

Figure 3.8 sMunc18-1 binds to the C-terminus of the synaptobrevin SNARE motif.

(A). $^{1}H-^{15}N$ HSQC spectra of 40 μM synaptobrevin(29−96) in the absence (black) and presence (red) of 40 μM sMunc18-1. Well-resolved cross-peaks that were strongly broadened and correspond to residues at the C-terminus of the synaptobrevin SNARE motif are labeled in blue. Three well-resolved cross-peaks that do not exhibit such strong broadening and correspond to the region spanning residues 60−70 are labeled in black.

(B). Ribbon diagram of the SNARE complex with synaptobrevin colored red; residues corresponding to the cross-peaks labeled in blue in panel A are colored yellow.

(C and D). ITC analysis of binding of synaptobrevin(49−96) (C) or synaptobrevin(77−96) (D) to sMunc18-1.

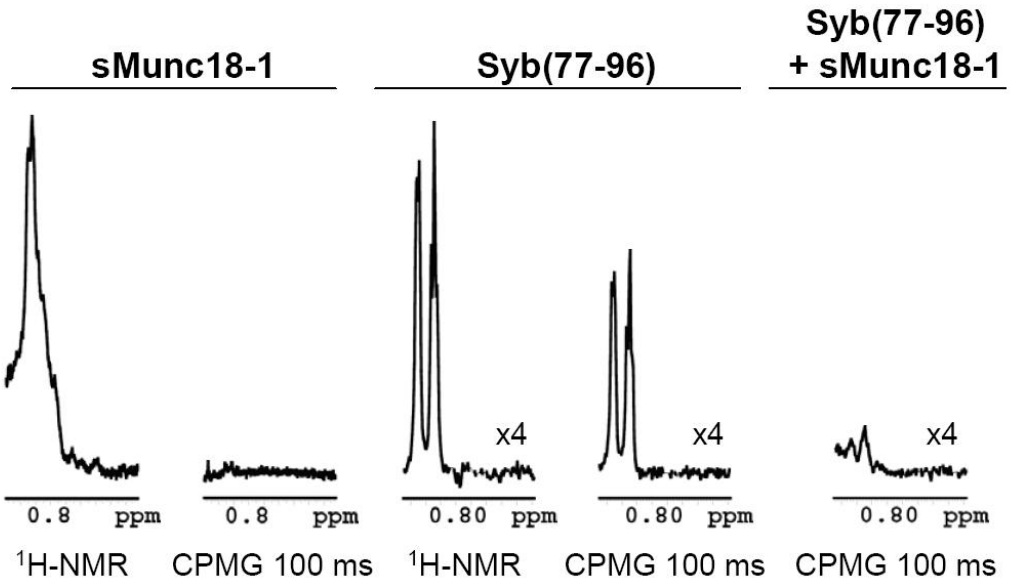

Figure 3.9

Figure 3.9 1D NMR and ITC experiments showing that sMunc18-1 binds to the C-terminus of the synaptobrevin SNARE motif.

Methyl regions of 1D ^{1}H NMR spectra without (^{1}H-NMR) and with application of a CPMG sequence for 100 ms (CPMG 100 ms) of samples containing 50 μM sMunc18-1, or 50 μM synaptobrevin(77-96) or both. The vertical scale of the three spectra on the right was increased four-fold compared to the two spectra on the left because the peptide has much weaker signal than sMunc18-1. The CPMG sequence allows T_2 relaxation during the 100 ms delay and leads to almost complete relaxation of the sMunc18-1 methyl signals because of the large size of this protein, while only a moderate reduction of the methyl signals of the synaptobrevin(77-96) peptide is observed because of its much smaller size. However, the methyl signals of the sMunc18-1/synaptobrevin(77-96) mixture are strongly decreased during the 100 ms CPMG period, showing that the peptide indeed binds to sMunc18-1.

glutamic acid, referred to as synaptobrevin(29-96) K83ER86E. I labeled these mutants with Texas Red as fluorescence acceptor probes. I observed no FRET between Munc18-308-BP and synaptobrevin-R86EK87E-61-TR or synaptobrevin-K83ER86E-61-TR (Figure 3.10A,B), suggesting these residues on the synaptobrevin SNARE motif were responsible for the binding to Munc18-1.

To test the binding of Munc18-1 to SNARE four-helix bundle (mini-core complex, mcc) containing mutant synaptobrevin, I performed FRET using Munc18-308-BP and mini-core complexes containing synaptobrevin-R86EK87E-61-TR or synaptobrevin-K83ER86E-61-TR. Efficient FRET between Munc18-308-BP and mini-core complexes was observed (Figure 3.10C). A possible interpretation could be that there are many residues from other SNARE motifs flanking the Munc18-1 binding region in the SNARE complex, and mutations at the C-terminus of synaptobrevin were not enough to break the Munc18-1 interaction. This result was consistent with the competition assay showing that complexin partially competes for the SNARE complex four-helix bundle with Munc18-1 (Figure 3.11). The crystal structure of the complexin/mini-SNARE complex revealed that complexin binds to the center of the groove between synaptobrevin and the syntaxin-1 SNARE motif (Chen *et al.* 2002). Complexin competing with Munc18-1 for mini-SNARE complex binding suggested that they shared similar binding sites on the mini-SNARE complex. Another possible interpretation could be that those mutated residues in synaptobrevin were not involved in SNARE four-helix bundle binding to Munc18-1.

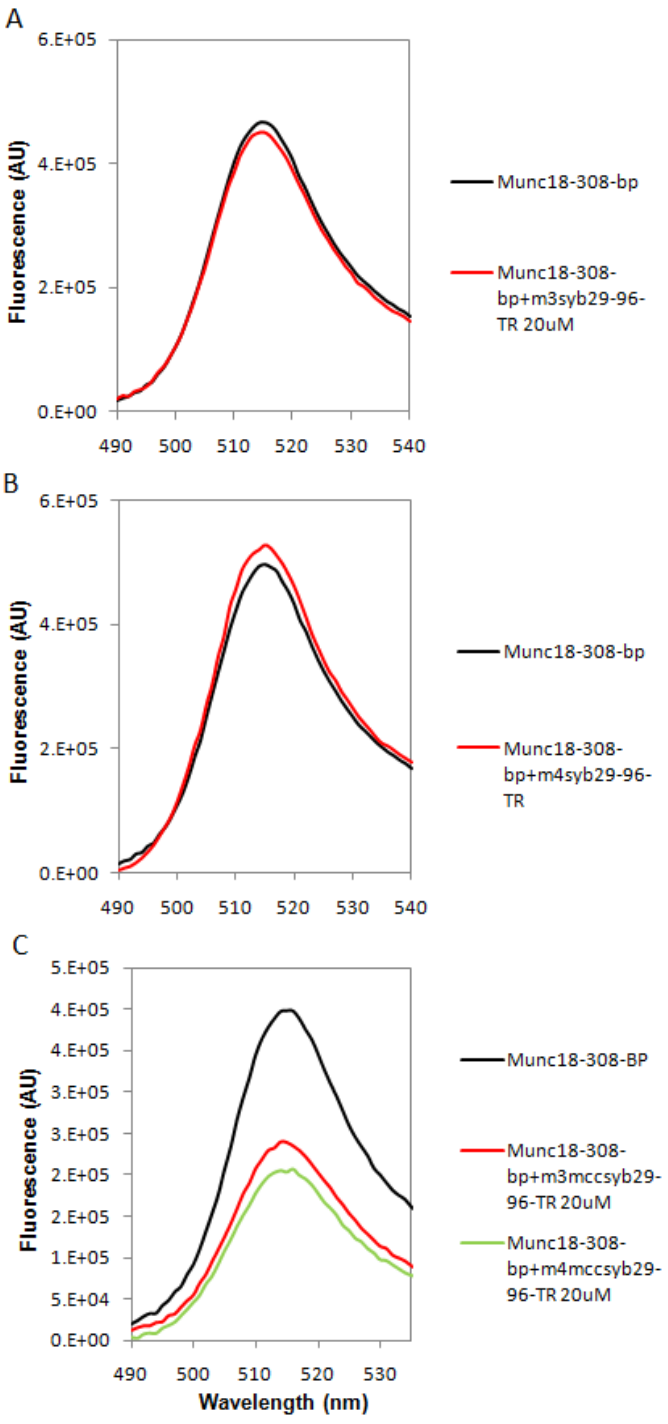
A
6.E+05
4.E+05
2.E+05
0.E+00
Fluorescence (AU)
490
500
510
520
530
540
Munc18-308-bp
Munc18-308-bp+m3syb29-96-TR 20uM
B
6.E+05
4.E+05
2.E+05
0.E+00
Fluorescence (AU)
490
500
510
520
530
540
Munc18-308-bp
Munc18-308-bp+m4syb29-96-TR
C
5.E+05
4.E+05
4.E+05
3.E+05
3.E+05
2.E+05
2.E+05
1.E+05
5.E+04
0.E+00
Fluorescence (AU)
490
500
510
520
530
Wavelength (nm)
Munc18-308-BP
Munc18-308-bp+m3mccsyb29-96-TR 20uM
Munc18-308-bp+m4mccsyb29-96-TR 20uM

Figure 3.10

Figure 3.10 Munc18-1 does not bind to synaptobrevin mutants but still binds the SNARE four-helix bundle containing the synaptobrevin mutants.

(A and B). Emission fluorescence spectra of 50 nM Munc18-308-BP in the absence (black) or presence (red) of 20 μM synaptobrevin-R86EK87E-61-TR (A) or synaptobrevin-K83ER86E-61-TR (B).

(C). Emission fluorescence spectra of 50 nM Munc18-308-BP alone (black) or in the presence of 20 μM SNARE four-helix bundle containing synaptobrevin-R86EK87E-61-TR (red) or synaptobrevin-K83ER86E-61-TR (green) and the SNARE motifs of syntaxin-1 and SNAP-25. m3syb29-96-TR stands for synaptobrevin-R86EK87E-61-TR; m4syb29-96-TR stands for synaptobrevin-K83ER86E-61-TR. mcc stands for mini-core complex (SNARE four-helix bundle).

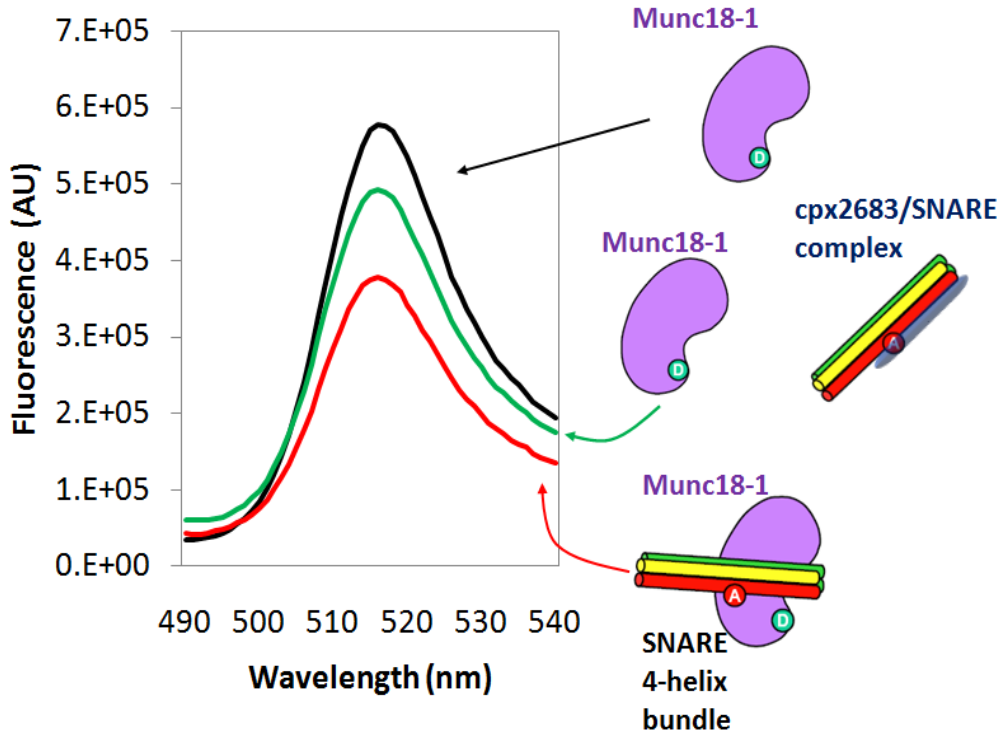

Figure 3.11

Figure 3.11 Cpx2683 partially competes with Munc18-1 for the binding to the SNARE complex four-helix bundle.

Emission fluorescence spectra of 50 nM Munc18-308-BP alone (black) or in the presence of 10 μM SNARE four-helix bundle containing synaptobrevin-61-TR and the SNARE motifs of syntaxin-1 and SNAP-25, before (red) or after (green) addition of 50 μM cpx2683. The diagrams next to the spectra represent Munc18-1 (purple) with a donor fluorescence probe (green), cpx2683 (dark blue), and SNARE four-helix bundles containing labeled synaptobrevin(1−96) (red) with an acceptor fluorescence probe (red) and the SNARE motifs of syntaxin-1 (yellow) and SNAP-25 (green).

3.4 Discussion

SM proteins are central components of the intracellular membrane fusion machinery but their main role is still highly unclear. This uncertainty arises in part because of the diversity of SM protein/SNARE interactions that have been identified (see chapter 1), and in part because no definitive evidence has been presented for the various models of SM protein function that have been proposed. To explain the very strong blocks in membrane fusion observed in the absence of SM proteins (Rizo and Südhof 2002; Verhage and Toonen 2007) , one of these models predicted that SM proteins bind to the SNARE four-helix bundle, enabling application of force to the membranes by the SNAREs (Rizo *et al.* 2006). Reconstitution experiments showed that Munc18-1 can strongly enhance the ability of the SNAREs to induce lipid mixing and suggested that this ability depends on Munc18-1/synaptobrevin interactions, but no biochemical evidence for such interactions was described (Shen *et al.* 2007). We now show that Munc18-1 binds directly to both synaptobrevin and the SNARE four-helix bundle with an affinity in the low micromolar range. Our data suggest that these interactions involve the same cavity of Munc18-1 where the closed syntaxin-1 binds. Furthermore, we find that the C-terminus of synaptobrevin is responsible for Munc18-1 binding, placing Munc18-1 right at the site where membrane fusion occurs. These results reinforce the notion that Munc18-1, and SM proteins in general, play a direct role in membrane fusion, and suggest a model whereby a sequence of distinct Munc18-1/SNARE interactions occurs during synaptic vesicle exocytosis (Figure3.12)

Multiple models of SM protein function have been proposed over the years (Rizo and Südhof 2002; Rizo and Rosenmund 2008). It is likely that several of these models are at least partially correct, since SM proteins may play several roles, but the key unanswered question is: why are SM proteins so critical for membrane fusion? The initial finding that Munc18-1 binds to syntaxin-1 led to the proposal that Munc18-1 forms part of the synaptic vesicle fusion machinery (Hata *et al.* 1993). This overall notion is now supported by overwhelming evidence, but the binary Munc18-1/syntaxin-1 interaction in itself imposes a roadblock that gates entry of syntaxin-1 into SNARE complexes (Dulubova *et al.* 1999; Yang *et al.* 2000; Chen *et al.* 2008; Gerber *et al.* 2008). Nevertheless, this binary interaction might play positive roles by stabilizing both proteins in vivo (Verhage *et al.* 2000; Gerber *et al.* 2008), and by assisting in vesicle docking, since syntaxin-1 and Munc18-1 play a role in docking in chromaffin cells, while synaptobrevin does not (Gerber *et al.* 2008). Importantly, overexpression of SNAP-25 rescues the docking defect in chromaffin cells from Munc18-1 KO mice, likely by promoting formation of syntaxin-1/SNAP-25 heterodimers that bind to synaptotagmin-1, but does not rescue the secretion defect (de Wit *et al.* 2009). Hence, Munc18-1 must play an additional function downstream of docking and syntaxin-1/SNAP heterodimer assembly. There is in fact evidence for participation of Munc18-1 in more than one of the steps that lead to exocytosis (Gerber *et al.* 2008; Guan *et al.* 2008; Deák *et al.* 2009).

Although Munc18-1 binding to closed syntaxin-1 hinders SNARE complex formation from an energetic point of view (Chen *et al.* 2008), Munc18-1 could still play a role in assisting SNARE complex assembly in downstream events (Dulubova *et al.* 1999;

Misura *et al.* 2000; Rizo and Rosenmund 2008). Indeed, Munc18-1 enhances assembly of SNARE complexes between co-expressed syntaxin-1/SNAP-25 heterodimers and synaptobrevin, which might underlie the stimulation of SNARE-dependent lipid mixing in reconstitution assays and depends on binding of Munc18-1 to the syntaxin-1 N-terminus (Shen *et al.* 2007). Since the co-expressed heterodimers appear to be in an inhibited state where the Habc domain hinders full interactions between the SNARE motifs (Starai *et al.* 2008), it seems likely that Munc18-1 helps to disinhibit this state by binding to the syntaxin-1 N-terminal region. It is unclear whether these events are related to the mechanism of neurotransmitter release in vivo, but in any case there is little doubt that interactions of Munc18-1 with the syntaxin-1 N-terminal region are important for release (Khvotchev *et al.* 2007; Deák *et al.* 2009). However, these interactions do not appear to play a role after vesicle priming (Deák *et al.* 2009). In addition, it seems unlikely that a mere role for Munc18-1 in assisting SNARE complex assembly can explain its essential nature for neurotransmitter release (Verhage *et al.* 2000), since SNARE complexes can be readily assembled in vitro. In addition, stimulation of SNARE-dependent lipid mixing by Munc18-1 appears to depend on interactions with synaptobrevin (Shen *et al.* 2007), and some evidence indicates that the SM protein Sec1p plays a key role in exocytosis downstream of SNARE complex formation (Grote *et al.* 2000).

These observations suggest that the key function of Munc18-1 and SM proteins in membrane fusion involves interactions with the SNARE four-helix bundle, as initially inferred for Sec1p (Carr *et al.* 1999) and as predicted by our previous model of how SM

proteins and SNAREs form the core fusion machinery (Rizo *et al.* 2006). Some results suggested the existence of such interactions (Togneri *et al.* 2006; Dai *et al.* 2007; Dulubova *et al.* 2007; Maximov *et al.* 2009), but ITC data indicated that Munc18-1 binding to the SNARE complex involves binding to only the syntaxin-1 N-terminal region (Burkhardt *et al.* 2008), and direct binding of SM proteins to the isolated SNARE four-helix bundle has not been reported. Our results now show unambiguously that Munc18-1 indeed binds to the SNARE four-helix bundle and to the very C-terminus of the synaptobrevin SNARE motif (Figures 3.6). It seems very likely that both interactions involve the same residues, since they have similar affinities and synaptobrevin competes with the SNARE four-helix bundle for Munc18-1 binding. Our data also provide strong evidence that these interactions involve the cavity of Munc18-1 where closed syntaxin-1 binds (Figure 3.5), which explains the ITC data obtained with Munc18-1 and the SNARE complex (Burkhardt *et al.* 2008). These results need to be interpreted with caution, since the interactions we report have moderate affinity and their physiological relevance remains to be established. However, the finding that Munc18-1 binds to the very C-terminus of the synaptobrevin SNARE motif is very intriguing, since it places Munc18-1 right at the site of fusion and hence suggests a fundamental new view whereby Munc18-1 is intimately and directly involved in fusion. Such a role could certainly explain the critical nature of Munc18-1 and SM proteins for membrane fusion in vivo.

The original idea of how Munc18-1 could help to induce fusion (Rodkey *et al.* 2008) was intended to provide such an explanation and was based on a simple mechanical principle: flexibility in the linker region between the SNARE motifs and TM

regions could hinder transduction of the energy of SNARE complex assembly onto the membranes and allow assembled SNARE complexes to diffuse to the middle of the interrmembrane space; however, binding of a bulky protein such as Munc18-1 to assembling SNARE complexes would prevent such diffusion and would help by applying torque on the two membranes to induce fusion, because Munc18-1 would push the membranes away while SNARE complexes bring them together. Note that the torque would be weakest if Munc18-1 binds to the N-terminus of the SNARE four-helix bundle and strongest if the binding site is at the C-terminus, as suggested by our data. Indeed, it seems impossible that SNARE complexes could form without fusion if Munc18-1 is bound to their C-termini (even if there is some flexibility in the linker regions). Moreover, Munc18-1 contains two highly positive surfaces surrounding the SNARE-binding cavity. These surfaces could bind to the two apposed membranes and actively help to bend them to induce fusion (Figure 3.12), as proposed for synaptotagmin-1 (Arac *et al.* 2006). In this context, only weak binding of Munc18-1 to liposomes has been reported (Starai *et al.* 2008), but such interactions could be greatly strengthened by the intrinsic cooperativity of the system.

Our model involves three different types of interactions of Munc18-1 with the SNAREs (Figure 3.12): first the binary interaction with closed syntaxin-1; second the interaction with the N-terminal region of syntaxin-1 as syntaxin-1 opens and SNARE complexes start to form via an as yet unknown mechanism that likely involves Munc13 (Guan *et al.* 2008; Ma *et al.* 2011); and third the binding to the C-terminus of synaptobrevin. Although the affinity of Munc18-1 for synaptobrevin is moderate, and

weaker than its affinity for the syntaxin-1 N-terminal regions in binding assays with isolated proteins, the transition from syntaxin-1 to synaptobrevin binding could be favored by strong cooperativity with the proposed interactions of Munc18-1 with both membranes, which would bring the membranes together and could therefore cooperate, in addition, with the pulling forces of the assembling SNARE complexes. Support for these ideas is provided by the finding that the HOPS complex, which includes the SM protein involved in yeast vacuolar fusion Vps33p, stabilizes *trans*-SNARE complexes as opposed to *cis*-SNARE complexes (Starai *et al.* 2008), since such stabilization must involve binding of HOPS to the two apposed membranes. Moreover, membranes appear to enhance binding of Munc18-1 to the SNARE four-helix bundle (Shen *et al.* 2007) and the functional importance of the synaptobrevin region that binds to Munc18-1 has been shown by the impairment in neurotransmitter release caused by mutation of two tryptophan residues in this region (Maximov *et al.* 2009), although the molecular target of this region in vivo remains to be determined. Candidates for such targets are also Munc13s, complexins and syntaptotagmin-1, factors that play key roles in neurotransmitter release and also bind to the SNARE four-helix bundle (Chen *et al.* 2002; Dai *et al.* 2007; Guan *et al.* 2008). These factors could provide additional cooperativity to the system, but they might also compete with Munc18-1 for binding to the four-helix bundle.

Clearly, this model remains highly speculative, and to better understand the mechanisms of membrane fusion and neurotransmitter release, it will be particularly important to study the interplay between the interactions among all these proteins and the

lipids in the context of trans-SNARE complexes formed between two apposed membranes. The data presented here have now yielded a hypothesis that can help guide these very challenging studies and proposes a fundamentally new view of how Munc18-1 might cooperate with the SNAREs to induce membrane fusion.

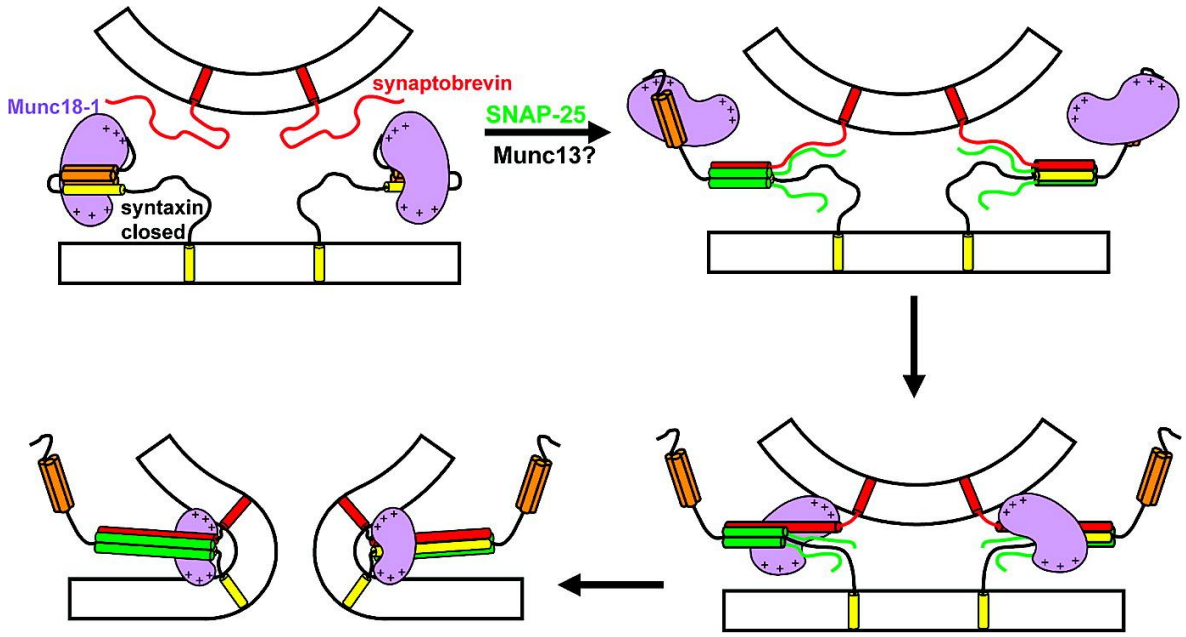

Figure 3.12

Figure 3.12 Proposed model of neurotransmitter release involving three types of Munc18-1−SNARE interactions.

The model assumes that Munc18-1 (purple) is initially bound to closed syntaxin-1 (Habc domain, orange; SNARE motif, yellow) (top left panel). Partial assembly of SNARE complexes of syntaxin-1 with synaptobrevin (red) and SNAP-25 (green) occurs by an unknown mechanism that likely involves Munc13 (not shown); here we propose that Munc18-1 is bound to only the N-terminal region of syntaxin-1 at this stage (top right panel). The next step is proposed to involve the transition of Munc18-1 from the syntaxin-1 N-terminal region to the C-terminus of the synaptobrevin SNARE motif, which could be favored by cooperativity with other interactions such as Munc18-1 binding to the vesicle membrane (bottom right panel). The central aspect of this model is that membrane fusion results from the cooperative action of Munc18-1 and the SNAREs, which would be favored by the binding of Munc18-1 to synaptobrevin and could involve interactions of basic residues of Munc18-1 (indicated by the + signs) with both membranes (bottom left panel; see the text for further details). Other proteins involved in triggering release and conferring its Ca^{2+} sensitivity are not represented for the sake of simplicity, but they are expected to cooperate with Munc18-1 and the SNAREs to trigger release.

Chapter 4 Is Munc18-1 the Sole Fusion Protein?

4.1 Introduction

Neurotransmitter release is actually a process of membrane fusion. Membrane fusion is a very important and universal event involved in a variety of cellular activities (Bennett and Scheller 1993; Rothman 1994; Orci *et al.* 1996). As a major component of the synaptic vesicle membrane, lipids play an essential role during the membrane fusion process. The vesicle membrane consists of three classes of lipids: phospholipids, glycolipids, and cholesterols. Among them, phospholipids are the most abundant.

As discussed in the previous chapters, numerous essential proteins involved in membrane fusion have been identified. The SNARE proteins synaptobrevin, syntaxin-1 and SNAP-25, as well as SM proteins, form the core of the membrane fusion machinery (Chen and Scheller 2001; Rizo and Südhof 2002; Südhof and Rothman 2009). Many other neuronal-specific proteins, such as Munc13s, RIMs and complexins, are required for the regulation of the specialized membrane fusion event at the last step of neurotransmitter release (Richmond *et al.* 1999; Koushika *et al.* 2001; Reim *et al.* 2001; Schoch *et al.* 2002; Varoqueaux *et al.* 2002). In previous studies, the interactions among these proteins were mostly analyzed in aqueous solution. However, native SNARE proteins are membrane proteins and the membrane environment might change their biochemical behavior dramatically (Dai *et al.* 2007; Guan *et al.* 2008).

Many of these important regulators are also membrane proteins and some of them have been shown to interact with membranes directly (Guan *et al.* 2008). To adequately understand the cooperative function of these proteins, researchers started to consider the membrane environment. Phospholipids can form lipid vesicles and membrane proteins can be reconstituted into the lipid vesicle, thus providing a tool to examine various membrane protein functions. Reconstitution of membrane proteins of interest mimics the native vesicle membrane environment and at the same time circumvents the complexity of the native membranes, which contain ion channels and other constituents.

Many reconstitution experiments have been reported in recent years, but different groups yielded different results mainly due to non proper procedures to set up these kinds of assays. The group headed by James Rothman was the first one to reconstitute recombinant v- and t-SNARE proteins into lipid bilayer vesicles. They found that two vesicles were docked but unfused at 4 ℃ by forming SNARE-complexes, and when brought to a physiological temperature spontaneous lipid mixing happened. Thus they claimed that SNAREs are sufficient to mediate fusion (Weber *et al.* 1998; Parlati *et al.* 1999). A big concern of this assay was that they used an extremely high protein:lipid molar ratio of 1:20 for synaptobrevin; for comparison, synaptic vesicles have a synaptobrevin to lipid ratio of ~ 1:200 (Takamori *et al.* 2006). Proteoliposomes with such a large amount of protein might be unstable and prone to artificial lipid mixing. Edwin Chapman's group repeated the same experiments except they used a lower synaptobrevin:lipid molar ratio and they observed less efficient lipid mixing (Tucker *et al.*

2004). There were also other groups that strived to repeat Chapman's original experiments. In their systems, the reconstitution procedures and conditions are different, including liposome size, amount of detergent, detergent type, and the detergent removal method. The results gave rise to opposite conclusions, since the SNAREs failed to mediate lipid mixing in these other reconstitution systems (Hu *et al.* 2002; Kweon *et al.* 2003; Chen *et al.* 2006).

These early reconstitution experiments bypassed the need for Munc18. Later the Rothman group found that Munc18-1 could enhance the lipid mixing mediated by SNAREs with a more physiological system (Shen *et al.* 2007; Shen *et al.* 2010). They claimed that the four-helix SNARE bundle, the syntaxin-1 N-peptide and Munc18-1 represent a minimal fusion machinery, whereas the rest of the SNARE sequences, including the syntaxin-1 Habc domain, are dispensable (Shen et al., 2010, Rothore et al., 2010) However, single-vesicle fusion assays showed that Munc18-1 and the SNARE four-helix bundle are sufficient to induce lipid mixing (Diao *et al.* 2010).

It is not clear how these technical differences in the reconstitution experiment could have such dramatic effects on membrane fusion and lead to contradictory results. Thus, development of a reliable reconstitution system is of considerably importance.

It is possible that Munc18-1 is involved in the last step of membrane fusion, but the exact role remains unclear. Structurally, Munc18-1 contains two conserved highly positive surfaces surrounding the SNARE-binding cavity that theoretically could bind to the two membranes and help bend them to induce fusion (Bracher *et al.* 2000; Misura *et*

al. 2000; Xu *et al.* 2010). Though weak binding of Munc18-1 to liposomes has been reported (Guan *et al.* 2008), there is no evidence for an effect of Munc18-1 on membranes or of membranes on Munc18-1.

To study the influence of the membrane on Munc18-SNARE proteins interactions, I reconstituted the SNARE proteins to the artificial proteoliposomes. I found that membranes did not help Munc18-1 binding to synaptobrevin, and Munc18-1 did not interact with membranes directly at room temperature. I also tried to set up the lipid mixing assay to study the biological relevance of Munc18-1/synaptobrevin interactions as well as the function of Munc18-1 in membrane fusion. I found that Munc18-1 causes lipid mixing even in the absence of SNAREs. Biochemistry studies showed that it was the denaturation of Munc18-1 that cause membrane lipid mixing in the absence of SNARE proteins.

4.2 Material and Methods

4.2.1 Recombinant Protein DNA Constructs

The construct expressing a GST fusion of full length synaptobrevin 2 (residues 1-116; abbreviated as Syb2) was a generous gift from Yeon-Kyum Shin's laboratory. The DNA construct containing co-expressed full length Syntaxin-SNAP25 (abbreviated as SyxSN25) was a gift from Jingshi Shen's lab. Mutations of Syb2(S61C), sMunc18-1(K319EK323E), sMunc18-1(K117ER122E), sMunc18-1(K330EK331E) and sMunc18-1(K20EK21E) were generated from the WT constructs using the QuickChange site-

directed mutagenesis kit (Stratagene) and custom designed primers, and verified by sequencing.

These constructs were transformed into *Escherichia coli* BL21 (DE3) cells for expression and stored in glycerol stocks (40% glycerol) at -80 ℃.

4.2.2 Expression and Purification of Recombinant Proteins

The expression and purification of full length synaptobrevin was as described in Chapter 2. Syb2 has a C-terminal trans-membrane region, so that detergents were required in all the purification steps.

The expression of Syb2 in pGex-KT was the same as for Syb(29-93) (see chapter 2). The purification procedures were similar except that detergents were required in all the purification steps. The buffer for re-suspension of harvested cells was PBS buffer containing 2 mM EDTA, 5 mM EGTA, 0.5 mM ABESF and 10 µl/ml sigma inhibitor cocktail (Sigma), 0.05% Tween-20, 0.5% n-lauroyl sarcosine, 0.4% Triton X-100, 10 mM β-ME and 1 mM DTT. The washing buffer, to remove non-specifically bound proteins from glutathione beads, contained PBS buffer, 1% Triton X-100 and 1 mM DTT. The Benzonase buffer, which is used to cleave double-stranded DNA, contained 50 mM Tris pH 8.0, 2 mM $MgCl_2$, 1 mM DTT and 1% Triton X-100. The thrombin cleavage buffer, which usually contained 50 mM Tris pH 8.0, 200 mM NaCl, 2.5 mM $CaCl_2$, had additional 1 mM DTT and 0.8% (w/v) β-OG. At this point, the detergent was changed to β-OG by washing the beads three times with 10 ml of 0.8% (w/v) β-OG containing

thrombin cleavage buffer. The elution buffer to elute the protein fraction contained 25 mM HEPES, pH 6.4, 1 mM DTT and 1% (w/v) *β*-OG. Buffers for Vivapure S column contained 1 mM DTT and 1% (w/v) *β*-OG as well. The typical yield of Syb2 is 2-3 mg per liter LB culture.

Dr. Shailendra Singh Rathore from Jingshi Shen's laboratory kindly sent me the DNA construct containing co-expressed full length SyxSN25, and 4 cysteines in SNAP-25 were mutated to serine (Rathore *et al.* 2010). The plasmid was transformed into *E.coli* BL21 (DE3) cells and the cells were then grown on a plate with kanamycin. Single colonies were then transferred to an overnight culture. The next day, 15 ml of this culture was transferred to 1 L of LB media containing 50 μg/ml kanamycin. Cells were then incubated at 37 ℃ and shaken at 250 rpm until OD_{600} reached 0.6-0.8, at which point 0.8 ml 1M IPTG was added to induce protein expression. Induction of protein expression then continued for 3.5 hr at 37 ℃. The cells were harvested by centrifugation at 4000 rpm for 30 min and re-suspended in 40 ml buffer A with protease inhibitors. Buffer A contained 25 mM HEPES pH 7.4, 400 mM KCl, 10% glycerol, 1 mM DTT. The cells were passed through an 18 gauge needle using a 60 ml syringe. 10 ml buffer A with 20% Triton X-100 was added to the suspension before passing through the cell disruptor 2-3 times. The resulting lysate was centrifuged at 20,000 rpm for 40 min. The supernatant was filtered with a 0.45 μM syringe filter (Nalgene) and mixed with 1.5 ml slurry of the prewashed Ni-NTA beads (Qiagen) per liter of culture and incubated in the cold room for 2 hr. The mixture was then put through a gravity flow column to allow unbound proteins to flow through the beads. The beads were then washed with imidazole gradient (in

buffer A and 1% β-OG) and eluted with 400 mM imidazole in buffer A and 1% β-OG. The eluate was subjected to ion exchange chromatography (Source Q) using 50 mM Tris pH 8.0, 2 mM DTT, and 1% β-OG as buffer QA and 50 mM Tris pH 8.0, 2 mM DTT, 1 M NaCl, and 1% β-OG as buffer QB. Purity and stoichiometry of the complex was then assessed by SDS-PAGE, and the protein concentration was determined by UV280 absorbance.

4.2.3 Preparation of Liposomes and Reconstitution of the SNAREs

Two different lipid compositions were used for preparation of liposomes:

1. A lipid composition commonly used in the field (Webber 1998, parlati 1999, Kweon 2003): 85% POPC (1-palmitoyl, 2-oleoyl phosphatidylcholine) and 15% DOPS (1,2-dioleoyl phosphatidylserine).

2. A lipid composition also used for reconstitutions and more similar to those of synaptic vesicles (Shen 2007, Shen2010): 60% POPC (1-palmitoyl, 2-oleoyl phosphatidylcholine), 20% POPE (1-palmitoyl-2-oleoyl-sn-glycero-3-phosphoethanolamine), 10% DOPS (1,2-dioleoyl-sn-glycero-3-phospho-L-serine) and 10% cholesterol.

All lipids were obtained from Avanti Polar Lipids and kept in chloroform at -20 ℃. For fluorescent donor liposomes, 1.5% NBD PE (1,2-dipalmitoyl-sn-glycero-3-phosphoethanolamine-N-(7-nitro-2-1,3-benzoxadiazol-4-yl)) and 1.5% Rho PE (1,2-

dioleoyl-sn-glycero-3-phosphoethanolamine-N-(lissamine rhodamine B sulfonyl)) were included.

Two main methods have been used to reconstitute SNAREs into proteoliposome. One is the "direct" method (Kweon 2003). 200 µl of 15 mM lipids with either composition 1 or composition 2 were mixed in chloroform. The lipid mixture was dried under a nitrogen stream to form a thin film at the bottom of a glass tube. The resulting lipid film was then dried thoroughly under vacuum overnight at room temperature. The lipid film was then rehydrated with 200 µl of reconstitution buffer (25 mM HEPES pH 7.4, 100 mM KCl, 2 mM $MgCl_2$, 2 mM DTT, 10% glycerol) and vortexed thoroughly for 5 minutes. The mixture was then subjected to 5 freeze/thaw cycles in liquid nitrogen. The lipid suspension was then forced through an 80 nm pore size filter for at least 21 times. After extrusion, the liposomes were subjected to dynamic light scattering to assess their homogeneity and size. For preparation of the Syb2 liposomes (*v*-liposomes), 200 µl of purified Syb2 (40 µM) and 100 µl of the preformed donor liposomes (15 mM) were mixed. For preparation of the SyxSN25 liposomes (*t*-liposomes), 200 µl of purified SyxSN25 (15 µM) and 100 µl of the preformed acceptor liposomes (15 mM) were mixed. The mixture was rotated for 30 min at room temperature. Detergent was then removed by extensive dialysis. The mixture was transferred to a Slide-A-Lyzer 10 kDa cutoff dialysis cassette (Pierce) and first dialyzed in 1 L reconstitution buffer containing 1g/L Biobeads SM2 beads (Bio-Rad) for one hour at room temperature, followed by another dialysis against 1L of fresh reconstitution buffer containing 1g/L SM2 beads for two more hours. Finally, the sample was transferred to 2 L reconstitution buffer containing 2 g/l SM2

beads and dialyzed at 4 ℃ overnight. After the final dialysis, the quality of the liposomes was assessed by DLS. The protein was analyzed by SDS-PAGE followed by Coomassie Blue staining.

The other method to prepare liposome is the "standard" method (Weber 1998). The procedure to make thin lipid films were the same as the direct method. The dried lipids were hydrated with reconstitution buffer and 1-2% *β*-OG, or mixed directly with SNARE proteins with a proper protein to lipid molar ratio and incubated for 15min at room temperature. The resulting solution was quickly diluted at least 3 times until the concentration of *β*-OG was below its critical micellar concentration (CMC) to spontaneously form SNARE-liposomes. Residual *β*-OG was removed by extensive dialysis as described for the direct method.

4.2.4 Purification of Liposomes by Floatation

A Histodenz gradient was used to purify the proteoliposomes and separate the unincorporated proteins from liposomes (Shen *et al.* 2007). Typically, 150 µl of reconstituted liposomes were mixed with an equal volume of 80% (w/v) Histodenz (Sigma) and placed on the bottom of 5 × 41 mm ultracentrifuge tubes (Beckman). Then the liposomes were overlaid with 250 µl of 30% (w/v) Histodenz. Additional 50 µl reconstitution buffer (without glycerol) was placed on the top of the tube. The samples were centrifuged in a SW55 rotor (Beckman) at 48,000 rpm for 4 hours at 4 ℃. The top 75 µl of gradient was collected and analyzed by SDS-PAGE and Coomassie Blue staining.

4.2.5 Fluorescence Resonance Energy Transfer (FRET) Assays

Single cysteine mutant Munc18-1(K125C) was purified and labeled with *N*-(2-aminoethyl) maleimide BODIPY-FL (Molecular Probes) as a donor fluorescence probe in 20 mM HEPES (pH 7.4) and 100 mM KCl. Syb2(S61C) was labeled with tetramethylrhodamine-5-iodoacetamide dihydroiodide (Molecular Probes) as a fluorescence acceptor probe. The FRET assays were performed as described in Chapter 3. As for Munc18-1-lipid binding tests, the liposomes were composed of 20% DOPS, 5% Dansyl PE, 5% PI, 70% POPC and were prepared by extrusion. FRET from the tryptophan residues of rat Munc18-1 to the dansyl chromophore in liposomes was monitored by recording dansyl emission at 515 nm with excitation at 290 nm, using 10 nm bandwidths for both excitation and emission. The data were recorded on a PTI fluorimeter at room temperature.

4.2.6 Dynamic Light Scattering Tests

Dynamic light scattering (DLS) experiments were performed on a Protein Solutions DynaPro instrument equipped with a temperature-controlled microsampler (Wyatt Technology), using 10 s acquisition time and 10% laser power. The samples were prepared in a total volume of 20 µl and each measurement was done as an average of 30 data points. The samples were diluted to a final lipid concentration of 30 µM and centrifuged at 13,000 rpm for 10 min, or immediately placed in the cuvette for measurement. The results were then processed with the program Dynamics V6. The radii

and the size distribution were calculated with the regularization algorithm provided by this software.

4.2.7 Thermal Denaturation

Thermal Denaturation curves were recorded on an Aviv model 62DS spectropolarimeter using a 1 mm path length cell monitoring the CD absorption at 220 nm. The sample contained 2 μM rMunc18-1, or 4 μM WT, or mutant sMunc18s in PBS buffer in the presence or absence of 30 μM liposomes. The fraction of unfolded protein at each temperature was calculated by using the formula $(I_{obs}-I_f)/(I_u+I_f)$, where I_{obs} is the observed signal intensity, and I_u and I_f are the signal intensities of the unfolded and folded states, respectively.

4.2.8 Lipid Mixing Assays

Proteoliposomes containing either synaptobrevin-2 (v-SNARE) or SyxSN25 (t-SNARE) were reconstituted with P/L mol ratios of 1:200 and 1:500, respectively. t-liposomes contained a 6:2:1:1:1 mixture of POPC, POPE, POPS and cholesterol. v-liposomes contained the same lipid mixture but replaced 20% PE with 17% PE, 1.5% NBD PE and 1.5% Rho PE. 5 μl v-liposomes (2 mM lipids, 10 μM Syb2) and 45 μl t-liposomes (1 mM lipids, 2 mM SyxSN25) were mixed in the presence of 4 μM Munc18 and incubated for 3 hr at 4 ℃. A 50 μl quartz fluorometer cuvette ((Nova Biotech) was preincubated at 37 ℃. Lipid mixing was followed by NBD fluorescence emission at 533 nm (460 nm excitation) monitored with a Photon Technology Incorporated (PTI)

fluorimeter. At the end of the reaction, 1% (w/v) Triton X-100 was added to solubilize the proteoliposomes and the resulting NBD fluorescence was used as the maximal signal for normalization.

4.2.9 Cryo-*Electron Microscopy*

Reaction samples contained high concentrations of lipids (3 mg/ml; DOPS/POPC = 15:85) in the presence or absence of 30 μM sMunc18-1. The samples were incubated at 37 ℃ for 5 min, and 3 μl were loaded on carbon-coated holey grids (Quantifoil Micro Tools GMBH) and blotted with Whatman #4 paper for 5 seconds. The grid was then frozen in liquid ethane using a Vitrobot automated vitrification device (FEI). Images were recorded on a 2K x 2K CCD camera and Kodak film using a JEOL 2200FS FEG transmission electron microscope. Sample temperature was kept at -175 ℃ with an Oxford holder. Electron density was kept at 20-30 electrons/$Å^2$ during each exposure by a minimum dosage system. An extensive examination of whole area on grids was necessary due to massive vesicle fusion.

4.3 Results and Discussion

4.3.1 Membranes do not Stimulate Munc18-Syb2 Binding

Munc18-125-BP binds to isolated synaptobrevin-61-Rho or TR in solution, where synaptobrevin contains only the cytoplasmic region (Xu *et al.* 2010)(see Chapter 3). ITC experiments and FRET have yielded *K*d values of 6-13 μM. Though this kind of

interaction is weak, it could be favored by strong cooperativity with the interactions of Munc18-1 with both membranes. To test the hypothesis that one membrane could favor the Munc18-1/SNARE interactions, I used fluorescence labeled proteins and proteoliposomes. The single mutant of rat Munc18-1 where residue 125 was mutated to cysteine was purified as described previously (Chapter 3). Munc18-1(K125C) was then labeled with *N*-(2-aminoethyl) maleimide BODIPY-FL (Molecular Probes) as a donor fluorescence probe. The native cysteine (C103) in Syb2 was mutated to serine and a single-cysteine mutation was introduced at residue 61 (referred to as Syb2(S61C)). Purified Syb2(S61C) protein was labeled with tetramethylrhodamine-5-iodoacetamide dihydroiodide (Molecular Probes) as a fluorescence acceptor probe and then was incorporated into the liposomes with a protein:lipid ratio of 1:500. The liposomes were prepared with the commonly used lipid composition (POPC:DOPS=85:15 molar ratio) by extrusion. I refer to the labeled donor protein as Munc18-125-BP and acceptor proteoliposome as Syb2-61-v-Rho, respectively.

The Syb2 proteoliposomes were then further purified by gel filtration to remove the detergent and the unincorporated Syb2. The proteoliposome fractions were collected and analyzed by SDS-PAGE and Coomassie staining and the incorporated Syb2 concentration was estimated from the SDS-PAGE gel. After detergent removal, the Syb2 proteoliposomes were analyzed by DLS. The Syb2 proteoliposomes showed a narrow size distribution with an average radius of about 56 nm (Figure 4.1), indicating that the liposomes were quite homogeneous.

Titrations of Munc18-125-BP with variable Syb2 proteoliposome concentrations

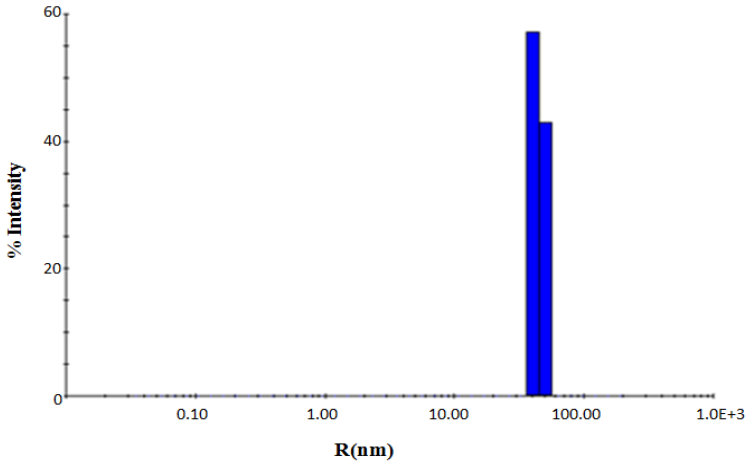

Item	R(nm)	%Pd
Peak	56.6	11.8

Figure 4.1

Figure 4.1 DLS analysis showing the radii and the size distribution of the Syb2 proteoliposomes.

The proteoliposomes were prepared with the commonly used lipid composition (85%POPC, 15% DOPS) by extrusion. R is the hydrodynamic radii and %Pd is the percentage of polydispersity.

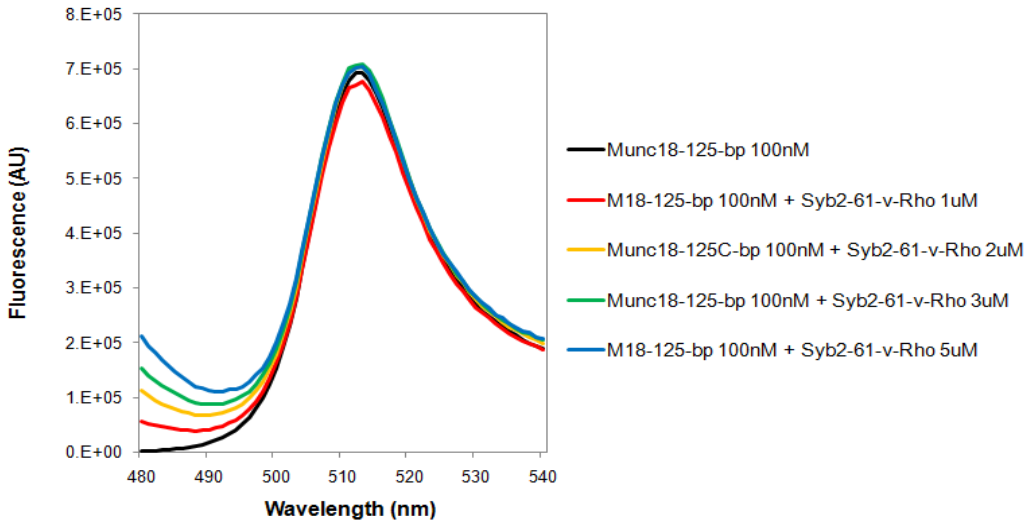

Figure 4.2

Figure 4.2 FRET experiments showing that proteoliposomes do not help Munc18-1 binding to Syb2.

Emission fluorescence spectra of 100 nM Munc18-125-BP and variable concentrations of Syb2-61-rho proteoliposomes.

did not yield observable FRET (Figures 4.2). Though I expected to observe more efficient FRET and tighter binding of Munc18-1/Syb2 with the help of these membranes than in solution, this result was not striking and to some extent it was consistent with the notion that synaptobrevin was restricted in the membrane. Thus, Hu and colleagues found that reconstituted Syb2 did not bind to soluble syntaxin-1 and SNAP-25 to form SNARE complexes, presumably because it was sequestered by the membrane (Hu *et al.* 2002). Later, using EPR and fluorescence quenching experiments, Kweon *et al*. (Kweon *et al.* 2003) showed that about 10 residues from the C-terminus of the synaptobrevin SNARE motif, responsible for Munc18-1 binding, are inserted in the membrane and form a short α-helix that is tilted ~33 °with respect to the plane of the membrane (Figure 4.3).

My data showed that the membrane did not favor the Munc18-1/Syb2 interaction, and even hindered the binding of Munc18-1 to Syb2. However, this result does not preclude the possibility that Munc18-1 cooperates with the membrane in binding to the SNAREs. I envision two scenarios of how such cooperation could arise. First, because of the membrane restriction of Syb2 as Kweon et al., described, there could be dynamic and transient states where the SNARE motif C-terminus is buried in the membrane or exposed to bind Munc18-1. It may be difficult to detect such flexible Munc18-1-Syb2 interaction in a reconstituted system by using FRET. However, this weak and transient binding might be sufficient to lower the energy barrier of the Syb2 release and thus favor the formation of the SNARE complex. Second, this study of the interactions of Munc18-1 with the reconstituted Syb2 proteoliposomes involved only one membrane. Munc18-1 contains two highly positive surfaces surrounding the SNARE-binding cavity that could

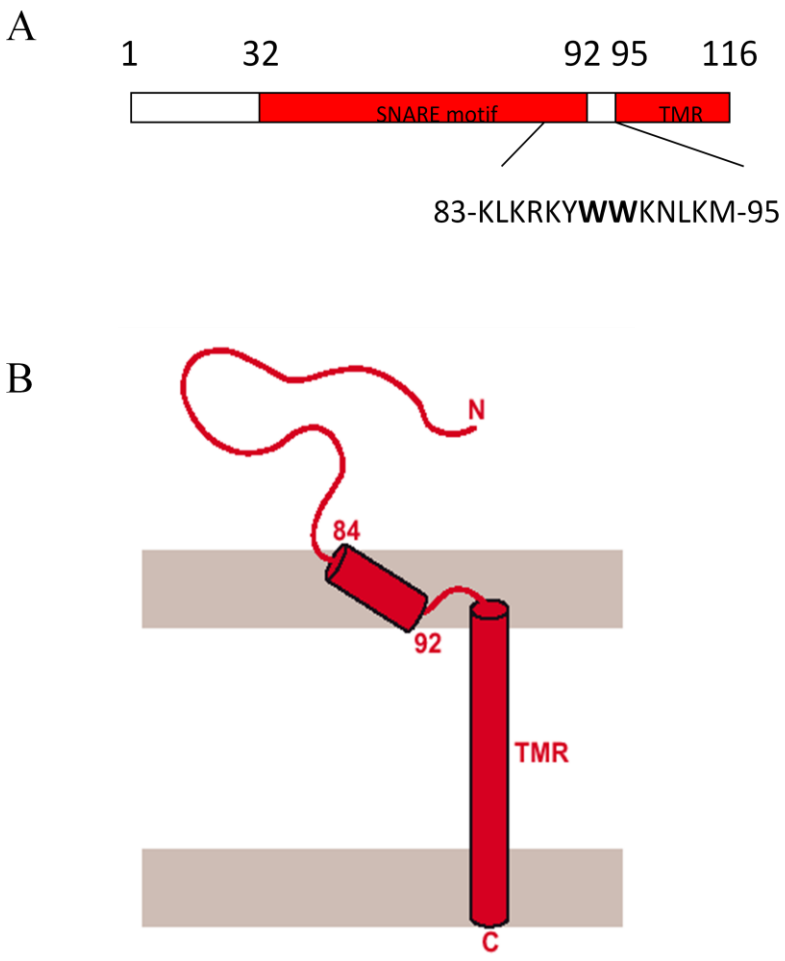
A
1
32
92 95
116
SNARE motif
TMR
83-KLKRKYWWKNLKM-95
B
N
84
92
TMR
C

Figure 4.3

Figure 4.3 Motif diagram summarizing the model of the structure of Syb2 in its membrane environment (Kweon *et al.* 2003).

(A). The domain structure of synaptobrevin2 with the SNARE motif and TMR colored in red. TMR stands for transmembrane region.

(B). The C-terminal transmembrane region (TMR) of synaptobrevin2, represented by a long cylinder, inserts perpendicularly into the lipid bi-layer. The SNARE motif of synaptobrevin2 comprises residues 28−93 and most of them are flexible and accessible (represented by a curving line). However, residues (84-92) form a short α-helix (short cylinder) in the interfacial region and is tilted ~33 ° with respect to the plane of the membrane. The interfacial regions of the membrane are gray (Kweon *et al.* 2003).

bind to two apposed membranes. Therefore, Munc18-1 might function by interaction with two membranes between v- and t- SNARE proteoliposomes, rather than Syb2 proteoliposomes alone. Further research will be necessary to test these possibilities.

4.3.2 Analysis of direct Munc18-1/lipid Interactions

In order to test the possibility that Munc18-1 might function by interaction with apposed liposome membranes, I first tested Munc18-1-lipid binding by monitoring the resonance energy transfer from the tryptophan residues of the rat Munc18-1 to a dansyl chromophore incorporated into the lipid vesicles (Zhao *et al.* 2005). If rat Munc18-1 indeed interacts with membranes, there should be an increase in dansyl fluorescence intensity upon addition to liposomes containing dansyl PE.

The dansyl liposomes were composed of 20%DOPS, 5% Dansyl PE, 5%PI, 70% POPC (or 20%DOPS, 10% Dansyl PE, 70% POPC) and were prepared by extrusion. The exposure of dansyl liposomes (30 μM) to rat Munc18-1 (7 μM) in 20 mM HEPES and 100 mM KCl at pH 7.4 did not increase dansyl fluorescence at 515 nm significantly following excitation of the tryptophan residues at 280 nm, thus indicating that rat Munc18-1 was not binding to membranes directly (Figure 4.4). Subsequently, Lijing Su performed 1D NMR assays using ^{15}N labeled sMunc18-1 and liposomes with 85% POPC and 15% POPC, and she confirmed that sMunc18-1 did not bind to liposomes at 20 ℃, although the signal of Munc18-1 started to drop upon incubation at 37 ℃.

The weak binding of rat Munc18-1 to liposomes was observed with a co-flotation

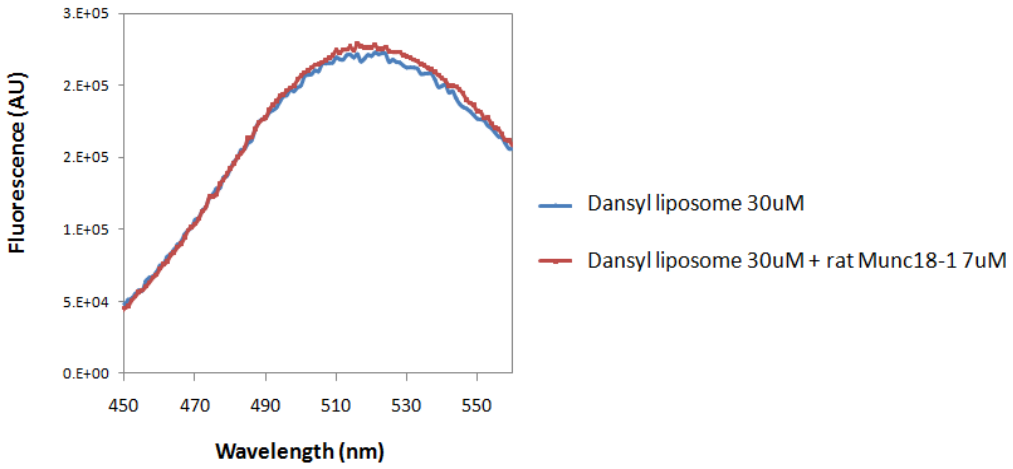

Figure 4.4

Figure 4.4 FRET experiments showing that Munc18-1 does not bind to dansyl liposomes.

Fluorescence intensities of 30 µM dansyl liposomes alone (**Blue**) are very similar in the presence of 7 µM rat Munc18-1 (**Red**), indicating that there is no interaction of the tryptophan with the dansyl chromophore. FRET experiments were done at room temperature.

assay (Guan *et al.* 2008). However this observation was debatable, since Shen and his colleagues showed that Munc18-1 did not bind to protein-free or v-SNARE liposomes in a flotation assay (Shen *et al.* 2007). The data from Shen *et al.,* suggested that Munc18-1 binds to the assembled trans-SNARE complex, indicating that Munc18-1 enhanced lipid mixing through interaction with the SNARE complex rather than membranes (Shen *et al.* 2007). Considering that Munc18-1s also enhances the syntaxin-1 stability and the transition to the docking stage, a possible explanation for the indispensable function of Munc18-1 in fusion could be that Munc18-1 is a key regulator of SNARE proteins and could boost SNARE complex formation in the last fusion step. Nevertheless, Munc18-1 may have a more direct function than a regulatory role. In fact, Munc18-1s are not the unique binding partners or regulators for the SNARE complex, and other proteins may play alternative/compensatory roles in initiating the complex formation, although none of them seems as important as Munc18-1 (Novick *et al.* 2006; Darios *et al.* 2009).

How Munc18-1s are involved directly in the fusion and how the functions of SM proteins and the SNARE family are coupled remains a mystery. Diverse models have been proposed to explain these questions. For example, SM proteins might bind to the SNARE four-helix bundle, by binding opposing membranes, enabling application of force to the membranes by the SNAREs (Rizo *et al.* 2006). Recently Shen and his colleagues reported that the N-peptide of syntaxin-1 recruits the SM protein Munc18-1/nSec1 to the SNARE four-helix bundle, thus promoting downstream assembly into a fusion complex (Rathore *et al.* 2010; Shen *et al.* 2010). It is still possible that SM

proteins are recruited to the trans-SNARE four-helix bundles through alternative routes, for example, interaction with membranes under certain conditions.

4.3.3 Munc18 can induce Membrane Rearrangements

To study the biological relevance of the Munc18-1/synaptobrevin interaction, a lipid mixing assay was employed. I tried to build up a well-characterized fusion system (Weber et al. 1998; Shen et al. 2007) in our lab, in which regulator proteins can be added to reconstituted SNAREs proteoliposomes. This assay involves fluorescence resonance energy transfer (FRET) between NBD-DPPE, the donor, and rhodamine-DPPE, the energy acceptor. When both fluorescent dyes are present in liposomes at appropriate surface densities, for example 1.5% each, the NBD fluorescence will be quenched because of the energy transfer. The liposomes with both fluorescence lipids are called the donor liposomes. Once they fuse with nonfluorescent acceptor liposomes, the surface densities of both fluorescent lipids are reduced, resulting in a decrease in quenching and an increase in NBD fluorescence (see Figure 4.5).

Liposomes were initially prepared with a commonly used composition (POPC:DOPS 85:15 molar ratio) and by the "standard method" (Rigaud and Levy 2003), in which dried lipids were dissolved in a detergent solution of proteins, followed by removal of detergent. The protein:lipid ratios for v- or t-SNARE liposomes were 1:1000, which is below the protein densities in synaptic vesicles (Takamori *et al.* 2006). After detergent removal by extensive dialysis, the liposomes were analyzed by DLS. All the plain donor or acceptor liposomes and SNAREs liposomes showed an average radius of

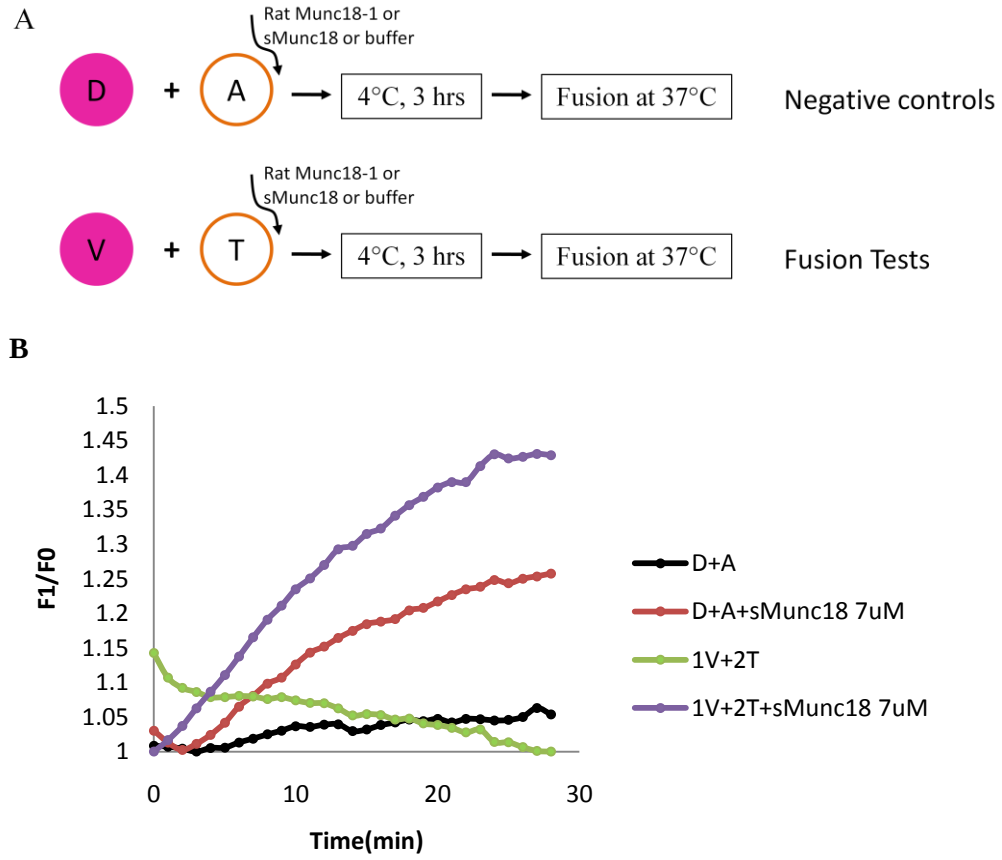
A
Rat Munc18-1 or sMunc18 or buffer
D
+
A
4°C, 3 hrs
Fusion at 37°C
Negative controls
Rat Munc18-1 or sMunc18 or buffer
V
+
T
4°C, 3 hrs
Fusion at 37°C
Fusion Tests
B
F1/F0
1.5
1.45
1.4
1.35
1.3
1.25
1.2
1.15
1.1
1.05
1
0
10
20
30
Time(min)
D+A
D+A+sMunc18 7uM
1V+2T
1V+2T+sMunc18 7uM

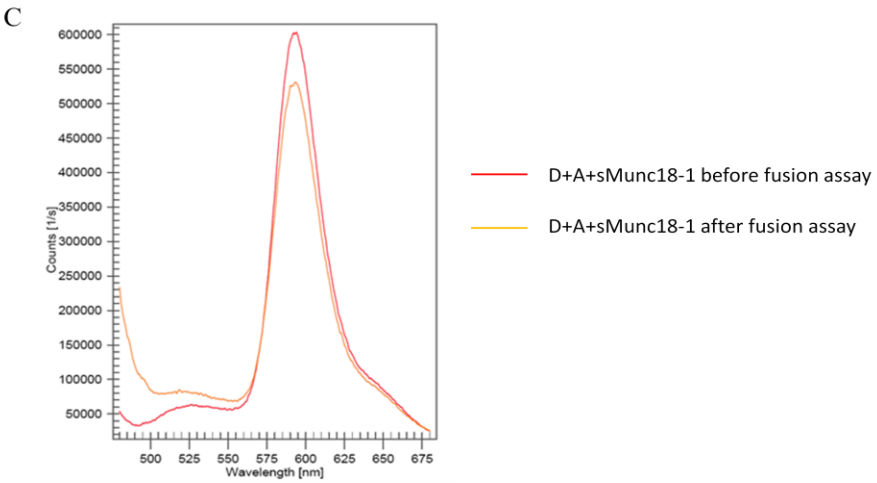
C
Counts [1/s]
600000
550000
500000
450000
400000
350000
300000
250000
200000
150000
100000
50000
500
525
550
575
600
625
650
675
Wavelength [nm]
D+A+sMunc18-1 before fusion assay
D+A+sMunc18-1 after fusion assay

Figure 4.5

Figure 4.5 sMunc18-1 activates lipid mixing.

(A) Incubation procedures for lipid mixing reactions catalyzed by preassembled SNARE complexes. D and A represent protein free donor liposomes and acceptor liposomes, respectively. V represents donor liposomes reconstituted with v-SNARE. T represents acceptor liposomes reconstituted with t-SNAREs.

(B) v- and t- liposomes were incubated with sMunc18-1 or buffer for 3 hr at 4 ℃ before the temperature was elevated to 37 ℃ to initiate lipid mixing. Plain donor liposomes were preincubated with sMunc18-1 or buffer at the 4 ℃ for 3 hr (negative control).

(C) Emission scans, exited at 465 nm, of negative control samples at the beginning or at the end of fusion assay. D stands for protein free donor liposomes. A stands for protein free acceptor liposomes.

about 60 nm (Figure 4.6). Consistent with DLS results, Cryo-EM images showed that the liposomes display a nice round shape of about 120 nm in diameter (Figure 4.7).

Recombinant squid Munc18 protein was expressed in *E.coli* and directly added to liposomes reconstituted with SNAREs (co-expressed SyxSN25 and Syb2) (Figure 4.5A). When t- and v-liposomes were mixed in the absence of sMunc18-1 at the beginning of the fusion assay, little lipid mixing was observed (Figure 4.5B). In contrast, in the presence of sMunc18-1, effective lipid mixing occurred. I next considered whether sMunc18-1 had the same effect on the fusion kinetics of plain liposomes. To my surprise, sMunc18-1 stimulated the initial rate of lipid mixing as well (Figure 4.5B). It seemed that sMunc18-1 could bypass the SNARE proteins to cause effective lipid mixing. To further investigate whether the increased fluorescence intensities resulted from donor liposomes mixing with acceptor liposomes or other routes, I took one emission scan before the repeated fusion assay and another afterwards. I observed a slight decrease in the acceptor emission intensity and an increase in the donor intensity. Moreover, most of this increase arises from a large scattering tail (Figure 4.5C). Since the intensity of scattered light depends on average molecular weight and particle size, the increased light scattering in the emission scan indicated that particles in suspension become larger or become clustered. To confirm that it was the scattering, I analyzed the fusion assay sample by DLS at the beginning and at the end of fusion assay, respectively. DLS data showed that the sample containing plain liposomes alone or reconstituted liposomes in the presence or absence of sMunc18-1 before fusion assay had average radii of ~ 72.8 nm (Figure 4.6). At the end of the fusion assay, I took the sample for DLS again, and I saw increased radii

~ 672 nm from those having sMunc18-1 in suspension (Figure 4.6), suggesting liposome clustering. Furthermore, addition of 20 μM syntaxin-1 or 1 M NaCl did not reverse the clustering of liposomes (Figure 4.6; Table 4.1).

I have tried various protein:lipid ratios with t-SNAREs ranging from 1:200 to 1:1000 and v-SNAREs from 1:100 to 1:2000, as well as various lipid composition, for example POPC:POPE:DOPS:cholesterol=60:20:10:10 molar ratio or POPC:POPE:DOPS:PI:cholesterol=50:20:10:10:10 molar ratio, and different ratios of v- and t-liposomes in the fusion assay. Though the Munc18-1 enhancement was not always reliable, the light clustering was always evident in the presence of Munc18-1 (Figure 4.8 E). Note that sMunc18-1 always gave a stronger effect on the acceleration of lipid mixing than rMunc18-1 (Figure 4.8 A-D). Preincubation seemed not to be important. However, the liposome preparation method mattered, because I observed much less stimulation of lipid mixing by Munc18-1 in separate experiments where the liposomes were prepared with the "direct method" (Chen *et al.* 2006)(Figure 4.8 D). These results are in conflict with the observation that preincubation of Munc18-1 with either t- or v-SNARE liposomes alone resulted in little activation and the claim that the effect of Munc18-1 was evident even in liposomes prepared by the direct method (Shen *et al.* 2007)(Figure 4.8). It is not clear why the difference in the fusion assay could lead to such different outcomes, whereas extensive studies are required to decipher the effect of Munc18 on membranes. Since sMunc18-1 has similar or even stronger effects than rMunc18-1 in the fusion assay, I used sMunc18-1 for the following tests.

It is not clear what happened in the sample containing Munc18 and liposomes,

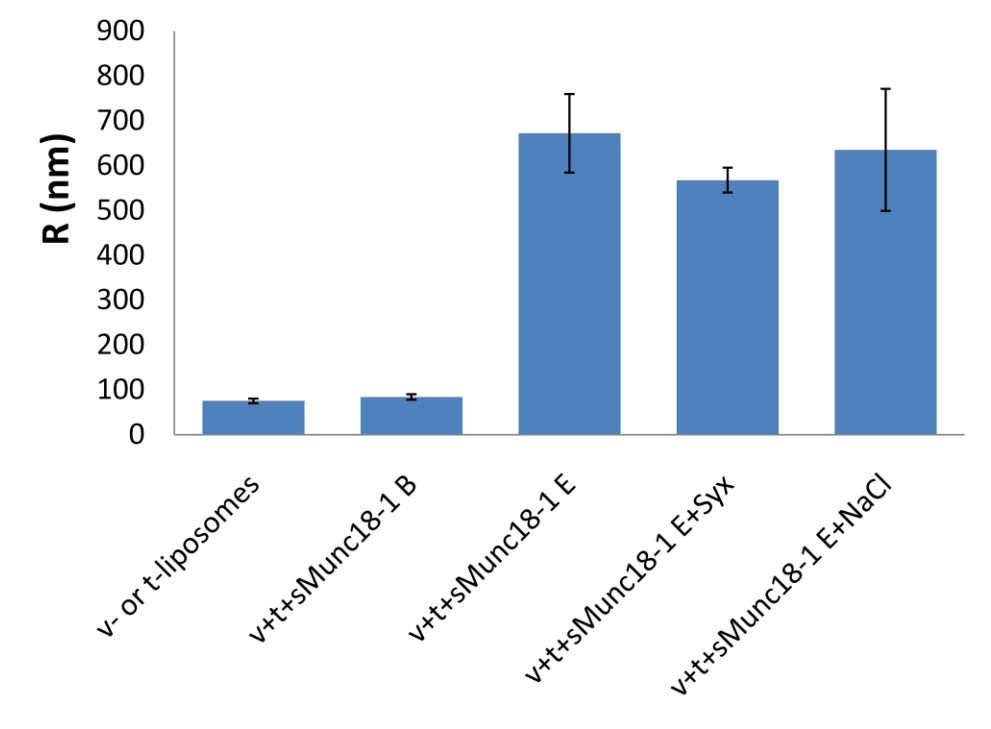

Figure 4.6

Figure 4.6 Summary of DLS analysis

DLS measurements of radius of samples containing reconstituted 30-50 μM vesicles either without additions (first bar), with 4 μM sMunc18-1 at the beginning of the fusion assay (second bar), at the end of the fusion assay of the same sample (third bar), upon adding 5 μM syntaxin-1 after the fusion assay (fourth bar), or upon adding 1 M NaCl after the fusion assay (fifth bar). All experiments were done at 37 ℃. Vesicles were made of 85%POPC and 15% DOPS via the direct method.

but the increased radius observed by DLS did suggest that the particles in the sample have larger molecular weight. Note that 1M NaCl and 20 μM syntaxin-1 could not reverse the clustering caused by sMunc18-1 (Figure 4.6), and temperature seemed important. sMunc18-1 did not induce vesicle clustering at room temperature overnight, but induced vesicle clustering in 5 min at 37 ℃ (Table 4.1). All these observations led us to the speculation that there might be some lipid mixing in addition to clustering. To clarify this assumption, I prepared phospholipid vesicles with 85%POPC and 15%DOPS and used Cryo-EM to visualize the vesicle clusters. 30 μM sMunc18-1 was incubated with 3 mM vesicles (DOPS/POPC = 15:85) at 37 ℃ for 5 min and then applied to a carbon-coated grid and fast frozen in liquid ethane. Images were collected on a JEOL Cryo-electron microscope by Alpay B. Seven, a graduate student in the Rizo lab. Consistent with DLS data, vesicles appeared to be dispersed in control experiments with an average diameter of ~ 75 nm in the absence of sMunc18-1, whereas vesicle clusters of diverse sizes were observed in the presence of 30 μM sMunc18-1 (Figure 4.7B,C). Importantly, giant vesicles with diameters over 1000 nm were observed and many vesicle pairs appeared to come into close contact with mass density being observed between the vesicles (Figure 4.7B). Moreover, some images showed the lipid bilayers from adjacent vesicles were very close and some vesicles were hemifused (Figure 4.7C).

Regardless of whether the lipid mixing caused by Munc18-1 is biologically relevant or artificial, my results show that Munc18-1 can cause dramatic membrane rearrangements under the conditions that are commonly used in all defined fusion systems. Hence, lipid mixing effect should be carefully interpreted. For instance, in

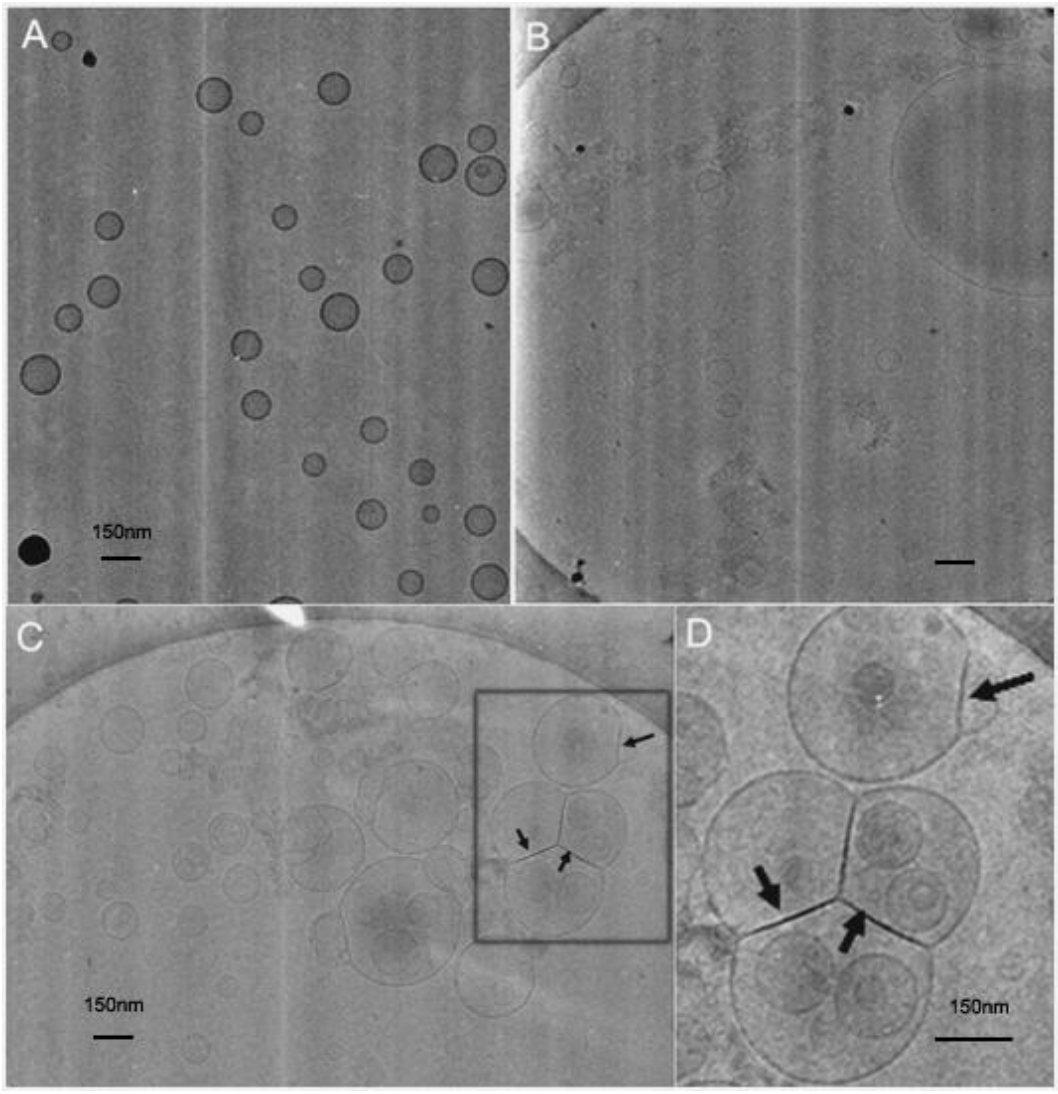

Figure 4.7

Figure 4.7 Cryo-EM of vesicle clustering and lipid mixing.

Cryo-EM images of samples containing 3 mM phospholipid vesicles in the absence (A) or presence (B,C) of 30 μM sMunc18-1. (C). The images illustrate the close proximity between membranes and the hemifusion of the vesicles (arrow). (D) Zoom-in view of a region of (C).

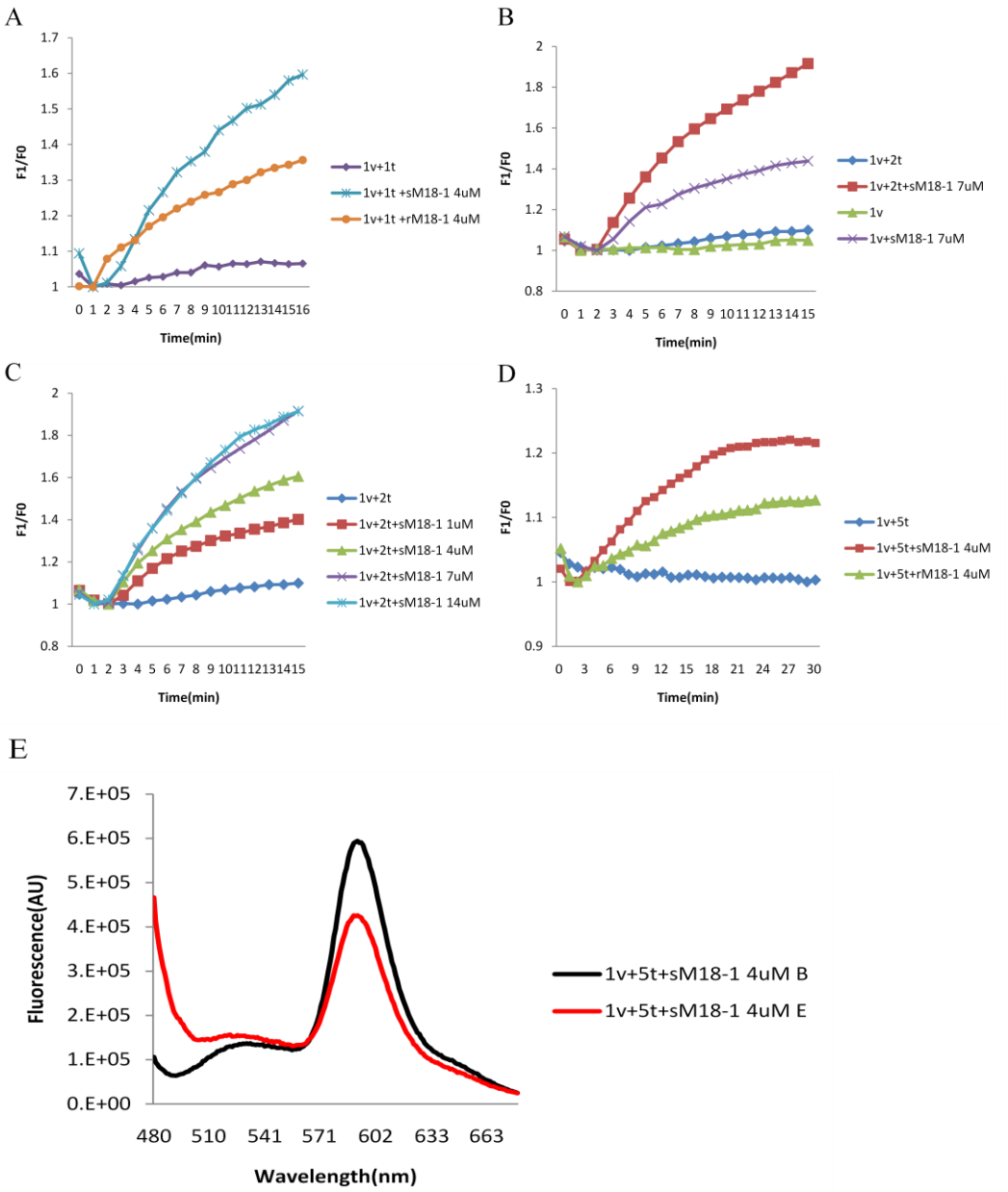
A
F1/F0
Time(min)
1v+1t
1v+1t +sM18-1 4uM
1v+1t +rM18-1 4uM
B
F1/F0
Time(min)
1v+2t
1v+2t+sM18-1 7uM
1v
1v+sM18-1 7uM
C
F1/F0
Time(min)
1v+2t
1v+2t+sM18-1 1uM
1v+2t+sM18-1 4uM
1v+2t+sM18-1 7uM
1v+2t+sM18-1 14uM
D
F1/F0
Time(min)
1v+5t
1v+5t+sM18-1 4uM
1v+5t+rM18-1 4uM
E
Fluorescence(AU)
Wavelength(nm)
1v+5t+sM18-1 4uM B
1v+5t+sM18-1 4uM E

Figure 4.8

Figure 4.8 Summary of various fusion assays.

Proteoliposomes were made of 50%POPC, 20% POPE, 10% POPS, 10% PI and 10% cholesterol via the standard method (A.B.C.E) or the direct method (D). Protein to lipid molar ratio was 1:1000 for both v- and t- proteoliposomes. v- and t- proteoliposomes were preincubated at equal molar ratio (A) or 1:2 molar ratio (B, C) or 1:5 molar ratio (D) with sMunc18-1 or rMunc18-1 for 3 hr at 4 ℃ before the temperature was elevated to 37 ℃ to initiate fusion assay. Note that 7 μM sMunc18-1 was added to v- liposomes directly and preincubated for 3 hr at 4 ℃ (B).

(E). Emission scans of the same samples from (D) at the beginning (black) and at the end (red) of the fusion assay, respectively. B represents beginning. E represents end.

	Temperature(℃)	Time	R(nm)
30 μM Vesicles	25/37	/	55-80
30 μM Vesicles+4 μM sMunc18-1	25	2 hr	60
30 μM Vesicles+4 μM sMunc18-1	25	O/N	131
30 μM Vesicles+4 μM sMunc18-1 O/N+0.5 M NaCl	25		128
30 μM Vesicles+4 μM sMunc18-1 O/N+ 20 μM Syx	25		137
30 μM Vesicles+4 μM sMunc18-1	37	5 min	151
30 μM Vesicles+4 μM sMunc18-1	37	10 min	> 500
30 μM Vesicles+4 μM sMunc18-1 after 10min+ 20 μM Syx	37		> 500
30 μM Vesicles+4 μM sMunc18-1 after 10min+ 1 M NaCl	37		> 500
30 μM Vesicles+4 μM sMunc18-1+4 μM Syx	37	10 min	139
30 μM Vesicles+4 μM sMunc18-1+1M NaCl	37	10 min	55
30 μM t-vesicles+60 μm v-vesicles	37	1 hr (at the end of fusion assay)	55-65
30 μM t-vesicles+60 μm v-vesicles +4 μM sMunc18-1	37	1 hr (at the end of fusion assay)	> 500

Table 4.1 Summary of DLS measurements.

Plain vesicles are made of 85% POPC and 15%DOPS. Proteoliposomes were made of 50%POPC, 20% POPE, 10% POPS, 10% PI and 10% cholesterol.

Figure 4.5B, if I regard the stimulation that is caused by sMunc18-1 on plain liposomes as noise, which could happen in any sample containing both Munc18 and liposomes, the real enhancement of sMunc18-1 was quite small.

In summary, I could not establish a reliable fusion system or repeat what happened in other reconstituted systems as defined in the literature. However, I observed liposome clustering and lipid mixing that was caused solely by Munc18-1, as shown by DLS analysis and Cryo-EM images.

4.3.4 Denaturation of Munc18 causes Lipids Clustering and Mixing

Admitting that there were no direct binding of Munc18-1 to liposomes, Munc18-1 indeed causes membrane lipid mixing by itself and it has to contact the membranes in some manner. To explore whether Munc18s act as fusion proteins and how they could contact membranes, I looked into the sequence and a structure-based alignment of Sec1/Munc18 (SM) proteins. Yeast Vps33, Sly1, rat Munc18-1 and squid Munc18-1 have strikingly similar crystal structures, despite relatively low primary sequence homology (Pieren *et al.* 2010). They all contain two highly positive surfaces surrounding the SNARE-binding cavity (Figure 4.9), which presumably could touch both membranes. To obliterate the capability of sMunc18-1 to fuse membranes, we designed double-mutations on the conserved positive surface as follows, sMunc18-1(K319EK323E), sMunc18-1(K117ER122E), sMunc18-1(K330EK331E) and sMunc18-1(K20EK21E).

To test whether these four mutants of sMunc18-1 lost the ability to cause lipid mixing, I employed DLS to examine the scattering in sample suspension. 4 μM purified sMunc18-1 mutant protein was added to 30 μM plain liposomes made by extrusions. All mutants induced scattering after several minutes at 37 ℃ and stimulated lipid mixing (Figure 4.10). Note that, since the mixture of Munc18-1 and syntaxin-1 could inhibit the liposome clustering as indicated by DLS measurements (Table 4.1), I speculated that the clustering might be attributable to the instability of Munc18-1. To test this possibility, I purified WT rMunc18-1, WT sMunc18-1 and mutant sMunc18-1s. Thermal melting experiments monitored by circular dichroism showed that the melting (transition midpoint) temperature (T_m) of the WT rMunc18-1 was about 8 ℃ lower than that of the WT sMunc18-1 (43 ℃ for the WT sMunc18-1 and 51 ℃ for the WT rMunc18-1) (Figure 4.11A). The obtained T_m of sMunc18-1 mutants was close to the WT sMunc18-1, but the slope of the denaturation curve of sMunc18-1(K20EK21E) appeared to be smaller than the other mutants (Figure 4.12B). The fact that sMunc18-1(K20EK21E) was thermolabile compared to wild type and other mutant sMunc18-1 was in agreement with the lipid mixing assay data, which showed that sMunc18-1(K20EK21E) enhanced lipid mixing most effectively (Figure 4.10).

To investigate the effect of sMunc18-1 on the liposomes, I recorded CD spectra every 2 minutes and collected DLS data with the same samples. As shown in figure 4.12A, the signal of sMunc18-1 kept dropping, which indicated the unfolding of sMunc18-1, while the average radii of liposomes kept increasing (Figure 4.12B). Since it became clear that it was the denaturation of Munc18-1 that caused the liposome

clustering and lipid mixing, chemicals such as glycerol or sucrose that stabilize proteins should be able to eliminate the effect of sMunc18-1 on liposomes. Indeed, melting experiments revealed that the T_m of the sMunc18-1 in PBS with 10% glycerol was about 2 ℃ higher than that of the sMunc18-1 in PBS alone (Figure 4.13). Furthermore, DLS data showed 15% glycerol was enough to stabilize sMunc18-1 without causing liposome clustering or lipid mixing over the course of an hour (Figure 4.14).

It has been recognized that insertion of hydrophobic peptides into the membrane can cause disorders in membrane lipid packing and thus can help to overcome the energy required for fusion (White 1992; Bentz 2000). Without a chaperone to stabilize Munc18, it tends to denature at 37 ℃, and unfolded Munc18-1 in turn inserts into the membrane, causing lipid mixing. Most defined reconstitution systems require 37 ℃ incubation for lipid mixing. Hence, caution should be taken when interpreting the results of lipid mixing assays, and one should ensure that the results are not due, at least in part, to protein denaturation.

4.4 Conclusion

The study of the relevance of membranes and Munc18-SNARE proteins interactions indicates that membranes did not help Munc18-1 bind to synaptobrevin, and there is no direct interaction between membranes and Munc18-1 at room temperature. But when brought to 37 ℃, which is required for most reconstitution systems, Munc18-1 gets denatured, and unfolded Munc18-1 tends to cause lipid rearrangement.

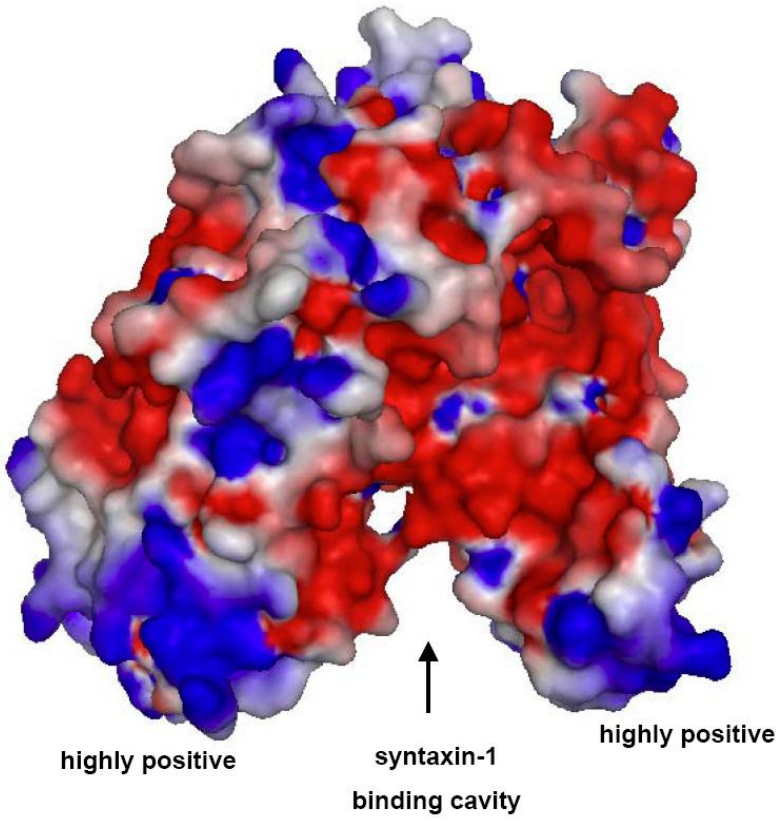

Figure 4.9

Figure 4.9 Surface electrostatic potential of rat Munc18-1.

The electrostatic potential was contoured at the 5 kT/e level, with red denoting negative potential and blue denoting positive potential. The location of the syntaxin-1 binding cavity is indicated. Note the two highly positive regions on both sides of the cavity.

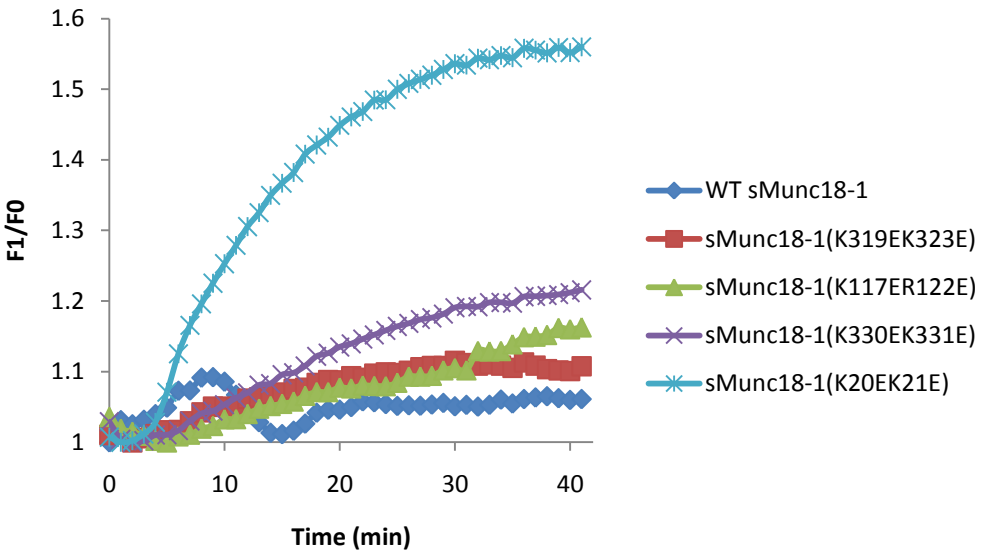

Figure 4.10

Figure 4.10 Mutant sMunc18-1s stimulate neuronal SNARE-mediated lipid mixing.

Lipid mixing of neuronal v- and t- SNARE liposomes in the presence of 4 μM WT and mutant sMunc18-1s.

A

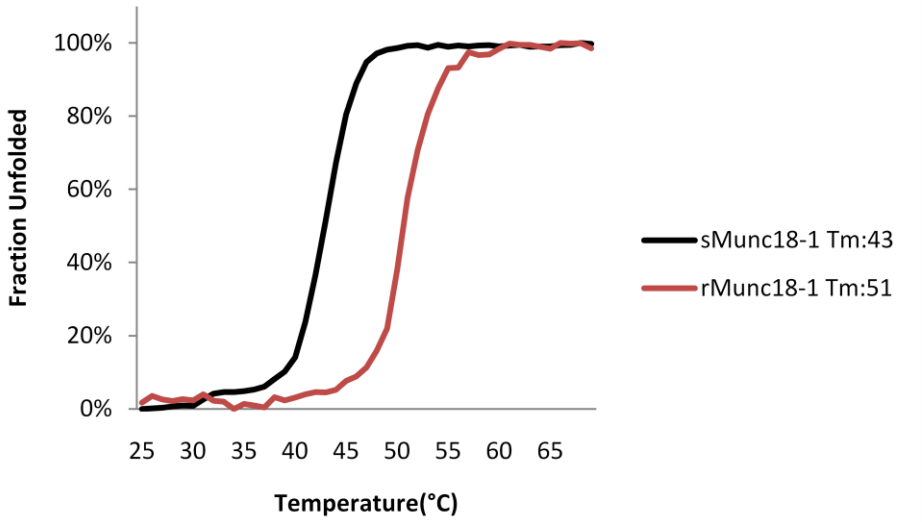

B

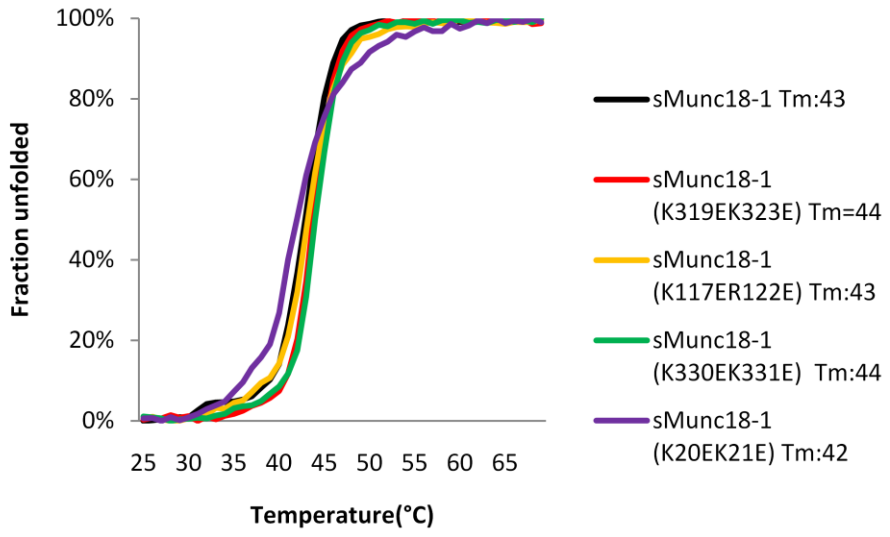

Figure 4.11

Figure 4.11 Analysis of mutant sMunc18-1s by thermal denaturation.

(A). Thermal denaturation curves of 4 μM WT rMunc18-1 (red) or sMunc18-1 (black).

(B). Thermal denaturation curves of 4 μM mutant sMunc18-1s.

Denaturation as a function of temperature was monitored by the decrease in the CD absorbance at 220 nm associated with the loss of helical structure upon disassembly. Thermal denaturation curves were normalized to the fraction of unfolded protein.

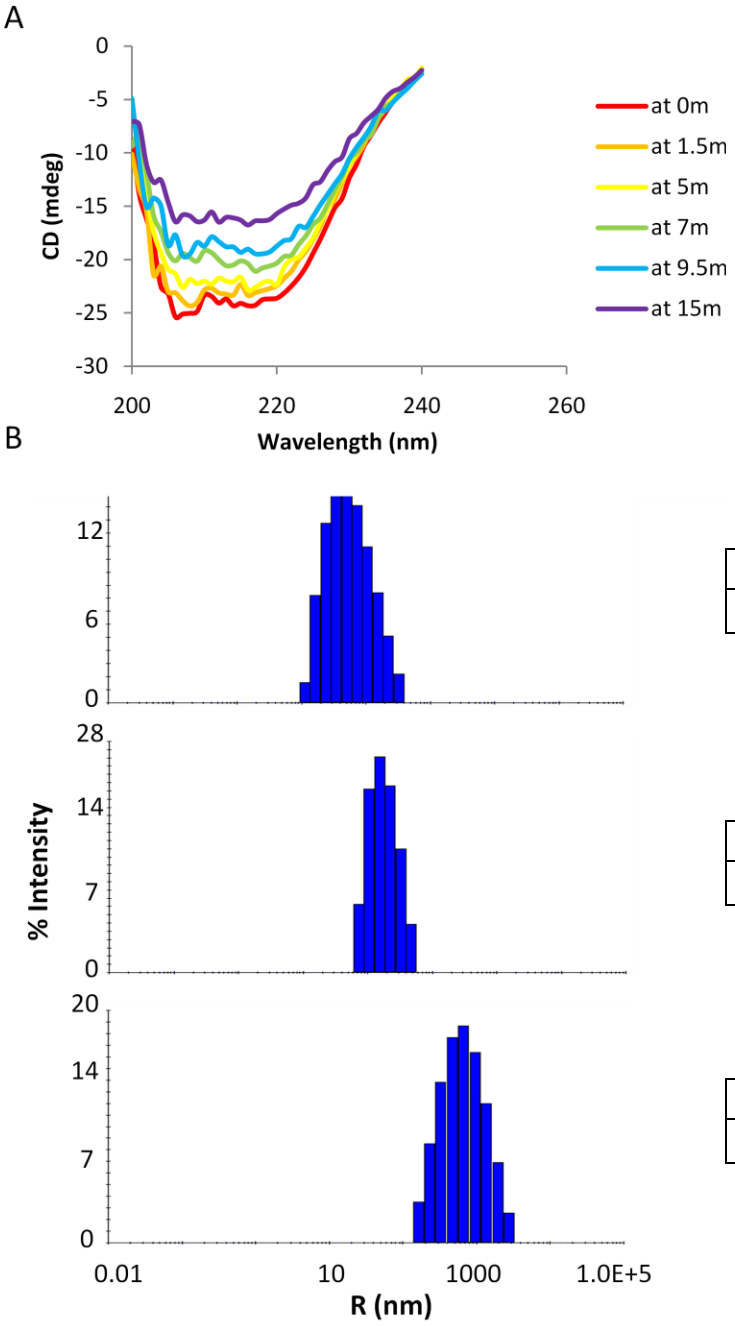

Time	R(nm)	%Pd
0 m	71.5	87.3

Time	R(nm)	%Pd
3 m	201.1	52.3

Time	R(nm)	%Pd
15 m	817.9	71.3

Figure 4.12

Figure 4.12 CD and DLS analysis of K117ER122E mutant sMunc18-1.

(A). CD spectra of 4 μM mutant K117ER122E sMunc18-1 in the presence of 30 μM phospholipid vesicles at different time points.

(B). DLS analysis of 4 μM mutant K117ER122E sMunc18-1 in the presence of 30 μM phospholipid vesicles at different time points. The sample for CD and DLS analysis was identical.

All experiments were done at 37 ℃.

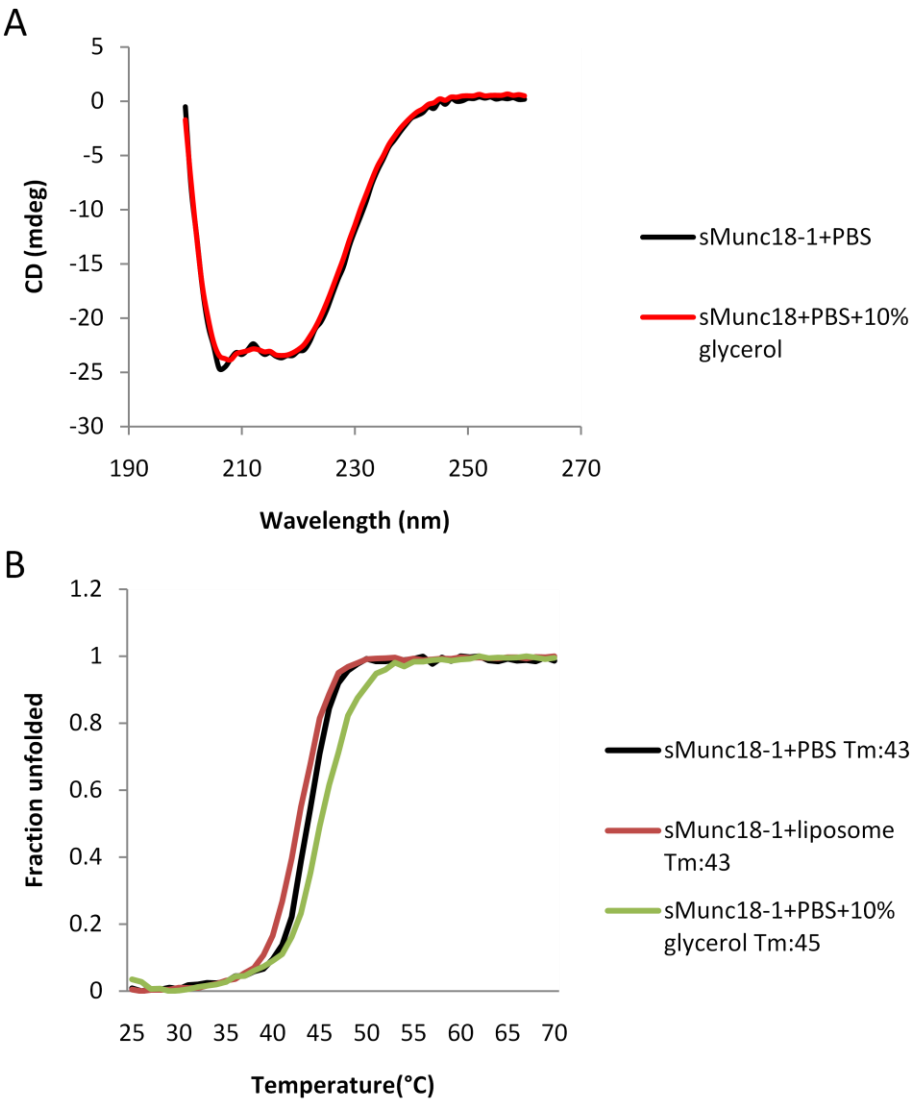
A
5
0
-5
-10
-15
-20
-25
-30
CD (mdeg)
190
210
230
250
270
Wavelength (nm)
sMunc18-1+PBS
sMunc18+PBS+10% glycerol
B
1.2
1
0.8
0.6
0.4
0.2
0
Fraction unfolded
25
30
35
40
45
50
55
60
65
70
Temperature(°C)
sMunc18-1+PBS Tm:43
sMunc18-1+liposome Tm:43
sMunc18-1+PBS+10% glycerol Tm:45

Figure 4.13

Figure 4.13 Analysis of the WT sMunc18-1s by circular dichroism and thermal denaturation

(A). Circular dichroism spectra of 4 μM WT sMunc18-1 in the presence of PBS buffer (black), or PBS buffer with 10% glycerol (red),

(B). Thermal denaturation curves of 4 μM WT sMunc18-1 in the presence of PBS buffer (black), or PBS buffer with 10% glycerol (green), or in the presence of 30 μM liposomes (red).

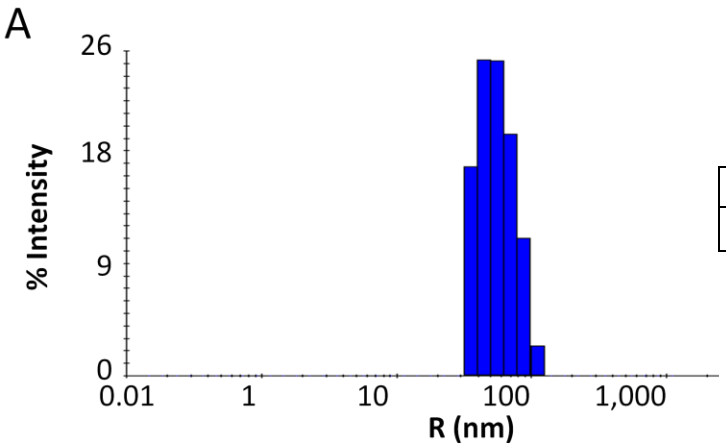

Time	R(nm)	%Pd
0 m	57.4	31.7

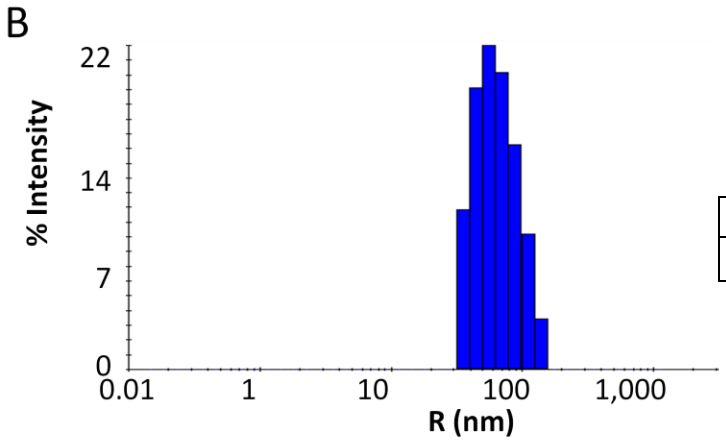

Time	R(nm)	%Pd
42 m	67.5	38.2

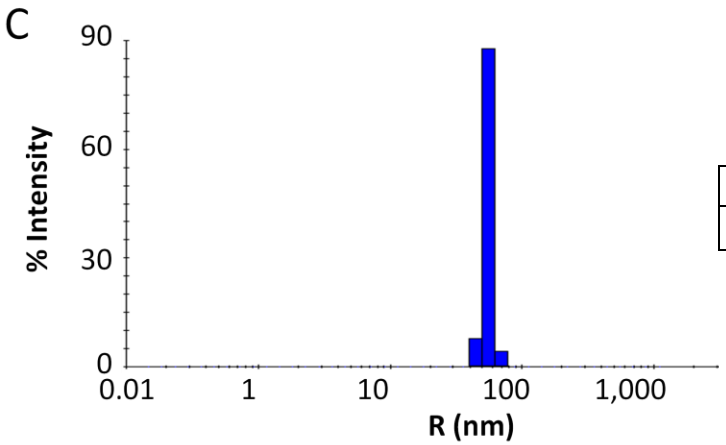

Time	R(nm)	%Pd
65 m	56.9	12.1

Figure 4.14

Figure 4.14 DLS analysis of phospholipid vesicles with sMunc18-1 in the presence of 15% glycerol.

DLS analysis showing the radii and the size distribution of 30 μM phospholipid vesicles with 4 μM WT sMunc18-1 in the presence of 15% glycerol at 0 minute (A), 42 minutes (B), or 65 minutes (B). Experiments were done at 37 ℃.

Chapter 5 Future Directions

Extensive studies of the neurotransmitter release machinery have led to the identification of the important components and to several models for their regulatory roles in the mechanism of release. The major actors for synaptic vesicle fusion include the neuronal SNAREs and Munc18-1. Their homologous proteins have been found to be conserved from yeast to humans, suggesting that synaptic vesicle fusion shares a common mechanism with many other types of intracellular vesicular traffic (Rizo and Südhof 2002). Neurotransmitter release, basically a membrane fusion process, is one of the most fundamental events in life, and research in this field has entered a new era while raising further questions.

The absolute requirement of Munc18-1 as well as SNAREs in neurotransmitter release has been widely acknowledged. Structural and functional analyses of Munc18-1 through rescue strategies in Munc18-1 null neurons, chromaffin cells, and Munc18-1/-2 knockdown cells have shown that Munc18-1 controls nearly all steps in the secretion cascade in conjunction with syntaxin-1 or with the SNARE complex (Khvotchev *et al.* 2007; Arunachalam *et al.* 2008; de Wit *et al.* 2009; Deák *et al.* 2009; Han *et al.* 2009). Different binding modes of Munc18-1 to SNARE proteins are now firmly established and different modes could control different steps (Toonen *et al.* 2006; Han *et al.* 2010). However, the most crucial question for understanding not only synaptic vesicle exocytosis but also intracellular membrane fusion in general remains unclear: why do fusion reactions universally require SM proteins?

To answer this broad question, we have to start somewhere with more specific subjects.

First, SM proteins are known as regulators of SNARE-mediated membrane fusion, but are they directly involved in fusion or present at the final stages of fusion, in addition to having a role in promoting the SNARE-complex assembly? Cryo-EM has great potential of producing moderate-resolution images of biological samples in their native environment. Recent advances in single-particle Cryo-EM have pushed the limit to near atomic resolution (Jiang *et al.* 2008; Yu *et al.* 2008; Zhang *et al.* 2008). Since only protein backbone models can be built from moderate Cryo-EM images, the value of such models for functional interpretation has been significantly limited. However a recent paper reported a 3.3Å full-atom structure of a nonenveloped virus at the priming state was obtained by Cryo-EM (Zhang *et al.* 2010). The development of Cryo-EM technology with high resolution but without the requirement for high symmetry could make it possible to "see" the proteins complexes on the vesicles at whatever stage. Alpay B. Seven is now working on the trans-SNARE complex anchored on the liposomes with Cryo-EM. Eventually, he would like to "see" how essential components of membrane fusion work together.

The binding of Munc18-1 to the SNARE complex is mediated partially through its interaction with the N-terminal peptide, as shown by the finding that mutations that abolish Munc18-1-syntaxin-1 binding impair the Munc18-1/SNARE complex interaction (Zilly *et al.* 2006; Rickman *et al.* 2007; Shen *et al.* 2007). Other mutations of residues of Munc18-1 that do not interact with the N-terminal peptide of syntaxin-1 have been

suggested to abolish binding to the SNARE complex (Boyd *et al.* 2008; Deák *et al.* 2009). The results from these studies suggest Munc18-1/SNARE complex assembly include interactions with the syntaxin-1 N-peptide and Habc domain. Thus, the second crucial question is: what is the structural basis for the interaction between Munc18-1 and the neuronal SNARE complex? Lijing Su has been putting a lot of effort into solving the structure of Munc18-1/SNARE complex. We expect that in the near future high-resolution structures of SM protein-SNARE complex assemblies, which could potentially be obtained from NMR spectroscopy or X-ray crystallography, will help decipher the mechanisms of fusion.

There are diverse models showing that Munc18-1 may be recruited from closed syntaxin-1 to the SNARE complex by the N-peptide (Rathore *et al.* 2010), through interaction with synaptobrevin (Xu *et al.* 2010), or via Munc13s (Ma *et al.* 2011). All these interactions could be integrated into one model whereby Munc13s open closed syntaxin-1 via binding to its SNARE motif (Figure 5.1), while Munc18-1 remains bound to the N-peptide of syntaxin-1, and after the SNARE complex is partially assembled, Munc18-1 moves to synaptobrevin and promotes the SNARE complex to extend to the membrane. The third set of questions is: assuming that all these binding modes of Munc18 and SNAREs are biologically relevant, do they occur simultaneously or sequentially? If sequentially, how and when do the two modes transit? Is Munc18 dissociated in the transition? Is the SM protein recruitment mechanism universal and applicable to all SNARE-mediated fusion events? Again, high-resolution Cryo-EM images and biophysical studies would help in answering these questions.

It has been clear that the SNARE complex is central in membrane fusion and that many factors, including Munc13s, synaptotagmins and complexins, interact with this complex to control its assembly. Synaptotagmin-1 and complexins are clearly involved in the Ca^{2+}-triggered step of release (Rizo *et al.* 2006), and both may play a role in fusion via interaction with the SNARE complex. Moreover, it is plausible that Munc13s also have a direct role in fusion. Nevertheless, it is unclear whether these interactions occur simultaneously or sequentially, and what is the exact mechanism of their interplay with the SNAREs. The HOPS complex in yeast is an Ypt7p (Rab)-effector complex with a Sec1/Munc18-family subunit, Vps33p. HOPS interact directly with membrane lipids, and stimulates fusion via tethering the membranes followed by SNARE complex interactions (Hickey and Wickner 2010)**.** Reconstitution experiments have shown that SNAREs and Sec17p/Sec18p (homologues of SNAP and NSF), Ypt7p (the rab7 homologue of *Saccharomyces cerevisiae*) and the HOPS complex, are required for competent yeast membrane fusion (Wickner 2010). This system has been reconstituted with high efficiency, but this is not the case for synaptic vesicle fusion. Rizo-Rey's lab will continue putting efforts to reconstitute this system more efficiently and in a manner that depends on Munc18-1 and other key regulators will shed light into functions of all these proteins.

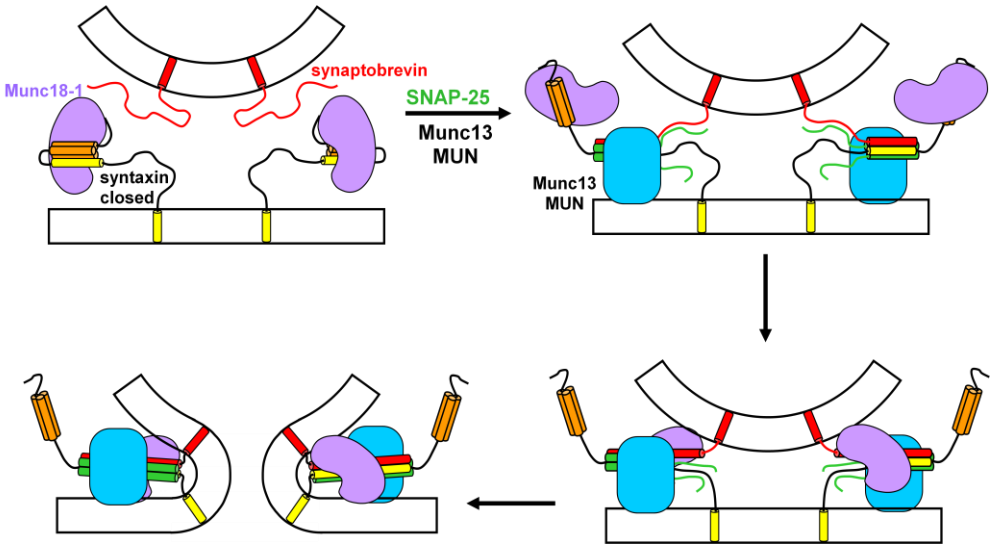

Figure 5.1

Figure 5.1 Functional model of Munc18-1, Munc13-1 and SNAREs in membrane fusion.

Syntaxin-1 (Habc domain, orange; SNARE motif, yellow) is initially within the complex of Munc18-1 (purple) in a closed conformation (top left panel). The MUN domain (blue) of Munc13 opens closed syntaxin-1 via binding to its SNARE motif, while Munc18-1 remains bound to the N-terminal region of syntaxin-1 at this stage (top right panel). After the SNARE complex is partially assembled, Munc18-1 moves to synaptobrevin and Munc13 MUN domain remains bound to the SNARE four-helix bundle. Eventually, Munc13 MUN domain and Munc18-1 cooperate with membrane-anchored SNARE complexes to facilitate membrane fusion.

BIBLIOGRAPHY

Arac, D., Murphy, T., and Rizo, J. (2003). "Facile detection of protein-protein interactions by one-dimensional NMR spectroscopy." Biochemistry 42(10): 2774-2780.

Arac, D., Chen, X., Khant, H.A., Ubach, J., Ludtke, S.J., Kikkawa, M., Johnson, A.E., Chiu, W., Südhof, T.C., and Rizo, J. (2006). "Close membrane-membrane proximity induced by Ca(2+)-dependent multivalent binding of synaptotagmin-1 to phospholipids." Nat Struct Mol Biol 13(3): 209-217.

Arunachalam, L., Han, L., Tassew, N.G., He, Y., Wang, L., Xie, L., Fujita, Y., Kwan, E., Davletov, B., Monnier, P.P., Gaisano, H.Y., and Sugita, S. (2008). "Munc18-1 is critical for plasma membrane localization of syntaxin1 but not of SNAP-25 in PC12 cells." Mol Biol Cell 19(2): 722-734.

Atwell, S., Ultsch, M., De Vos, A.M., and Wells, J.A. (1997). "Structural plasticity in a remodeled protein-protein interface." Science 278(5340): 1125-1128.

Augustine, G.J., Burns, M.E., DeBello, W.M., Pettit, D.L., and Schweizer, F.E. (1996). "Exocytosis: proteins and perturbations." Annual review of pharmacology and toxicology 36(1): 659-701.

Barakauskas, V.E., Beasley, C.L., Barr, A.M., Ypsilanti, A.R., Li, H.Y., Thornton, A.E., Wong, H., Rosokilja, G., Mann, J.J., Mancevski, B., Jakovski, Z., Davceva, N., Ilievski, B., Dwork, A.J., Falkai, P., and Honer, W.G. (2010). "A novel mechanism and treatment target for presynaptic abnormalities in specific striatal regions in schizophrenia." Neuropsychopharmacology 35(5): 1226-1238.

Basu, J., Shen, N., Dulubova, I., Lu, J., Guan, R., Guryev, O., Grishin, N.V., Rosenmund, C., and Rizo, J. (2005). "A minimal domain responsible for Munc13 activity." Nat Struct Mol Biol 12(11): 1017-1018.

Bennett, M.K., Calakos, N., and Scheller, R.H. (1992). "Syntaxin: a synaptic protein implicated in docking of synaptic vesicles at presynaptic active zones." Science 257(5067): 255-259.

Bennett, M.K. and Scheller, R.H. (1993). "The molecular machinery for secretion is conserved from yeast to neurons." Proceedings of the National Academy of Sciences of the United States of America 90(7): 2559.

Bentz, J. (2000). "Membrane fusion mediated by coiled coils: a hypothesis." Biophys J 78(2): 886-900.

Betz, A., Okamoto, M., Benseler, F., and Brose, N. (1997). "Direct interaction of the rat unc-13 homologue Munc13-1 with the N terminus of syntaxin." J Biol Chem 272(4): 2520-2526.

Borisovska, M., Zhao, Y., Tsytsyura, Y., Glyvuk, N., Takamori, S., Matti, U., Rettig, J., Südhof, T., and Bruns, D. (2005). "v-SNAREs control exocytosis of vesicles from priming to fusion." EMBO J 24(12): 2114-2126.

Boyd, A., Ciufo, L.F., Barclay, J.W., Graham, M.E., Haynes, L.P., Doherty, M.K., Riesen, M., Burgoyne, R.D., and Morgan, A. (2008). "A random mutagenesis approach to isolate dominant-negative yeast sec1 mutants reveals a functional role for domain 3a in yeast and mammalian Sec1/Munc18 proteins." Genetics 180(1): 165-178.

Bracher, A., Perrakis, A., Dresbach, T., Betz, H., and Weissenhorn, W. (2000). "The X-ray crystal structure of neuronal Sec1 from squid sheds new light on the role of this protein in exocytosis." Structure 8(7): 685-694.

Bracher, A. and Weissenhorn, W. (2002). "Structural basis for the Golgi membrane recruitment of Sly1p by Sed5p." EMBO J 21(22): 6114-6124.

Brenner, S. (1974). "The genetics of Caenorhabditis elegans." Genetics 77(1): 71-94.

Brunger, A. (2005). "Structure and function of SNARE and SNARE-interacting proteins." Quarterly reviews of biophysics 38(01): 1-47.

Burkhardt, P., Hattendorf, D.A., Weis, W.I., and Fasshauer, D. (2008). "Munc18a controls SNARE assembly through its interaction with the syntaxin N-peptide." EMBO J 27(7): 923-933.

Carr, C.M., Grote, E., Munson, M., Hughson, F.M., and Novick, P.J. (1999). "Sec1p binds to SNARE complexes and concentrates at sites of secretion." J Cell Biol 146(2): 333-344.

Carr, C.M. and Rizo, J. (2010). "At the junction of SNARE and SM protein function." Curr Opin Cell Biol 22(4): 488-495.

Castillo, M.A., Ghose, S., Tamminga, C.A., and Ulery-Reynolds, P.G. (2010). "Deficits in syntaxin 1 phosphorylation in schizophrenia prefrontal cortex." Biol Psychiatry 67(3): 208-216.

Chen, X., Tomchick, D., Kovrigin, E., Ara , D., Machius, M., Südhof, T., and Rizo, J. (2002). "Three-dimensional structure of the complexin/SNARE complex." Neuron 33(3): 397-409.

Chen, X., Arac, D., Wang, T.M., Gilpin, C.J., Zimmerberg, J., and Rizo, J. (2006). "SNARE-mediated lipid mixing depends on the physical state of the vesicles." Biophys J 90(6): 2062-2074.

Chen, X., Lu, J., Dulubova, I., and Rizo, J. (2008). "NMR analysis of the closed conformation of syntaxin-1." Journal of biomolecular NMR 41(1): 43-54.

Chen, Y.A. and Scheller, R.H. (2001). "SNARE-mediated membrane fusion." Nat Rev Mol Cell Biol 2(2): 98-106.

Clary, D.O., Griff, I.C., and Rothman, J.E. (1990). "SNAPs, a family of NSF attachment proteins involved in intracellular membrane fusion in animals and yeast." Cell 61(4): 709-721.

Collins, K.M., Thorngren, N.L., Fratti, R.A., and Wickner, W.T. (2005). "Sec17p and HOPS, in distinct SNARE complexes, mediate SNARE complex disruption or assembly for fusion." EMBO J 24(10): 1775-1786.

Dai, H., Shen, N., Arac, D., and Rizo, J. (2007). "A quaternary SNARE-synaptotagmin-Ca2+-phospholipid complex in neurotransmitter release." J Mol Biol 367(3): 848-863.

Darios, F., Wasser, C., Shakirzyanova, A., Giniatullin, A., Goodman, K., Munoz-Bravo, J.L., Raingo, J., Jorgacevski, J., Kreft, M., Zorec, R., Rosa, J.M., Gandia, L., Gutierrez, L.M., Binz, T., Giniatullin, R., Kavalali, E.T., and Davletov, B. (2009). "Sphingosine facilitates SNARE complex assembly and activates synaptic vesicle exocytosis." Neuron 62(5): 683-694.

de Wit, H., Walter, A., Milosevic, I., Gulyás-Kovács, A., Riedel, D., Sørensen, J., and Verhage, M. (2009). "Synaptotagmin-1 docks secretory vesicles to syntaxin-1/SNAP-25 acceptor complexes." Cell 138(5): 935-946.

Deák, F., Xu, Y., Chang, W., Dulubova, I., Khvotchev, M., Liu, X., Südhof, T., and Rizo, J. (2009). "Munc18-1 binding to the neuronal SNARE complex controls synaptic vesicle priming." The Journal of cell biology 184(5): 751.

DiAntonio, A., Parfitt, K.D., and Schwarz, T.L. (1993). "Synaptic transmission persists in synaptotagmin mutants of Drosophila." Cell 73(7): 1281-1290.

Diao, J., Su, Z., Lu, X., Yoon, T., Shin, Y., and Ha, T. (2010). "Single-vesicle fusion assay reveals Munc18-1 binding to the SNARE core is sufficient for stimulating membrane fusion." ACS Chemical Neuroscience 1(3): 168-174.

Dulubova, I., Sugita, S., Hill, S., Hosaka, M., Fernandez, I., Südhof, T.C., and Rizo, J. (1999). "A conformational switch in syntaxin during exocytosis: role of munc18." EMBO J 18(16): 4372-4382.

Dulubova, I., Yamaguchi, T., Wang, Y., Südhof, T.C., and Rizo, J. (2001). "Vam3p structure reveals conserved and divergent properties of syntaxins." Nat Struct Biol 8(3): 258-264.

Dulubova, I., Yamaguchi, T., Gao, Y., Min, S.W., Huryeva, I., Südhof, T.C., and Rizo, J. (2002). "How Tlg2p/syntaxin 16 'snares' Vps45." EMBO J 21(14): 3620-3631.

Dulubova, I., Yamaguchi, T., Arac, D., Li, H., Huryeva, I., Min, S.W., Rizo, J., and Südhof, T.C. (2003). "Convergence and divergence in the mechanism of SNARE binding by Sec1/Munc18-like proteins." Proc Natl Acad Sci U S A 100(1): 32-37.

Dulubova, I., Lou, X., Lu, J., Huryeva, I., Alam, A., Schneggenburger, R., Südhof, T.C., and Rizo, J. (2005). "A Munc13/RIM/Rab3 tripartite complex: from priming to plasticity?" EMBO J 24(16): 2839-2850.

Dulubova, I., Khvotchev, M., Liu, S., Huryeva, I., Südhof, T.C., and Rizo, J. (2007). "Munc18-1 binds directly to the neuronal SNARE complex." Proc Natl Acad Sci U S A 104(8): 2697-2702.

Fasshauer, D., Sutton, R.B., Brunger, A.T., and Jahn, R. (1998). "Conserved structural features of the synaptic fusion complex: SNARE proteins reclassified as Q- and R-SNAREs." Proc Natl Acad Sci U S A 95(26): 15781-15786.

Fernandez-Chacon, R., Konigstorfer, A., Gerber, S.H., Garcia, J., Matos, M.F., Stevens, C.F., Brose, N., Rizo, J., Rosenmund, C., and Südhof, T.C. (2001). "Synaptotagmin I functions as a calcium regulator of release probability." Nature 410(6824): 41-49.

Fernandez-Chacon, R., Shin, O.H., Konigstorfer, A., Matos, M.F., Meyer, A.C., Garcia, J., Gerber, S.H., Rizo, J., Südhof, T.C., and Rosenmund, C. (2002). "Structure/function analysis of Ca2+ binding to the C2A domain of synaptotagmin 1." J Neurosci 22(19): 8438-8446.

Fernandez, I., Ubach, J., Dulubova, I., Zhang, X., Südhof, T.C., and Rizo, J. (1998). "Three-dimensional structure of an evolutionarily conserved N-terminal domain of syntaxin 1A." Cell 94(6): 841-849.

Fernandez, I., Arac, D., Ubach, J., Gerber, S.H., Shin, O., Gao, Y., Anderson, R.G., Südhof, T.C., and Rizo, J. (2001). "Three-dimensional structure of the synaptotagmin 1 C2B-domain: synaptotagmin 1 as a phospholipid binding machine." Neuron 32(6): 1057-1069.

Fujiwara, T., Mishima, T., Kofuji, T., Chiba, T., Tanaka, K., Yamamoto, A., and Akagawa, K. (2006). "Analysis of knock-out mice to determine the role of HPC-1/syntaxin 1A in expressing synaptic plasticity." J Neurosci 26(21): 5767-5776.

Geppert, M., Goda, Y., Hammer, R.E., Li, C., Rosahl, T.W., Stevens, C.F., and Südhof, T.C. (1994). "Synaptotagmin I: a major Ca2+ sensor for transmitter release at a central synapse." Cell 79(4): 717-727.

Gerber, S.H., Rah, J.C., Min, S.W., Liu, X., de Wit, H., Dulubova, I., Meyer, A.C., Rizo, J., Arancillo, M., Hammer, R.E., Verhage, M., Rosenmund, C., and Südhof, T.C. (2008). "Conformational switch of syntaxin-1 controls synaptic vesicle fusion." Science 321(5895): 1507-1510.

Glavan, G., Schliebs, R., and Zivin, M. (2009). "Synaptotagmins in neurodegeneration." Anat Rec (Hoboken) 292(12): 1849-1862.

Gray, L.J., Dean, B., Kronsbein, H.C., Robinson, P.J., and Scarr, E. (2010). "Region and diagnosis-specific changes in synaptic proteins in schizophrenia and bipolar I disorder." Psychiatry Res 178(2): 374-380.

Grote, E., Carr, C.M., and Novick, P.J. (2000). "Ordering the final events in yeast exocytosis." J Cell Biol 151(2): 439-452.

Guan, R., Dai, H., and Rizo, J. (2008). "Binding of the Munc13-1 MUN domain to membrane-anchored SNARE complexes." Biochemistry 47(6): 1474-1481.

Gulyás-Kovács, A., de Wit, H., Milosevic, I., Kochubey, O., Toonen, R., Klingauf, J., Verhage, M., and Sørensen, J.B. (2007). "Munc18-1: sequential interactions with the fusion machinery stimulate vesicle docking and priming." J Neurosci 27(32): 8676-8686.

Han, G., Malintan, N., Collins, B., Meunier, F., and Sugita, S. (2010). "Munc18 1 as a key regulator of neurosecretion." Journal of neurochemistry.

Han, L., Jiang, T., Han, G., Malintan, N., Xie, L., Wang, L., Tse, F., Gaisano, H., Collins, B., and Meunier, F. (2009). "Rescue of Munc18-1 and-2 double knockdown reveals the essential functions of interaction between Munc18 and closed syntaxin in PC12 cells." Molecular biology of the cell 20(23): 4962.

Hanson, P.I., Heuser, J.E., and Jahn, R. (1997). "Neurotransmitter release - four years of SNARE complexes." Curr Opin Neurobiol 7(3): 310-315.

Hanson, P.I., Roth, R., Morisaki, H., Jahn, R., and Heuser, J.E. (1997). "Structure and conformational changes in NSF and its membrane receptor complexes visualized by quick-freeze/deep-etch electron microscopy." Cell 90(3): 523-535.

Hata, Y., Slaughter, C.A., and Sudhof, T.C. (1993). "Synaptic vesicle fusion complex contains unc-18 homologue bound to syntaxin." Nature 366(6453): 347-351.

Hazzard, J., Südhof, T.C., and Rizo, J. (1999). "NMR analysis of the structure of synaptobrevin and of its interaction with syntaxin." J Biomol NMR 14(3): 203-207.

Hickey, C.M. and Wickner, W. (2010). "HOPS initiates vacuole docking by tethering membranes before trans-SNARE complex assembly." Mol Biol Cell 21(13): 2297-2305.

Hikita, T., Taya, S., Fujino, Y., Taneichi-Kuroda, S., Ohta, K., Tsuboi, D., Shinoda, T., Kuroda, K., Funahashi, Y., Uraguchi-Asaki, J., Hashimoto, R., and Kaibuchi, K. (2009). "Proteomic analysis reveals novel binding partners of dysbindin, a schizophrenia-related protein." J Neurochem 110(5): 1567-1574.

Hosono, R., Hekimi, S., Kamiya, Y., Sassa, T., Murakami, S., Nishiwaki, K., Miwa, J., Taketo, A., and Kodaira, K.I. (1992). "The unc-18 gene encodes a novel protein affecting the kinetics of acetylcholine metabolism in the nematode Caenorhabditis elegans." J Neurochem 58(4): 1517-1525.

Hu, K., Carroll, J., Fedorovich, S., Rickman, C., Sukhodub, A., and Davletov, B. (2002). "Vesicular restriction of synaptobrevin suggests a role for calcium in membrane fusion." Nature 415(6872): 646-650.

Hu, S.H., Latham, C.F., Gee, C.L., James, D.E., and Martin, J.L. (2007). "Structure of the Munc18c/Syntaxin4 N-peptide complex defines universal features of the N-peptide binding mode of Sec1/Munc18 proteins." Proc Natl Acad Sci U S A 104(21): 8773-8778.

Hu, S.H., Christie, M.P., Saez, N.J., Latham, C.F., Jarrott, R., Lua, L.H., Collins, B.M., and Martin, J.L. (2011). "Possible roles for Munc18-1 domain 3a and Syntaxin1 N-peptide and C-terminal anchor in SNARE complex formation." Proc Natl Acad Sci U S A 108(3): 1040-1045.

Jahn, R. and Südhof, T.C. (1999). "Membrane fusion and exocytosis." Annual review of biochemistry 68(1): 863-911.

Jahn, R. and Scheller, R. (2006). "SNAREs-engines for membrane fusion." Nature reviews Molecular cell biology 7(9): 631-643.

Jiang, W., Baker, M.L., Jakana, J., Weigele, P.R., King, J., and Chiu, W. (2008). "Backbone structure of the infectious epsilon15 virus capsid revealed by electron cryomicroscopy." Nature 451(7182): 1130-1134.

Johnson, J.R., Ferdek, P., Lian, L.Y., Barclay, J.W., Burgoyne, R.D., and Morgan, A. (2009). "Binding of UNC-18 to the N-terminus of syntaxin is essential for neurotransmission in Caenorhabditis elegans." Biochem J 418(1): 73-80.

Kandel, E.R., Schwartz, J.H., Jessell, T.M., Mack, S., and Dodd, J. (1991). Principles of neural science, Elsevier New York.

Khvotchev, M., Dulubova, I., Sun, J., Dai, H., Rizo, J., and Südhof, T.C. (2007). "Dual modes of Munc18-1/SNARE interactions are coupled by functionally critical binding to syntaxin-1 N terminus." J Neurosci 27(45): 12147-12155.

Koushika, S.P., Richmond, J.E., Hadwiger, G., Weimer, R.M., Jorgensen, E.M., and Nonet, M.L. (2001). "A post-docking role for active zone protein Rim." Nat Neurosci 4(10): 997-1005.

Kweon, D.H., Kim, C.S., and Shin, Y.K. (2003). "Regulation of neuronal SNARE assembly by the membrane." Nat Struct Biol 10(6): 440-447.

Lin, R. and Scheller, R. (2000). "M ECHANISMS OF S YNAPTIC V ESICLE E XOCYTOSIS." Annual Review of Cell and Developmental Biology 16(1): 19-49.

Link, E., Edelmann, L., Chou, J.H., Binz, T., Yamasaki, S., Eisel, U., Baumert, M., Südhof, T.C., Niemann, H., and Jahn, R. (1992). "Tetanus toxin action: inhibition of neurotransmitter release linked to synaptobrevin proteolysis." Biochem Biophys Res Commun 189(2): 1017-1023.

Littleton, J.T., Stern, M., Schulze, K., Perin, M., and Bellen, H.J. (1993). "Mutational analysis of Drosophila synaptotagmin demonstrates its essential role in Ca(2+)-activated neurotransmitter release." Cell 74(6): 1125-1134.

Liu, J., Guo, T., Wu, J., Bai, X., Zhou, Q., and Sui, S.F. (2007). "Overexpression of complexin in PC12 cells inhibits exocytosis by preventing SNARE complex recycling." Biochemistry (Mosc) 72(4): 439-444.

Ma, C., Li, W., Xu, Y., and Rizo, J. (2011). "Munc13 Mediates the Transition from the Closed Syntaxin/Munc18 complex to the SNARE complex." Nature structural & molecular biology, in press.

Mackler, J.M. and Reist, N.E. (2001). "Mutations in the second C2 domain of synaptotagmin disrupt synaptic transmission at Drosophila neuromuscular junctions." J Comp Neurol 436(1): 4-16.

Mackler, J.M., Drummond, J.A., Loewen, C.A., Robinson, I.M., and Reist, N.E. (2002). "The C(2)B Ca(2+)-binding motif of synaptotagmin is required for synaptic transmission in vivo." Nature 418(6895): 340-344.

Maximov, A., Tang, J., Yang, X., Pang, Z.P., and Südhof, T.C. (2009). "Complexin controls the force transfer from SNARE complexes to membranes in fusion." Science 323(5913): 516-521.

McMahon, H.T., Missler, M., Li, C., and Südhof, T.C. (1995). "Complexins: cytosolic proteins that regulate SNAP receptor function." Cell 83(1): 111-119.

McMahon, H.T., Kozlov, M.M., and Martens, S. (2010). "Membrane curvature in synaptic vesicle fusion and beyond." Cell 140(5): 601-605.

Medine, C.N., Rickman, C., Chamberlain, L.H., and Duncan, R.R. (2007). "Munc18-1 prevents the formation of ectopic SNARE complexes in living cells." J Cell Sci 120(Pt 24): 4407-4415.

Misura, K.M., Scheller, R.H., and Weis, W.I. (2000). "Three-dimensional structure of the neuronal-Sec1-syntaxin 1a complex." Nature 404(6776): 355-362.

Nishiki, T. and Augustine, G.J. (2004). "Dual roles of the C2B domain of synaptotagmin I in synchronizing Ca2+-dependent neurotransmitter release." J Neurosci 24(39): 8542-8550.

Nonet, M.L., Grundahl, K., Meyer, B.J., and Rand, J.B. (1993). "Synaptic function is impaired but not eliminated in C. elegans mutants lacking synaptotagmin." Cell 73(7): 1291-1305.

Novick, P. and Schekman, R. (1979). "Secretion and cell-surface growth are blocked in a temperature-sensitive mutant of Saccharomyces cerevisiae." Proc Natl Acad Sci U S A 76(4): 1858-1862.

Novick, P., Field, C., and Schekman, R. (1980). "Identification of 23 complementation groups required for post-translational events in the yeast secretory pathway." Cell 21(1): 205-215.

Novick, P., Medkova, M., Dong, G., Hutagalung, A., Reinisch, K., and Grosshans, B. (2006). "Interactions between Rabs, tethers, SNAREs and their regulators in exocytosis." Biochem Soc Trans 34(Pt 5): 683-686.

Ohya, T., Miaczynska, M., Coskun, U., Lommer, B., Runge, A., Drechsel, D., Kalaidzidis, Y., and Zerial, M. (2009). "Reconstitution of Rab- and SNARE-dependent membrane fusion by synthetic endosomes." Nature 459(7250): 1091-1097.

Orci, L., Schekman, R., and Perrelet, A. (1996). "Interleaflet clear space is reduced in the membrane of COP I and COP II-coated buds/vesicles." Proc Natl Acad Sci U S A 93(17): 8968-8970.

Pabst, S., Hazzard, J.W., Antonin, W., Südhof, T.C., Jahn, R., Rizo, J., and Fasshauer, D. (2000). "Selective interaction of complexin with the neuronal SNARE complex. Determination of the binding regions." J Biol Chem 275(26): 19808-19818.

Parlati, F., Weber, T., McNew, J.A., Westermann, B., Sollner, T.H., and Rothman, J.E. (1999). "Rapid and efficient fusion of phospholipid vesicles by the alpha-helical core of a SNARE complex in the absence of an N-terminal regulatory domain." Proc Natl Acad Sci U S A 96(22): 12565-12570.

Peng, R. and Gallwitz, D. (2004). "Multiple SNARE interactions of an SM protein: Sed5p/Sly1p binding is dispensable for transport." EMBO J 23(20): 3939-3949.

Pevsner, J., Hsu, S.C., Braun, J.E., Calakos, N., Ting, A.E., Bennett, M.K., and Scheller, R.H. (1994). "Specificity and regulation of a synaptic vesicle docking complex." Neuron 13(2): 353-361.

Pieren, M., Schmidt, A., and Mayer, A. (2010). "The SM protein Vps33 and the t-SNARE H(abc) domain promote fusion pore opening." Nat Struct Mol Biol 17(6): 710-717.

Poirier, M.A., Xiao, W., Macosko, J.C., Chan, C., Shin, Y.K., and Bennett, M.K. (1998). "The synaptic SNARE complex is a parallel four-stranded helical bundle." Nat Struct Biol 5(9): 765-769.

Rathore, S., Bend, E., Yu, H., Hammarlund, M., Jorgensen, E., and Shen, J. (2010). "Syntaxin N-terminal peptide motif is an initiation factor for the assembly of the SNARE-Sec1/Munc18 membrane fusion complex." Proceedings of the National Academy of Sciences 107(52): 22399.

Reim, K., Mansour, M., Varoqueaux, F., McMahon, H., Südhof, T., Brose, N., and Rosenmund, C. (2001). "Complexins regulate a late step in Ca2+-dependent neurotransmitter release." Cell 104(1): 71-81.

Reim, K., Wegmeyer, H., Brandstatter, J.H., Xue, M., Rosenmund, C., Dresbach, T., Hofmann, K., and Brose, N. (2005). "Structurally and functionally unique complexins at retinal ribbon synapses." J Cell Biol 169(4): 669-680.

Richmond, J.E., Davis, W.S., and Jorgensen, E.M. (1999). "UNC-13 is required for synaptic vesicle fusion in C. elegans." Nat Neurosci 2(11): 959-964.

Rickman, C., Medine, C.N., Bergmann, A., and Duncan, R.R. (2007). "Functionally and spatially distinct modes of munc18-syntaxin 1 interaction." J Biol Chem 282(16): 12097-12103.

Riento, K., Galli, T., Jansson, S., Ehnholm, C., Lehtonen, E., and Olkkonen, V.M. (1998). "Interaction of Munc-18-2 with syntaxin 3 controls the association of apical SNAREs in epithelial cells." J Cell Sci 111 (Pt 17): 2681-2688.

Rigaud, J.L. and Levy, D. (2003). "Reconstitution of membrane proteins into liposomes." Methods Enzymol 372: 65-86.

Rizo, J. and Südhof, T. (2002). "Snares and Munc18 in synaptic vesicle fusion." Nature Reviews Neuroscience 3(8): 641-653.

Rizo, J., Chen, X., and Ara, D. (2006). "Unraveling the mechanisms of synaptotagmin and SNARE function in neurotransmitter release." Trends in cell biology 16(7): 339-350.

Rizo, J. and Rosenmund, C. (2008). "Synaptic vesicle fusion." Nature structural & molecular biology 15(7): 665-674.

Rodkey, T.L., Liu, S., Barry, M., and McNew, J.A. (2008). "Munc18a scaffolds SNARE assembly to promote membrane fusion." Mol Biol Cell 19(12): 5422-5434.

Rothman, J.E. (1994). "Intracellular membrane fusion." Adv Second Messenger Phosphoprotein Res 29: 81-96.

Rowe, J., Corradi, N., Malosio, M.L., Taverna, E., Halban, P., Meldolesi, J., and Rosa, P. (1999). "Blockade of membrane transport and disassembly of the Golgi complex by expression of syntaxin 1A in neurosecretion-incompetent cells: prevention by rbSEC1." J Cell Sci 112 (Pt 12): 1865-1877.

Rowe, J., Calegari, F., Taverna, E., Longhi, R., and Rosa, P. (2001). "Syntaxin 1A is delivered to the apical and basolateral domains of epithelial cells: the role of munc-18 proteins." J Cell Sci 114(Pt 18): 3323-3332.

Schaub, J.R., Lu, X., Doneske, B., Shin, Y.K., and McNew, J.A. (2006). "Hemifusion arrest by complexin is relieved by Ca2+-synaptotagmin I." Nat Struct Mol Biol 13(8): 748-750.

Schiavo, G., Benfenati, F., Poulain, B., Rossetto, O., Polverino de Laureto, P., DasGupta, B.R., and Montecucco, C. (1992). "Tetanus and botulinum-B neurotoxins block neurotransmitter release by proteolytic cleavage of synaptobrevin." Nature 359(6398): 832-835.

Schoch, S., Deak, F., Konigstorfer, A., Mozhayeva, M., Sara, Y., Südhof, T.C., and Kavalali, E.T. (2001). "SNARE function analyzed in synaptobrevin/VAMP knockout mice." Science 294(5544): 1117-1122.

Schoch, S., Castillo, P.E., Jo, T., Mukherjee, K., Geppert, M., Wang, Y., Schmitz, F., Malenka, R.C., and Südhof, T.C. (2002). "RIM1alpha forms a protein scaffold for regulating neurotransmitter release at the active zone." Nature 415(6869): 321-326.

Shao, X., Fernandez, I., Südhof, T.C., and Rizo, J. (1998). "Solution structures of the Ca2+-free and Ca2+-bound C2A domain of synaptotagmin I: does Ca2+ induce a conformational change?" Biochemistry 37(46): 16106-16115.

Shen, J., Tareste, D., Paumet, F., Rothman, J., and Melia, T. (2007). "Selective activation of cognate SNAREpins by Sec1/Munc18 proteins." Cell 128(1): 183-195.

Shen, J., Rathore, S., Khandan, L., and Rothman, J. (2010). "SNARE bundle and syntaxin N-peptide constitute a minimal complement for Munc18-1 activation of membrane fusion." The Journal of cell biology 190(1): 55.

Smyth, A.M., Duncan, R.R., and Rickman, C. (2010). "Munc18-1 and syntaxin1: unraveling the interactions between the dynamic duo." Cell Mol Neurobiol 30(8): 1309-1313.

Starai, V., Hickey, C., and Wickner, W. (2008). "HOPS proofreads the trans-SNARE complex for yeast vacuole fusion." Molecular biology of the cell 19(6): 2500.

Stein, A., Weber, G., Wahl, M.C., and Jahn, R. (2009). "Helical extension of the neuronal SNARE complex into the membrane." Nature 460(7254): 525-528.

Stevens, D.R., Wu, Z.X., Matti, U., Junge, H.J., Schirra, C., Becherer, U., Wojcik, S.M., Brose, N., and Rettig, J. (2005). "Identification of the minimal protein domain required for priming activity of Munc13-1." Curr Biol 15(24): 2243-2248.

Stroupe, C., Collins, K.M., Fratti, R.A., and Wickner, W. (2006). "Purification of active HOPS complex reveals its affinities for phosphoinositides and the SNARE Vam7p." EMBO J 25(8): 1579-1589.

Südhof, T. (2004). "The synaptic vesicle cycle." Annual review of neuroscience 27: 509.

Südhof, T. (2004). "The synaptic vesicle cycle." Neuroscience 27(1): 509.

Südhof, T.C. (1995). "The synaptic vesicle cycle: a cascade of protein-protein interactions." Nature 375(6533): 645-653.

Südhof, T.C. (2002). "Synaptotagmins: why so many?" J Biol Chem 277(10): 7629-7632.

Südhof, T.C. and Rothman, J.E. (2009). "Membrane fusion: grappling with SNARE and SM proteins." Science 323(5913): 474-477.

Sutton, R.B., Davletov, B.A., Berghuis, A.M., Südhof, T.C., and Sprang, S.R. (1995). "Structure of the first C2 domain of synaptotagmin I: a novel Ca2+/phospholipid-binding fold." Cell 80(6): 929-938.

Sutton, R.B., Fasshauer, D., Jahn, R., and Brunger, A.T. (1998). "Crystal structure of a SNARE complex involved in synaptic exocytosis at 2.4 A resolution." Nature 395(6700): 347-353.

Takamori, S., Holt, M., Stenius, K., Lemke, E.A., Gronborg, M., Riedel, D., Urlaub, H., Schenck, S., Brugger, B., Ringler, P., Muller, S.A., Rammner, B., Grater, F., Hub, J.S., De Groot, B.L., Mieskes, G., Moriyama, Y., Klingauf, J., Grubmuller, H., Heuser, J., Wieland, F., and Jahn, R. (2006). "Molecular anatomy of a trafficking organelle." Cell 127(4): 831-846.

Tang, J., Maximov, A., Shin, O.H., Dai, H., Rizo, J., and Südhof, T.C. (2006). "A complexin/synaptotagmin 1 switch controls fast synaptic vesicle exocytosis." Cell 126(6): 1175-1187.

Tellam, J.T., McIntosh, S., and James, D.E. (1995). "Molecular identification of two novel Munc-18 isoforms expressed in non-neuronal tissues." J Biol Chem 270(11): 5857-5863.

Terrian, D.M. and White, M.K. (1997). "Phylogenetic analysis of membrane trafficking proteins: a family reunion and secondary structure predictions." European journal of cell biology 73(3): 198.

Thurmond, D.C., Ceresa, B.P., Okada, S., Elmendorf, J.S., Coker, K., and Pessin, J.E. (1998). "Regulation of insulin-stimulated GLUT4 translocation by Munc18c in 3T3L1 adipocytes." J Biol Chem 273(50): 33876-33883.

Togneri, J., Cheng, Y.S., Munson, M., Hughson, F.M., and Carr, C.M. (2006). "Specific SNARE complex binding mode of the Sec1/Munc-18 protein, Sec1p." Proc Natl Acad Sci U S A 103(47): 17730-17735.

Toonen, R. and Verhage, M. (2003). "Vesicle trafficking: pleasure and pain from SM genes." Trends in cell biology 13(4): 177-186.

Toonen, R., Kochubey, O., De Wit, H., Gulyas-Kovacs, A., Konijnenburg, B., Sørensen, J., Klingauf, J., and Verhage, M. (2006). "Dissecting docking and tethering of secretory vesicles at the target membrane." The EMBO Journal 25(16): 3725-3737.

Tucker, W.C., Weber, T., and Chapman, E.R. (2004). "Reconstitution of Ca2+-regulated membrane fusion by synaptotagmin and SNAREs." Science 304(5669): 435-438.

Varoqueaux, F., Sigler, A., Rhee, J.S., Brose, N., Enk, C., Reim, K., and Rosenmund, C. (2002). "Total arrest of spontaneous and evoked synaptic transmission but normal synaptogenesis in the absence of Munc13-mediated vesicle priming." Proc Natl Acad Sci U S A 99(13): 9037-9042.

Verhage, M., Maia, A.S., Plomp, J.J., Brussaard, A.B., Heeroma, J.H., Vermeer, H., Toonen, R.F., Hammer, R.E., van den Berg, T.K., Missler, M., Geuze, H.J., and Südhof, T.C. (2000). "Synaptic assembly of the brain in the absence of neurotransmitter secretion." Science 287(5454): 864-869.

Verhage, M. and Toonen, R. (2007). "Regulated exocytosis: merging ideas on fusing membranes." Current opinion in cell biology 19(4): 402-408.

Voets, T., Toonen, R.F., Brian, E.C., de Wit, H., Moser, T., Rettig, J., Südhof, T.C., Neher, E., and Verhage, M. (2001). "Munc18-1 promotes large dense-core vesicle docking." Neuron 31(4): 581-591.

Washbourne, P., Thompson, P.M., Carta, M., Costa, E.T., Mathews, J.R., Lopez-Bendito, G., Molnar, Z., Becher, M.W., Valenzuela, C.F., Partridge, L.D., and Wilson, M.C. (2002). "Genetic ablation of the t-SNARE SNAP-25 distinguishes mechanisms of neuroexocytosis." Nat Neurosci 5(1): 19-26.

Weber, M., Chernov, K., Turakainen, H., Wohlfahrt, G., Pajunen, M., Savilahti, H., and Jantti, J. (2010). "Mso1p regulates membrane fusion through interactions with the putative N-peptide-binding area in Sec1p domain 1." Mol Biol Cell 21(8): 1362-1374.

Weber, T., Zemelman, B.V., McNew, J.A., Westermann, B., Gmachl, M., Parlati, F., Sollner, T.H., and Rothman, J.E. (1998). "SNAREpins: minimal machinery for membrane fusion." Cell 92(6): 759-772.

Weimbs, T., Low, S.H., Chapin, S.J., Mostov, K.E., Bucher, P., and Hofmann, K. (1997). "A conserved domain is present in different families of vesicular fusion proteins: a new superfamily." Proceedings of the National Academy of Sciences of the United States of America 94(7): 3046.

Weimer, R., Richmond, J., Davis, W., Hadwiger, G., Nonet, M., and Jorgensen, E. (2003). "Defects in synaptic vesicle docking in unc-18 mutants." Nature neuroscience 6(10): 1023-1030.

Weninger, K., Bowen, M.E., Choi, U.B., Chu, S., and Brunger, A.T. (2008). "Accessory proteins stabilize the acceptor complex for synaptobrevin, the 1:1 syntaxin/SNAP-25 complex." Structure 16(2): 308-320.

White, J.M. (1992). "Membrane fusion." Science 258(5084): 917-924.

Wickner, W. (2010). "Membrane fusion: five lipids, four SNAREs, three chaperones, two nucleotides, and a Rab, all dancing in a ring on yeast vacuoles." Annu Rev Cell Dev Biol 26: 115-136.

Xu, Y., Su, L., and Rizo, J. (2010). "Binding of Munc18-1 to synaptobrevin and to the SNARE four-helix bundle." Biochemistry 49(8): 1568-1576.

Xue, M., Craig, T.K., Xu, J., Chao, H.T., Rizo, J., and Rosenmund, C. (2010). "Binding of the complexin N terminus to the SNARE complex potentiates synaptic-vesicle fusogenicity." Nat Struct Mol Biol 17(5): 568-575.

Yamaguchi, T., Dulubova, I., Min, S.W., Chen, X., Rizo, J., and Südhof, T.C. (2002). "Sly1 binds to Golgi and ER syntaxins via a conserved N-terminal peptide motif." Dev Cell 2(3): 295-305.

Yang, B., Steegmaier, M., Gonzalez, L.C., Jr., and Scheller, R.H. (2000). "nSec1 binds a closed conformation of syntaxin1A." J Cell Biol 148(2): 247-252.

Yu, X., Jin, L., and Zhou, Z.H. (2008). "3.88 A structure of cytoplasmic polyhedrosis virus by cryo-electron microscopy." Nature 453(7193): 415-419.

Zhang, X., Settembre, E., Xu, C., Dormitzer, P.R., Bellamy, R., Harrison, S.C., and Grigorieff, N. (2008). "Near-atomic resolution using electron cryomicroscopy and single-particle reconstruction." Proc Natl Acad Sci U S A 105(6): 1867-1872.

Zhang, X., Jin, L., Fang, Q., Hui, W.H., and Zhou, Z.H. (2010). "3.3 A cryo-EM structure of a nonenveloped virus reveals a priming mechanism for cell entry." Cell 141(3): 472-482.

Zhao, H., Jutila, A., Nurminen, T., Wickstrom, S.A., Keski-Oja, J., and Kinnunen, P.K. (2005). "Binding of endostatin to phosphatidylserine-containing membranes and formation of amyloid-like fibers." Biochemistry 44(8): 2857-2863.

Zilly, F., Sørensen, J., Jahn, R., and Lang, T. (2006). "Munc18-bound syntaxin readily forms SNARE complexes with synaptobrevin in native plasma membranes." PLoS Biol 4(10): e330.